The Pennsylvania State University

The J. Jeffrey and Ann Marie Fox Graduate School

AUTOMATION OF URBAN BUILDING PARAMETER DATA EXTRACTION: ZERO-SHOT OBJECT DETECTION FOR WINDOW-TO-WALL RATIO ESTIMATION

A Thesis in

Architectural Engineering

by

Elnaz Ghasemi

Submitted in Partial Fulfillment
of the Requirements
for the Degree of

Master of Science

May 2025

The thesis of Elnaz Ghasemi was reviewed and approved by the following:

Rahman Azari
Associate Professor of Architecture
Thesis Advisor

Wangda Zuo
Professor of Architectural Engineering

Lisa Iulo
Professor of Architecture

Julian Wang
Associate Professor of Architectural Engineering

James Freihaut
Professor of Architectural Engineering
Program Head

ABSTRACT

Urban energy and carbon modeling rely on comprehensive and accurate building data, yet the limited availability of such data remains a major challenge for urban-scale simulations. This study addresses this gap by developing a data-driven methodology to extract and aggregate geometric and non-geometric attributes of urban buildings for energy simulation. Specifically, object detection and machine learning techniques were applied to publicly available street-view images to estimate the window-to-wall ratio (WWR), a key parameter in urban energy and carbon modeling. The extracted WWR data were then integrated with other urban building parameters using spatial join techniques to create a more detailed and accurate urban dataset.

The findings of this research contribute to the refinement of building archetypes by incorporating more precise WWR data and to the development of an urban carbon emission modeling framework for evaluating building-related greenhouse gas emissions. By providing urban planners and policymakers with actionable insights into the carbon implications of various urban forms and construction strategies, this study supports informed decision-making for sustainable urban development. Ultimately, this research advances efforts to reduce urban carbon footprints, aligning with global net-zero emission goals.

Keywords: Urban data, Data-driven method, Object detection, UBEM (Urban Building Energy Modeling)

TABLE OF CONTENTS

LIST OF FIGURES

LIST OF TABLES

ACKNOWLEDGEMENTS

I would like to take this opportunity to thank the many people who have supported me throughout the process of completing this thesis. First, I would like to express my appreciation, and gratitude to my advisor, Dr. Rahman Azari, for directing and supporting me throughout this research process. His advice and mentorship have helped me tremendously and I am grateful for his guidance. I also want to thank my committee members, Dr. Lisa Iulo, Dr. Julian Wang, and Dr. Wangda Zuo for their support and for taking the time to provide valuable suggestions for improvement.

Finally, I would like to thank my family for their continuous support in all my endeavors.

This research was conducted as part of the Baltimore Social Environmental Collaboration (BSEC) project and supported by funding from the U.S. Department of Energy. The findings and conclusions presented in this work are solely those of the author and do not necessarily reflect the views or policies of the Department of Energy or any other agency of the United States governmen

Chapter 1

Introduction

According to the 2022 Intergovernmental Panel on Climate Change (IPCC) report on the new net-zero needs, decarbonization initiatives need to scale up on urban and city levels for global warming to stay below the 1.5°C threshold. The construction sector, especially the morphological aspects of buildings, can make a significant impact on reducing carbon emissions (IPCC, 2022).

Data on the spatial characterization of the building's stock is required to achieve environmental goals defined by governments and national energy agencies. These data include building geometric and non-geometric attributes such as height, materials, and local climate. While the advancements in urban data collection allow for detailed analysis of building features, the dominant practices of data collection to use as input in energy modeling are often cumbersome and incomprehensive, particularly in less studied smaller cities which suffer from a scarcity of databases that would include detailed building information. Additionally, in many cases, national and global datasets lack necessary and detailed morphological information on buildings (Hecht et al., 2013; Herfort et al., 2023a).

Challenges also persist in computational costs and integrating diverse data to use as input for simulation, necessitating comprehensive, scalable, and accurate methods to gather data from various sources. The present research addresses this gap by utilizing advanced machine learning (ML) techniques and computer vision to provide a novel methodology to obtain certain building parameter data (such as WWR, in case of this research) for urban building analysis. In this work, two ML models and data mining methods are used to aggregate buildings' data from various sources.

To overcome these challenges, I used zero-shot image processing techniques to extract the necessary physical information of buildings from Google Maps Street View (SVS) images. The machine learning model employed in this phase has been pretrained to detect objects, specifically windows, within an image. Statistical and mathematical methods are then used to calculate window-to-wall ratio as critical building physical characteristics in urban energy studies. This methodology leverages real-world Google images, as input data for urban energy and carbon analysis, ensuring realism and relevance of the data.

Urban Building Energy Modeling

Cities have emerged as centers of energy consumption and carbon emissions, contributing significantly to global greenhouse gas emissions. They are responsible for consuming a significant portion of global energy in sectors including industry, transportation, commercial activities, buildings, and infrastructure, and they account for approximately 75% of primary energy use and 70% of greenhouse gas emissions (IEA, 2024). Among all sectors contributing to GHG emissions in urban areas, buildings contribute significantly to this consumption, with about 30% of global energy being utilized in buildings. Buildings play a critical role in global energy consumption and emissions, contributing to both direct on-site activities and indirect energy demands for heating, cooling, and electricity. Their environmental impact underscores the need for sustainable design strategies and decarbonization efforts to mitigate their contribution to climate change (IEA, 2023). Given this, developing accurate methods for evaluating, simulating, and forecasting energy usage in buildings is crucial to achieving low-carbon targets. Such analyses require detailed building characteristics, including information about HVAC systems, internal loads, and construction features, as inputs for urban building energy/carbon modeling. In Baltimore where this research focuses, buildings account for 64% of city's GHG emissions (*Joanna Birch et al, 2024*) and more than 6,000 new houses were built in 2023 (Bureau of the Census, 2023), presenting significant opportunity to reduce residential building emissions. Evaluating, simulating, and forecasting energy usage in the building sector are imperative to meet the low-carbon energy targets (Allan et al., 2022). This is not only important for new construction projects but also for existing buildings.

Previous studies have used urban building energy modeling (UBEM) to quantify different target variables including thermal comfort (Allan et al., 2022; Ang et al., 2020; J. Kim et al., 2025), energy usage, greenhouse gas emissions, and heat emissions (Excell et al., 2024; Hong et al., 2020; Sherif et al., 2025). For example, Natanian et al. (2020) evaluated total energy demand (Load Match index: LM), photovoltaic (PV) energy production, and daylight performance analysis (sDA) (Natanian & Auer, 2020). Also, Evola (2020) used Grasshopper plugins LadyBug and HoneyBee to evaluate the Universal Thermal Climate (UTC) Heat Gain of a canyon, an indicator of outdoor thermal comfort, and Mean Radiant Temperature (MRT) (Evola et al., 2020).

To create an energy model for physics-based UBEM approach, various data and input are required, that include building geometry (Width, length, height, window to wall ratio, and orientation), and non-geometry data consisting of construction material information, mechanical and lighting systems, occupancy schedules, and local climate data (Hong et al., 2020). Conversely, the data-driven strategy uses statistical or machine learning techniques to forecast energy consumption based on historical urban data (Ahmad et al., 2018). An example of data-driven methods is Ghorbany and Hu (2024) which provides a methodology to analyze embodied carbon emissions of over millions of houses in Chicago. Their research identified 157 archetypes in the city, and applied life cycle assessment for urban embodied carbon analysis (Ghorbany & Hu, 2024).

To gather input parameters for physics-based urban modeling, previous studies have used data-driven methods, filed survey, image processing, object detection methods, and photogrammetry. Dabirian et al (2022) used a data-driven approach to gather input data with a focus on reviewing the occupancy modeling i.e. occupant's presence and absence, and schedules of UBEM. They finally categorized occupant behavior modeling in UBEM and discussed the pros and cons of each model. In other studies, Mohammadiziazi et al (2021), and Ghorbany et al (2024) used object detection, and computer vision methods to get input parameters such as window to wall ratio, and number of floors.(Dabirian et al., 2022; Ghorbany et al., 2024; Mohammadiziazi et al., 2021).

Despite advancements in urban data collection methods, challenges remain concerning computation time, costs, and the integration of the input parameters used for simulation in the software. Ma et al. (2023) highlights that city-scale building energy simulation faces two main challenges: computational cost due to huge number of buildings and data limitations. Modern models address this issue by simplifying calculations or simulating smaller areas. Hence, archetype, which is one of the physics-based approaches used in UBEM studies, categorizes the building attributes of the study area based on their similarities in terms of type, climate, year of construction, size, number of floors, etc. This method aims to achieve a comprehensive analysis of the overall study area by taking each archetype building as a representative of a group of buildings (Ali et al., 2021; Pristerà et al., 2023).

There have also been studies that investigate carbon emissions in city scale, and energy use related carbon using physics-based methods, and some of them developed new tools such as UBIM.io. The overall process requires three roles: sustainability champion, GIS manager, and energy modeler, with eight workflows: feasibility check, project scope definition, GIS data preparation, baseline UBEM construction, baseline model execution, building upgrades creation, scenario analysis, and findings presentation (Ang et al., 2023)

According to the above discussion, previous studies in this area assessed energy efficiency, and carbon emissions on the scales of a building, neighborhood, and city, however, there are less papers investigating the modeling and analyzing carbon emissions in two sections of operational and embodied carbon at the scale of city or even one neighborhood (Ang et al., 2023; Javanroodi et al., 2018; Kamal et al., 2021). Hence, there is a challenge to an integrated assessment of the impact of urban design morphological choices on cumulative emissions, analyzing different densification strategies on a scale of one block of buildings (Allan et al., 2022). The other challenge as discussed earlier in introduction, is to gather an integrated, and accurate input data of all building attributes, as they are not always available for a city on the online municipality sources of the city, and building attribute dataset encompasses just 30-50% of the total number of buildings (Ali et al., 2020; Hoare et al., 2022). Therefore, this research aims to suggest a new workflow to gather input data, for urban carbon emission analysis using data-driven, and object detection methods, and understand the relationship between urban morphological parameters, and carbon emissions on the city scale.

State of Art

Despite previous research in this area which used supervised object detection methods, this study leverages an unsupervised zero-shot machine learning approach to detect buildings and windows in realistic urban street view images of Google map application programming interface (API), ensuring the realism and relevance of data. The approach used in this research is highly scalable, allowing for the extraction of Window-to-Wall Ratios across the entire city of

Baltimore, as well as other urban environments. I believe previous studies to detect buildings by fine-tuning datasets to detect buildings cannot be generalized to all building images while the approach used in this research utilizes the zero-shot learning power of multi-modal transformer-based models which is more reliable in practice (Chundawat et al., 2023).

Research Question

Based on the discussion above, the research questions in the present work are as follows:

1. (Primary) How can the advancements in object detection and zero-shot learning methods be leveraged to collect certain urban building data (such as window-to-wall ratio) that are needed for energy and carbon simulation and modeling?

2. (Secondary) What data integration methods can be used to combine geographical and numerical urban data?

Research Hypothesis

One of the main hypotheses of this research is that the application of object detection methods, especially the ongoing zero-shot large language models development can enhance the building physical attribute extraction for various urban analyses, such as energy, and carbon efficiency analysis.

Accuracy Hypothesis: Zero-shot object detection can achieve a comparable level of accuracy to supervised learning models for the estimation of WWR in urban buildings, while requiring significantly less labeled data, making it more applicable for usage for other untrained, and unseen locations.

Scalability Hypothesis: The use of object detection models will allow for the scalable and automated extraction of WWR data across an entire urban area, providing a cost-effective alternative to traditional methods of urban building parameter collection.

Research Objectives

- Aim 1: Provide a review of the applications of computer vision methods for collecting urban data, specifically for energy modeling.
- Aim 2: Develop a framework to obtain the window-to-wall ratio using available Google Street View Static (SVS) API data.
- Aim 3: Integrate the collected data to develop archetypes and analyze the distribution of window-to-wall ratios across different construction years in two selected neighborhoods.

Background

Figure 1-1 *Baltimore at night from : https://visibleearth.nasa.gov/images/79616/baltimore-at-night.*

Buildings in Urban Context

The study of urban areas is fundamental to understanding the intricate relationships between spatial patterns, cultural dynamics, and economic frameworks that define urban areas (Kropf, 2018). Urban morphology, encompassing the spatial configuration of streets, buildings, and open spaces, serves as a defining characteristic of cities. The layout of roads and buildings directly impacts microclimatic conditions, energy consumption, and the overall sustainability of urban development(Shi et al., 2020). For example, Figure 1-1 presents a nighttime image of

Baltimore, illustrating how roads and buildings contribute to the city's distinctive spatial characteristics.

Moreover, cities consume a significant portion of global energy across various sectors, accounting for approximately 75% of primary energy use and 70% of greenhouse gas emissions (IEA, 2023). Therefore, a comprehensive understanding of spatial patterns is essential for informing sustainable urban planning strategies aimed at mitigating environmental impact, enhancing livability, and promoting equitable development. Among all sectors contributing to greenhouse gas (GHG) emissions in urban areas, buildings account for a significant share, consuming approximately 30% of global energy. They also contribute about 26% of global energy-related emissions, with 8% being direct emissions and 18% indirect (IEA, 2023). Given this, developing accurate methods for evaluating, simulating, and forecasting energy usage in buildings is crucial to achieving low-carbon targets. Such analyses require detailed building characteristics, including information about HVAC systems, internal loads, and construction features, as inputs for urban building energy and carbon modeling.

Window to wall ratio (WWR)

Window-to-wall ratio (WWR), is a metric representing the proportion of the glazed area of a building's façade relative to its wall area, and has a direct impact on energy performance by influencing natural light penetration, thermal comfort, and energy consumption (Valladares-Rendón et al., 2017). WWR has been extensively studied to assess its effect on energy efficiency (Troup et al., 2019). Several studies have investigated its impact on indoor thermal comfort and energy demand. For instance, Chi et al. examined the influence of building orientation on air temperature, velocity, and daylight factors, identifying optimal WWR values for residential buildings(Chi et al., 2020). Similarly, Philips et al., argued that merely reducing WWR is insufficient to meet sustainability goals, emphasizing the need to consider broader façade design implications (Phillips et al., 2020). Furthermore, Xie et al. demonstrated that high WWRs (greater than 0.7) can cause significant indoor overheating during winter daylight hours due to increased solar radiation exposure on south-facing façades (Xie et al., 2022). Therefore, due to the impact of WWR on a building's heating and cooling loads, certain limitations exist on its percentage. For example, according to ASHRAE Standard 90.1, a maximum WWR of 40% is allowed for buildings in Climate Zone 4, which includes Baltimore (ASHRAE, 2000; IECC & International Code Council, 2021).

While building WWR data are critical for the digital representation of urban buildings and energy modeling to support environmental goals (Herfort et al., 2023b), traditional data collection methods are often cumbersome, incomprehensive. As a result, some studies rely on assumed ranges for building envelope characteristics. For example, in an energy modeling study of Boston, researchers adopted a WWR range of 0.10 to 0.80 for each building use type based on recommendations from city consultants, as the required data were not available in urban datasets (Cerezo Davila et al., 2016). In contrast, the methodology developed in this thesis employs machine learning techniques to extract WWR as a continuous numerical variable, avoiding the need to rely on assumed ranges or discrete buckets (e.g., 10%, 20%). This approach utilizes real-world (i.e., unidealized images, making it easier for models to distinguish buildings from their surroundings) Google images, as input data for urban energy, and carbon analysis, ensuring the realism and relevance of the data. To validate the method, I manually calculate WWR and report the associated error.

Zero-shot object detection

Zero-shot object detection (ZSD) is an unsupervised object detection approach that aims to identify object classes that have not been seen during the model's training phase (Bansal et al., 2018). This contrasts with traditional supervised learning, which relies on large volumes of labeled data and multiple training cycles to enable artificial intelligence (AI) models to recognize predefined object classes. While zero-shot learning (ZSL) enables models to understand and perform entirely new tasks, few-shot learning focuses on generalizing from a minimal number of labeled examples.

Unlike conventional object detection approaches that depend on fine-tuned datasets, zero-shot learning offers an alternative by leveraging multi-modal transformer-based models that associate visual and textual representations, enabling them to recognize unseen categories without task-specific training(Minderer et al., 2022). In this research, I selected a zero-shot model to address a novel task: extracting buildings and calculating WWRs, a task for which the model was not specifically trained. This approach allows the model to make predictions in unfamiliar domains—specifically, identifying buildings in various cities to obtain the WWR. By leveraging zero-shot object detection, I was able to bypass the need for an extensive labeled dataset, which is time-consuming, and often a limitation in urban energy modeling studies (Brown et al., 2020). Instead, the model utilizes semantic relationships between object descriptions and image features to infer building components, making it a scalable and adaptable method for large-scale urban analysis.

Chapter 2

Literature Review

Urban data collection

A critical aspect of each urban analysis, especially energy and carbon analysis, is to provide necessary input for accurate simulations. The type and format of input data vary depending on the chosen urban analysis approach, whether top-down or bottom-up. As shown in Figure 2-1, the top-down approach requires historical, socioeconomic, operational, and environmental data, while the bottom-up approach relies on building geometric, non-geometric, and weather data to perform urban analysis (Javanroodi et al., 2023). Data on the spatial characterization of the building's stock is essential to achieve environmental goals set by governments and national energy agencies.

In many cases, however, national and global datasets lack necessary and detailed morphological information required for such analysis (Hecht et al., 2013; Herfort et al., 2023a). In many cases, key building attributes such as geometry, materials, HVAC systems, and occupancy data are missing or insufficiently measured. As a result, many urban energy models rely on mathematically estimated parameters or broad assumptions derived from public datasets, online mapping tools, and national registers (Wate & Coors, 2015). For instance, WWR have often been considered within an acceptable range for energy analysis (Cerezo Davila et al., 2016). In response to such data gaps, researchers have developed computational methods to generate missing data (Reinhart & Davila, 2016). The choice of data collection methods significantly influences the accuracy, quality, and efficiency of analysis. Integrating diverse datasets—including energy use, spatial configuration, and thermal characteristics—requires balancing data availability, quality, and the computational complexity of the modeling approach (Oraiopoulos & Howard, 2022).

In the following paragraphs, I explore the types of data used in urban energy modeling, examine various sources, and discuss approaches to database development with a focus on building archetypes.

The large scale of urban data led to development of various strategies for managing urban-scale analysis. Urban-scale building geometry, such as footprints and heights, can be obtained using Light Detection and Ranging (LiDAR) technology (Y. Li, 2023). Other data sources include websites, application programming interface (API) , and Internet of Things (IoT) data which mostly rely on sensors are mentioned as sources of urban data (Dabirian et al., 2023). IoT refers to a network of physical devices and digital systems that enable real-time data collection and communication. In urban applications, IoT aims to enhance communication and sensing capabilities within and between internal and external environments by systematically collecting data related to environmental variables from building devices and sensors(Mu & Antwi-Afari, 2024; J. Xu et al., 2023). For example, Xu et al. integrated IoT with Building Information Modeling (BIM) to monitor real-time embodied carbon emissions from transportation, equipment, and construction materials (J. Xu et al., 2023). Dabirian et al. developed a flexible framework that combines real-time data from IOT or smart meters, and static data such as building models or occupancy schedules. Their method involves structuring data through a central model (CDM), organizing domain-specific catalogs (Occupancy, construction, and material, greenery system, neighborhood retrofit enrichment, and energy management catalogs), and using import/export mechanisms to interface with different data sources and simulation tools (Dabirian et al., 2023).

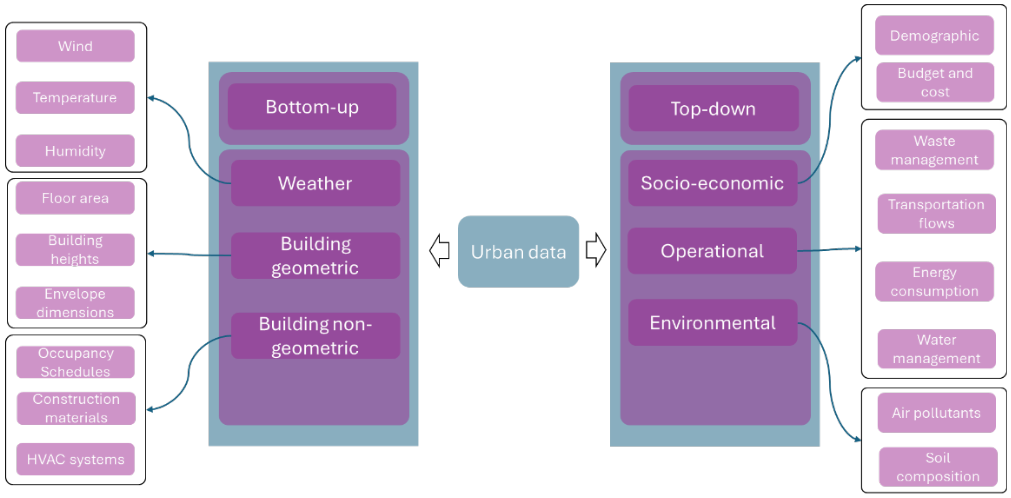

***Figure 2-1** summarizes the types of urban data required for both top-down and bottom-up approaches (Ali et al., 2021; Barns, 2018).*

Traditional relational databases have long been used to store and manage urban energy data. However, as the volume and complexity of urban data increases, more advanced database systems are being adopted. NoSQL databases, for instance, offer greater flexibility in handling unstructured data and can scale up to accommodate growing datasets. Spatial databases, integrated with Geographic Information Systems (GIS), enable the storage and manipulation of spatially referenced data, which is vital for urban energy modeling(Chen et al., 2024). GIS-based urban energy databases offer advantages over traditional database structures:

-Spatial context and visualization

- Multidisciplinary integration

GIS integration allows data to be mapped to specific geographic locations, enabling the visualization of building characteristics and energy use patterns. This helps identify high-consumption zones (Cai et al., 2021) and assess the impact of urban design on energy efficiency(Mutani & Todeschi, 2021; H. Yu et al., 2021). GIS-based urban energy databases can integrate a diverse set of data types, including building characteristics (such as age, type, and materials), energy consumption data, climate information, demographic data, transportation networks, and renewable energy potential. By combining multiple datasets, these systems offer a more holistic view of urban energy systems and their interactions (Bishop et al., 2024).

To effectively conduct urban modeling and simulation, it is essential to understand the types of urban data, their sources, strengths and limitations, and identify which formats are most appropriate for a given analysis. In my research, I primarily work with comma-separated values (CSV) files and shapefiles (SHP) to manage and analyze large datasets using ArcGIS software. However, given the complexity and volume of urban data, in bottom-up physics-based modeling and simulation approach, it is impractical to model each building to model each individual building with its unique characteristics. To overcome this challenge, the concept of building archetypes is used. Archetypes involve categorizing and clustering buildings into representative typologies, which can then be modeled and simulated to represent the entire city. In this study, the WWR extraction results provided insights into different building types in Baltimore. These data were used to develop building archetypes across different construction year intervals, which were then modeled and simulated in Rhino.

Researchers have developed various methods to compile and structure urban data efficiently. A recent approach by Ma et al., 2023 involves creating tiled datasets that divide cities into manageable patches. This method transforms whole-city simulations into distributed patch-based simulations, while incorporating interactions among urban objects. In their study, a dataset was developed for 30 major U.S. cities, encompassing over 8 million buildings, as well as vegetation, streets, and other urban features(Ma et al., 2023). By generalizing buildings into archetypes, these models support a range of applications, including urban energy planning, climate change mitigation, policy evaluation, and building stock retrofit analysis (Shen & Wang, 2024). Key attributes of building archetypes typically include geometry and physical properties, energy systems and equipment, and occupant-related parameters such as schedules. Shen & Wang(2024) categorize important factors for archetypes into four main areas(Shen & Wang, 2024). These four key archetypes are essential for accurately assessing energy performance. Form, refers to the building's structural characteristics such as orientation, number of floors, and floor height, influencing how the building interacts with environmental factors. Operation involves internal building schedules, including lighting, HVAC, and occupancy, affecting energy consumption. Envelope encompasses the external structure, such as walls, roofs, and windows, which impact insulation and heat transfer. Lastly, System includes HVAC types and other building systems that determine overall energy efficiency and sustainability(Shen & Wang, 2024). In this study, I focus specifically on collecting envelope-related properties as inputs for archetype development Common methods for developing archetypes include clustering algorithms, which group buildings based on shared characteristics, and rule-based classification systems, which assign archetypes according to predefined criteria (Colleto & Gomes, 2021; von Behren et al., 2023). Previous studies have demonstrated that the archetype approach can significantly reduce the complexity of urban energy models while maintaining high accuracy in predicting energy consumption patterns (Deng et al., 2023).

However, the effectiveness of archetype method hinges on the selection of appropriate criteria and the availability of detailed building data. An ongoing debate exists regarding the trade-off between the simplicity of archetype modeling and the precision of highly detailed, building-specific models (Dahlström et al., 2024). While archetypes enhance scalability and computational efficiency, they may overlook unique building features that influence energy usage.

One of the challenges in this study was integrating all datasets into a unified framework. To achieve this, it was necessary to identify a shared attribute across the datasets to enable merging. Two potential options were building addresses or spatial attributes (longitude and latitude). The latter proved more reliable, as multiple buildings (e.g., multi-family housing units) often share the same address but represent distinct structures. Therefore, I used the spatial coordinates of building footprint centroids—specifically, their longitude and latitude—to perform a spatial join and integrate all datasets accurately.

Object detection and computer vision

Applications of computer vision in urban analysis

Computer vision encompasses a diverse set of techniques and tasks, including object detection, which involves identifying and locating specific classes of objects within digital images (Zou et al., 2023). In this section, I provide a summary of the applications of computer vision in urban analysis and building energy modeling with a focus on object detection. The integration of object detection methods has gained attention due to their ability to automatically identify and analyze visual data across various fields(W. Li et al., 2020). For instance, object detection has been applied in healthcare and medical imaging to identify abnormalities in medical scans (Litjens et al., 2017), in agriculture to monitor crop health , and in environmental monitoring to detect changes in urban morphology, monitor urban sprawl, and assess the impacts of natural disasters through remote sensing (K. Li et al., 2020). In urban planning and building energy analysis, object detection models have been used for 3D reconstruction of existing buildings (Dino et al., 2020), monitoring construction progress by detecting site activities, identifying thermal insulation damages, and analyzing the thermal performance of buildings (Balaras & Argiriou, 2002). Recent studies have also focused on enhancing object detection accuracy in real-world weather conditions, particularly for urban traffic and mobility analysis (X. Yu & Lu, 2024). While many previous studies have concentrated on using aerial and satellite images for landscape change detection, especially for evaluating green spaces in support of carbon neutrality goals (Qin & Gruen, 2014), advancements in object detection continue to enhance the accuracy and scalability of data collection processes for energy models.

At the building scale, computer vision techniques have been used to create virtual representations of building façades, contributing to the automation of Building Energy Modeling (BEM) workflows through both automatic and semi-automatic methods (Y. Xu et al., 2021). These studies often focus on a single building or limited set of buildings, making it easier to collect the necessary data for modeling and analysis. Such approaches are commonly used for retrofitting evaluations or to support early-stage design through solar and energy performance simulations (Klimkowska et al., 2022; L. Zhao et al., 2021). One common method for façade reconstruction involves 3d laser scanning, which captures and translates measurements of the building into virtual building model (Balsa-Barreiro & Fritsch, 2018; Moyano et al., 2022; Zalama et al., 2011).

Beyond laser scanning, researchers are increasingly using computer vision, a machine learning technique using the computer to “see” and interpret information, to derive façade grammar and automate the detection of building components. Automating building extraction and parsing façades into components such as windows, doors, and walls remains a key research focus in photogrammetry and computer vision (Shahrabi, 2002). Two primary data sources are used in façade element detection: images and point clouds (Sun et al., 2022). Pattern recognition algorithms and grammar-based methods are frequently explored for this purpose. For example, Liu et al. introduced a symmetric loss function to enhance the accuracy of detecting repeating patterns in buildings, enabling more precise parsing of building facades and identification of architectural elements. Their model achieved detection accuracies of 97.6% for windows and 91.7% for walls across five datasets containing images of both historic and modern European architecture, representing improvements of 2.1% and 6%, respectively, over previous approaches. In a follow-up study, Liu and colleagues extended this work by incorporating translational symmetry, which identifies repeating architectural elements at regular intervals, not just mirrored across an axis. While the first study improved façade parsing by applying symmetry constraints during training, the second focused on generating 3dimensional models from 2dimensional images using shape grammars and procedural modeling tools such as Blender (Liu et al., 2021).

At the urban scale, data-driven methods have been employed to extract building information from street-level imagery. Luo et al. (2021) developed a deep learning-based segmentation and photogrammetry approach to generate Level of Detail 1 (LOD1) 3D urban models by combining building footprints from satellite images with height data (Luo et al., 2021). Wendel et al. (2010) proposed an unsupervised segmentation approach to extract individual facades from complex urban scenes by identifying repetitive patterns in images. Their algorithm assumes that facades have horizontal repetition, while separation boundaries are primarily vertical. Segmentation is performed by combining repetitive pattern analysis with superpixel segmentation, using a convex hull of repetitive interest points to improve accuracy and refine facade boundaries (Wendel et al., 2010).

Despite growing interest in computer vision for urban analysis, the application of object detection techniques for extracting WWRs specifically for building energy modeling remains underexplored in literature. This gap makes the proposed pipeline of this study particularly valuable and a key contribution for improving building-level data in cities where traditional data sources are incomplete or unavailable.

Application of Computer vision to obtain WWR

The integration of artificial intelligence (AI), particularly zero-shot learning (ZSL), presents a transformative approach to automating and improving the accuracy of urban data collection. Zero-shot object detection (ZSOD), a subset of ZSL that enables models to detect and classify previously unseen object categories based on semantic description, has emerged as a powerful solution, allowing for the identification and analysis of building features without requiring extensive labeled datasets. Notably, Zachariah et al. (2022) demonstrated the application of ZSL in sustainable building design, addressing the challenge of predicting energy usage for new or previously unclassified building types. Their study leveraged expert-provided side information to develop a ZSL-based method for identifying the closest known building types to a given unknown structure (Zachariah et al., 2022).

Among the various applications of computer vision in building and urban studies, detecting and segmenting windows has gained increasing attention due to its critical role in energy and thermal analysis of buildings. Since window detection aligns with the Level of Detail (LoD3) required for energy modeling, numerous studies across disciplines have explored this task (S. Kim et al., 2016; Sun et al., 2022). However, research specifically targeting the extraction of WWR at an urban scale remains relatively scarce, despite its significance in energy and carbon analysis.

Ghorbany et al. (2024) utilized Convolutional Neural Networks (CNN), specifically Region-based CNN (R-CNN), to extract WWR and analyze window shading for passive house design. Their study employed a supervised deep learning model trained on curated datasets. MohammadiZiazi et al. (2021) proposed a data-driven model to estimate WWR and the number of floors for commercial buildings in a neighborhood in Pittsburgh. Their method leveraged Street View Static (SVS) Google images API to extract relevant building features. De Simone et al. (2023) enhanced window detection using semantic segmentation techniques, including Fully Convolutional Networks (FCN) and SegFormer, to classify windows and façades at a pixel level. Another study aimed to develop a cost-effective method for determining WWR and the air conditioning (A/C) status of existing buildings (Ghorbany et al., 2024; Mohammadiziazi et al., 2021; Philip et al., 2023).

My methodology advances existing methods by employing a more sophisticated approach inspired by recent developments in artificial intelligence and computer vision. Unlike previous studies such as (Ghorbany et al., 2024) that trained their model on curated datasets (i.e., unrealistic, idealized images) such as COCO, I propose a zero-shot (without any training data) design. This approach consists of three main steps. First, it utilizes a multi-modal transformer-based model (OWL-ViT) (Minderer et al., 2022) in the zero-shot manner to detect the buildings in the noisy, realistic Google Street images. As the second step, it then uses the RoboFlow package (Traore, 2022) to extract the window location and their respective bounding boxes. Finally, it aggregates the detected building and window information to compute the WWR.

I believe previous approaches to building detection that use hand-curated datasets to fine-tune Region-based R-CNN on the COCO dataset to calculate bounding boxes cannot be generalized to all building images. Even though this would result in a faster design the model would not generalize to unseen examples and has a high chance of overfitting to the annotation artifacts within the training data (Z.-Q. Zhao et al., 2019). In addition, hand-curating the training dataset is a time-consuming and expensive process that further limits the generalizability of methods that rely on such datasets (Brown et al., 2020). De Simone et al. (2023) enhance window detection for individual buildings using semantic segmentation (Fully Convolutional Networks and SegFormer) to classify windows and façades in images, requiring explicit pixel-level labeling but do not propose a scalable method for city-wide WWR extraction (Simone et al., 2024). Their reliance on manually labeled datasets limits adaptability across diverse urban environments. Also, their approach applies a four-point perspective transformation to reproject images to a fronto-parallel view but struggles with distortions, especially in tall buildings. The approach developed in this research instead utilizes zero-shot learning power of multi-modal transformer-based models which are more reliable in practice (Minderer et al., 2022). RoboFlow's object detection models, especially those based on You only look once (YOLO), are designed to handle different perspectives, lighting conditions, and angles—making them more reliable when analyzing diverse urban environments (*Model & API*, 2024).

Despite previous research that use supervised object detection methods, the present study leverages an unsupervised zero-shot machine learning approach to detect buildings and windows in realistic urban street view images of Google map API, ensuring the realistic and relevant data. The approach used in this research is highly scalable, allowing for the extraction of WWRs across the entire city of Baltimore, as well as other urban environments. I believe previous studies to detect buildings by fine-tuning datasets to detect buildings cannot be generalized to all building images while the approach used in this research utilizes the zero-shot learning power of multi-modal transformer-based models which is more reliable in practice (Chundawat et al., 2023). Table 2-1 summarizes studies on the application of object detection in urban research, with a focus on extracting WWR.

Table 2-1: Studies on the applications of object detection in urban studies with a focus on extracting WWR.

Scope	Authors	Year	Scale	Objective	Method	Data Sources
___	K. Li et al.	2020	Urban	Monitor urban morphology and disaster impacts.	Remote sensing and GIS for morphology analysis.	Satellite images
____	Balaras & Argiriou,	2002	Building	Analyze thermal performance of buildings using object detection.	Thermal imaging and infrared detection methods.	Thermograph images

____	X. Yu & Lu,	2024	Urban	Improve object detection performance under real-world conditions.	Anchor free object detection	Cityscape, Foggy Cityscape, SIM 10K, BDD 100K and KITTI
WWR	Ghorbany et al.	2024	Urban	Data-driven model to extract WWR for passive house analysis	Region-based Convolutional Neural Networks (R-CNN)	COCO dataset
WWR	De Simone et al.	2023	Urban/district	Extract WWR as a computer vision task.	Semantic segmentation (Fully Convolutional Networks and SegFormer) for window detection	Manually labeled datasets for semantic segmentation
WWR	Mohammadiziazi et al.	2021	Urban block	Data-driven model to extarct WWR for energy analysis	Data-driven models to estimate window-to-wall ratio and number of floors	Street View Statics (SVS) and Google Images API

Chapter 3

Methodology

This section outlines the overall methodology, including the process of defining the boundaries of the two neighborhoods and explaining the format of geospatial building data, and the integration of multiple datasets in different formats. It then details the extraction of numerical WWR data from image-based sources using two object detection models, describes the models' properties, and explains their integration within the workflow. The methodology encompasses a series of steps beginning with the aggregation of diverse data to develop a comprehensive dataset of urban building parameter data for the City of Baltimore, using spatial join analysis technique. As part of this dataset, certain building parameter data (such as window-to-wall ratio) for buildings are extracted from available street view statics (SVS) application programming interface (API) in Google Map Street view images. Subsequently, ArcGIS is used to compile and integrate all relevant geospatial and numerical data.

The first step involved defining the boundaries of the selected neighborhoods. To achieve this, I used Shapefile (.shp) containing neighborhood borders in Baltimore, which is publicly available on the OpenBaltimore data portal (Table 3-1, Figure 3-1). A shapefile is a commonly used vector data format in Geographic Information Systems (GIS) for storing spatial features (Hong et al., 2020). It represents geographic areas using points (e.g., city locations), lines (e.g., roads, railways), and polygons (e.g., buildings), all defined through such as longitude and latitude for mapping (Environmental Systems Research Institute, 1998). This format differs from Comma-Separated Values (CSV), which store tabular data and lack spatial structure. Shapefiles can be analyzed and modified using Python libraries such as GeoPandas, which are designed for geospatial data analysis.

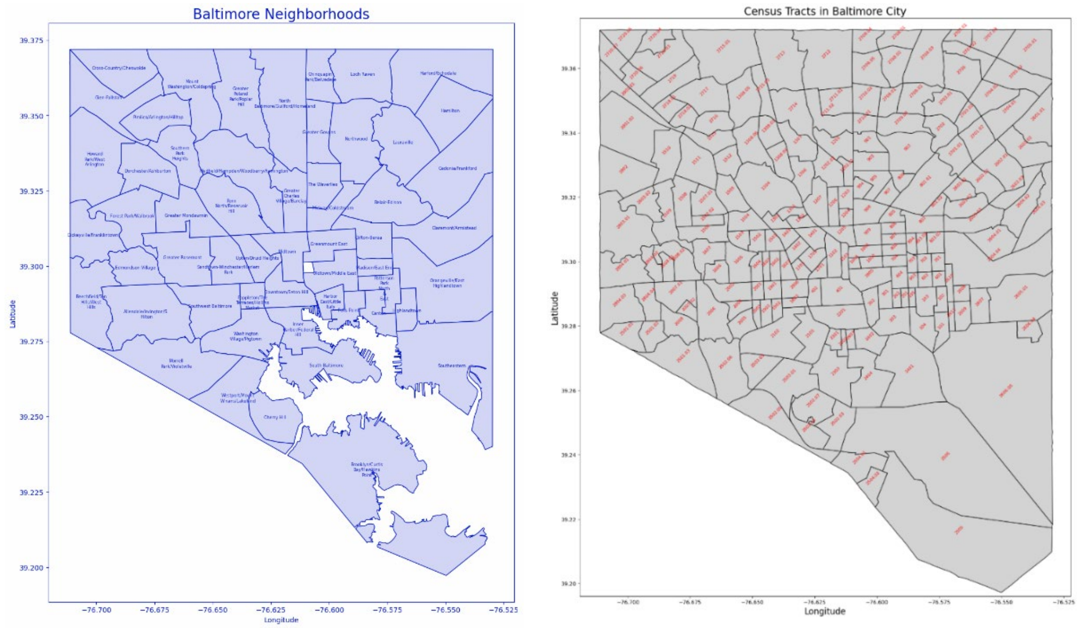

Figure 3-1 *The boundaries of the neighborhoods in Baltimore, as defined by the shapefile obtained from the city's open data portal. These boundaries were used to define the study area, identify residential building locations, and extract corresponding WWR data. Data obtained from: https://gisdata.baltometro.org/datasets/BMC::2020-census-tracts-census-tiger/explore?location=39.311777%2C-76.620338%2C14.65*

In the WWR data extraction method used in this research, WWR was estimated for the entire Broadway East neighborhood (comprising 522 buildings) and the Patterson Park neighborhood (comprising 960 buildings), following the initial round of data cleaning. Also building height data was obtained from Baltimore's Real Property Information database (*Baltimore City Real Property Assessments*, 2024). This dataset, along with WWR and other relevant building attributes, was integrated using each building's geographic coordinates to create a unified spatial dataset.

Table **3-1**: Source of geometrical and non-geometrical building information used in this research.

Types of attributes	**Building attributes**	**Sources**	**Type of data**

Geometrical	Footprint area,	OpenStreetMap building footprint data (*OpenStreetMap*, n.d.)	GIS base data
	Number of floors	Real Property Information of Baltimore (Smeriglio, 2022)	Text
	Window to Wall ratio (WWR)	Street Images from Google Map API	Image
	Building orientation	Real Property Information of Baltimore (Smeriglio, 2022)	Text
Non-geometrical	Year-built, material, zone code, block, parcel, ward, address, direction, longitude, latitude,	Real Property Information of Baltimore (*Baltimore City Real Property Assessments*, 2024)	Text

Data collection

Building and window detection

In the first step of this WWR extraction approach, I retrieved street images of buildings using the Google Street View Static (SVS) API, based on each building's address. I chose to use building addresses, rather than the longitude and latitude of the building footprints, to facilitate the integration of image with building height and non-geometric attributes obtained from Baltimore's Real Property Information database, which also uses addresses as the primary identifier. The geographical distribution of the buildings and data points used as input for the object detection models in Broadway East and Patterson Park neighborhoods is shown in Figure 3-2.

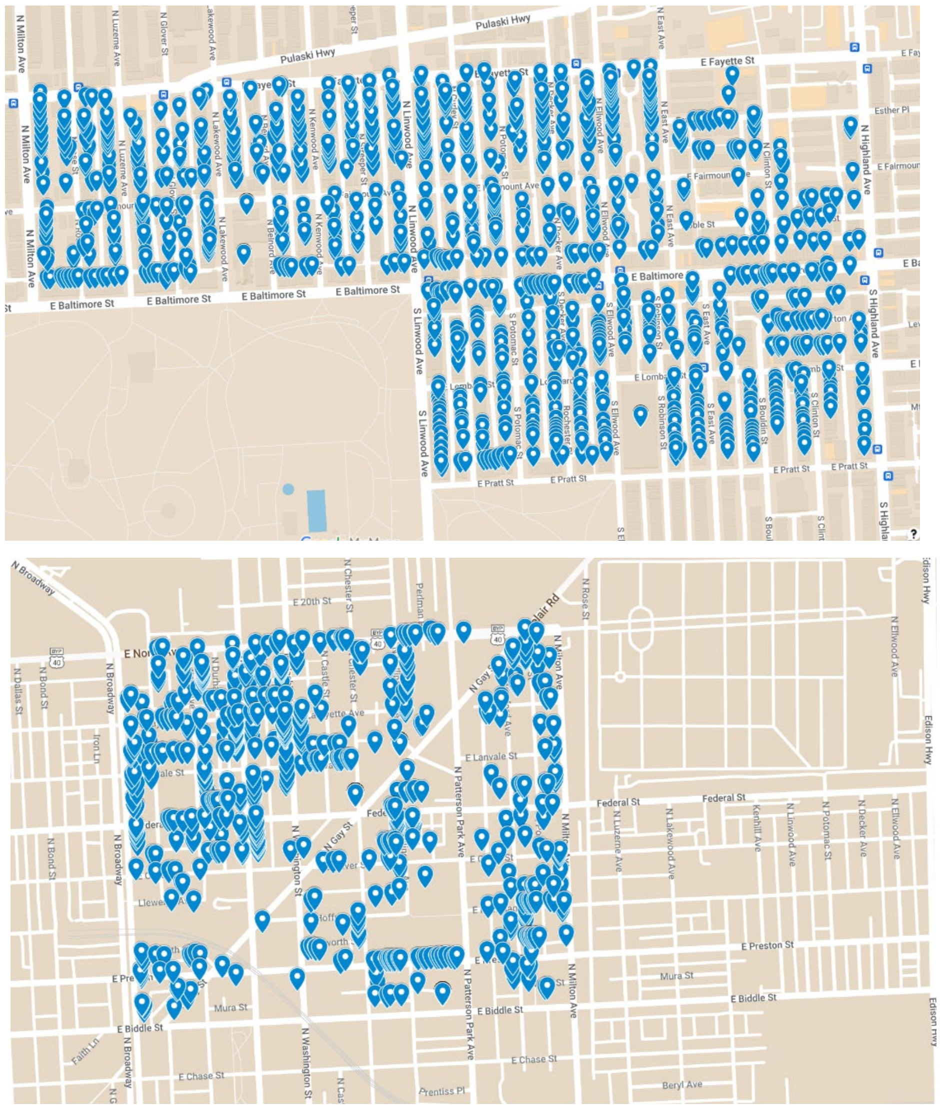

Figure 3-2*: Geographical scope of buildings used for WWR extraction.*

To ensure an unbiased selection process, I used simple random sampling (SRS) for selecting buildings for WWR extraction in each neighborhood. Since my dataset does not have an inherent order, and I did not aim to control specific values or impose spatial constraints (e.g., by zone, or block), SRS was the most appropriate method. This approach guarantees that each building has an equal probability of being selected, preventing biases introduced by clustering or stratification. Figure 3-3 represents the workflow of the WWR extraction methodology, which includes: 1. Scraping Street images from Google Street View Static API, 2. Detecting buildings in each image using Hugging face machine learning model, 3. Cropping the image to the bounding boxes of the detected buildings, 4. Identifying windows using RoboFlow model, and 5. Calculating WWR by computing the ratio of total window pixel area to the corresponding building façade area.

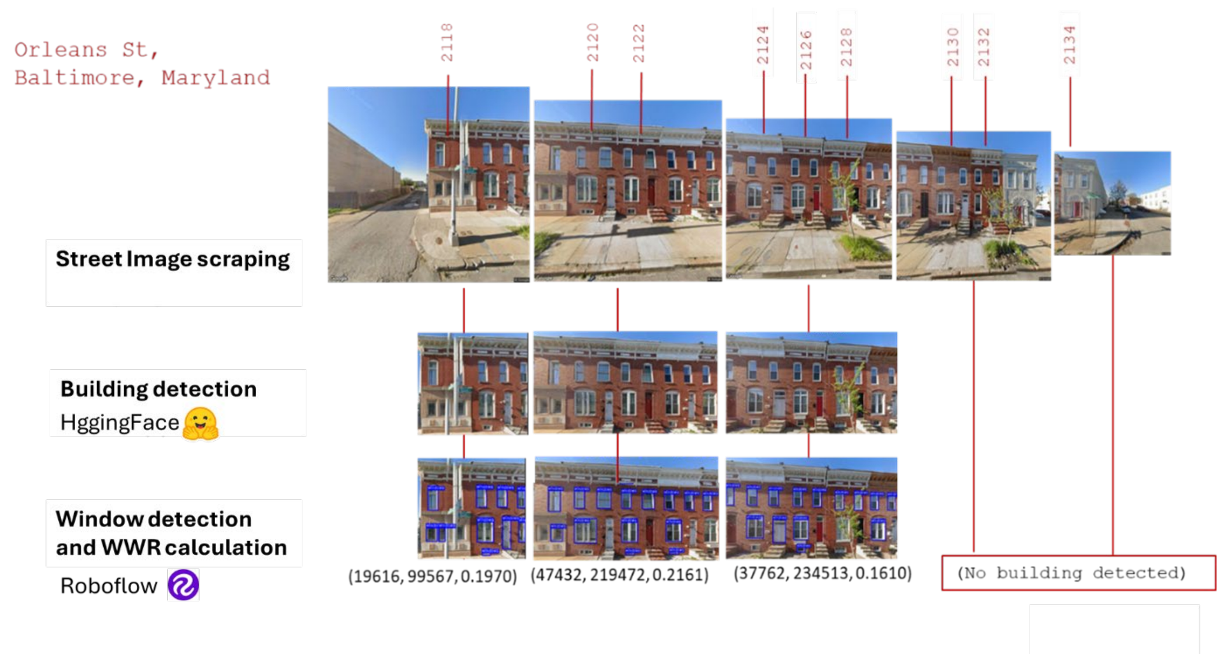

Figure 3-3: *My methodology of WWR extraction, which includes first, scraping street images from Google Streer View Statics API, second using a model to detect buildings in an image, third, crop the image to the bounding boxes of the buildings, fourth identify windows through another ML model, and finally calculate the window area to the building area.*

During the image extraction phase, I defined several key parameters. The Field of View (FOV) was set to 120°, representing the extent of the observable area within an individual image from the 360° panoramic images provided by Google Street View. The heading parameter, which specifies the camera's orientation, was set to 90° to capture side views of buildings effectively

(Figure3-4). Additionally, the pitch parameter was set to 0° to ensure straight-ahead images, minimizing tilted perspectives that could introduce inaccuracies in the calculation of WWR (Table 3-2).

Table **3-2**: Parameters, and assumptions used to obtain building images via the Google Maps API.

Parameter	Description	Value
api_key	Google Maps API key for Street View access	-
location	Address or coordinates (latitude, longitude) of the desired location	-
size	Size of the image in pixels (width * height)	600*300
fov	Field of View angle in degrees (wider view with higher values)	120°
pitch	Up/down tilting angle in degrees (positive for tilting up)	0°
heading	Compass direction of the view in degrees.	90°

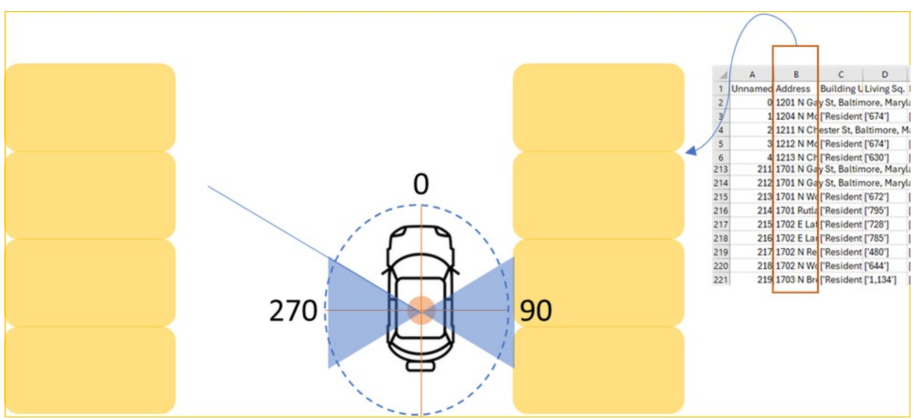

Figure 3-4 *The camera angle was set to 90° to capture buildings' façade.*

I also conducted several unsuccessful trials for WWR extraction by leveraging the saturation differences between glass areas and the surrounding façade, as well as the textural contrast between glass and brick surfaces (Figure 3-5).

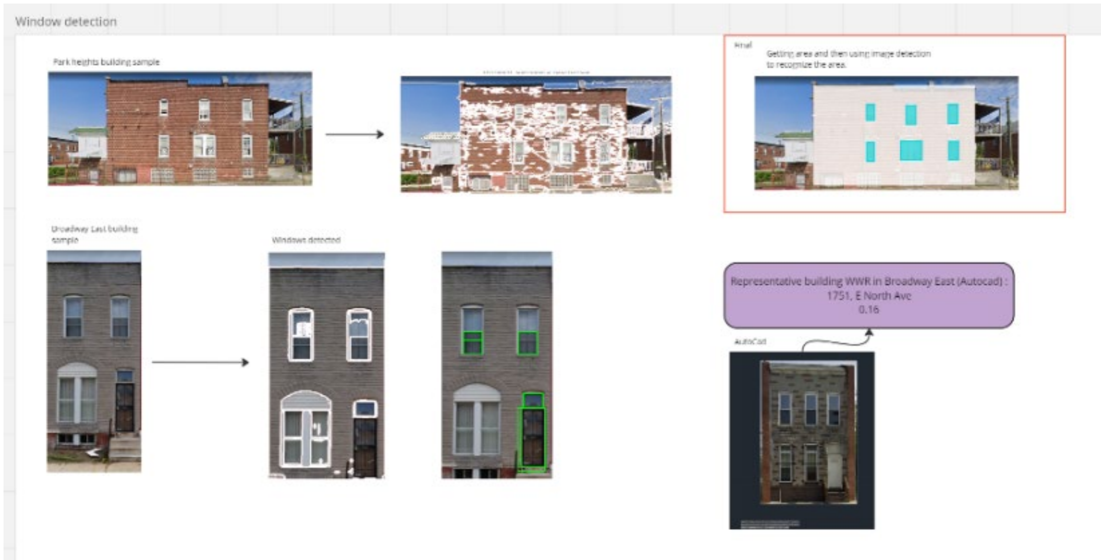

Figure 3-5 *Unsuccessful tries to get WWR through object detection methods, in which I considered the saturation difference of the glass areas with the facade, and difference among the textures of the glass and brick.*

The proposed method includes using two machine learning models, one for building detection and the other for window detection. For building detection, I utilized the Hugging Face model, a publicly available open-vocabulary object detection framework capable of identifying a wide range of object classes within an image (Hugging Face, n.d.; Minderer et al., 2022). For window detection, I used Roboflow, a computer vision platform optimized for high-precision object detection, specifically windows (Traore, 2022). The two models are advanced in one single task (i.e. Hugigng face to detect buildings and Roboflow to detect windows). However, in this work, they are repurposed and integrated into a multi-step workflow. The combined workflow includes collecting street images, applying the two object detection models, and calculating WWRs for buildings at the neighborhood or city scale in a single run of the automated pipeline. The Roboflow model used in this study was trained on approximately 1,018 images and employs Convolutional Neural Networks (CNNs), particularly YOLO (You Only Look Once) family, which produces bounding boxes around objects and is used for real-time object, making them especially suitable for large-scale urban analysis. According to Ouardani (2023), this Roboflow-based window detection model achieves a mean average precision (mAP) of 64.7% and a precision of 68.9% (Ouardani, 2023). Moreover, mean average precision(mAP) of OWL-ViT model of Hugging Face reaches 55.1%, while the best model zeroshot model today reaches 64.3% accuracy on ImageNet dataset(Klingler, 2025). Mean average precision(mAP) is a commonly used metric in object detection to evaluate the accuracy of detecting an object in the image. It is calculated using precision-recall curves and Intersection over Union (IoU) thresholds. The process involves determining precision (true positive rate among detected objects) and recall (ability to identify all relevant instances), then computing the Average Precision (AP) for each class by measuring the area under the precision-recall curve. The final mAP score is obtained by averaging the AP values across all classes. Evaluating mAP at different IoU thresholds helps assess localization accuracy. mAP is widely used in benchmarks like the COCO dataset to provide a comprehensive performance overview (Shah, 2022). Figure 3-6 represents IoU (Intersection over Union), which is defined as:

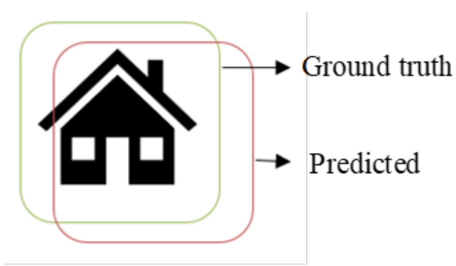

Figure 3-6: Schematic of IOU calculation.

$$IoU = \frac{Area\ of\ Overlap}{Area\ of\ Union}$$

After buildings were detected, the next step involved cropping the image to the bounding box of each building to determine its width and height, which were then used in subsequent WWR calculations. The final step involved computing the WWR by dividing the cumulative area of all detected windows by the area of the corresponding building façade. Since the calculation is a ratio, the unit of measurement is not relevant. The formula used to calculate WWR is:

$$WWR_i = \sum_{i=1}^{n} \frac{(Total\ detected\ window\ area)_i}{(Total\ detected\ building\ area)_i}$$

Where i= number of Google Street View images retrieved per building address, including both the target building and adjacent buildings in the frame. This approach is effective because it analyzes archetypal buildings that represent broader building stock within each neighborhood. To calculate WWR for all four sides of the buildings, I estimated building orientation based on the street address. Orientation was classified as either north-south (N) or east-west (E), depending on the building's alignment relative to the street (Figure 3-7).

WWR for four sides:

Addresses including " E "	Addresses including " N "
E = 0	E = Calculated via WWR extraction
W = 0	W = Calculated via WWR extraction*
N = Calculated via WWR extraction	N = 0
S = Calculated via WWR extraction*	S = 0

*Backyard façade WWR has been considered the same as the front.

Figure **3-7**: Schematic of identifying WWRs for each side of the buildings.

Data integration

Spatial join

To combine all available data on building information, I performed a spatial join to merge geometric and non-geometric attributes. These included building footprints, year built, residential building type, window-to-wall ratio, construction materials, and number of floors (used to estimate height). The spatial join was conducted in ArcGIS, linking building polygons (footprints) with building point data (Real Property Information) using the longitude and latitude coordinates of building centroids. Building footprints were sourced from OpenStreetMap, while non-geometric attributes, such as residential building type, were obtained from the Open Baltimore website ("OpenStreetMap," n.d.; Smeriglio 2022). The merged dataset formed the basis for the next stages of the study: developing building archetypes and modeling in Rhino. This methodology is consistent with previous studies, such as Abolhassani et al. (2022), who integrated building characteristics in Montreal by linking CityGML files with building footprints using shared coordinate attributes. Similarly, in this research, various shapefiles were spatially joined using building geometry and address-based attributes (Abolhassani et al. 2022).

As described earlier, buildings in this method are identified using their addresses, along with their polygon geometry from OpenStreetMap. While OpenStreetMap generally includes building geometry and height, one of the major challenges in this research was the lack of building height information. To address this, I supplemented the data with the number of floors and other attributes, such as construction year, usage type, and materials, obtained from Baltimore's municipal real property database (Table 3-1). To handle missing data, a combination of elimination and estimation methods was applied. Buildings with missing or incomplete real estate data were excluded, while missing construction years were estimated by assuming alignment with neighboring buildings’ construction dates.

Validation:

The validation of machine learning models requires careful selection of evaluation metrics aligned with the task’s objectives. In object detection tasks, as described in the methodology section, common evaluation metrics include mAP and IoU, which assess a model's ability to correctly classify objects within an image (Shah, 2022). These are based on confusion matrix components such as true positives and false positives and are widely used in classification-based tasks, like detecting windows or façades (Shah, 2022; Ultralytics, 2024). However, the present research does not solely focus on object classification; rather, it involves a regression analysis that predicts continuous values (WWRs of the buildings). Unlike object detection tasks that contain discrete classifications, WWR estimation involves numerical predictions, making precision-recall-based metrics less suitable for assessing model performance. Instead, Mean Absolute Error (MAE) and Mean Squared Error (MSE) is commonly used in regression problems to quantify the difference between predicted and actual values (aldean, 2023). A schematic of a regression model and calculation of MSE, and MAE has been shown in Figure 3-8.

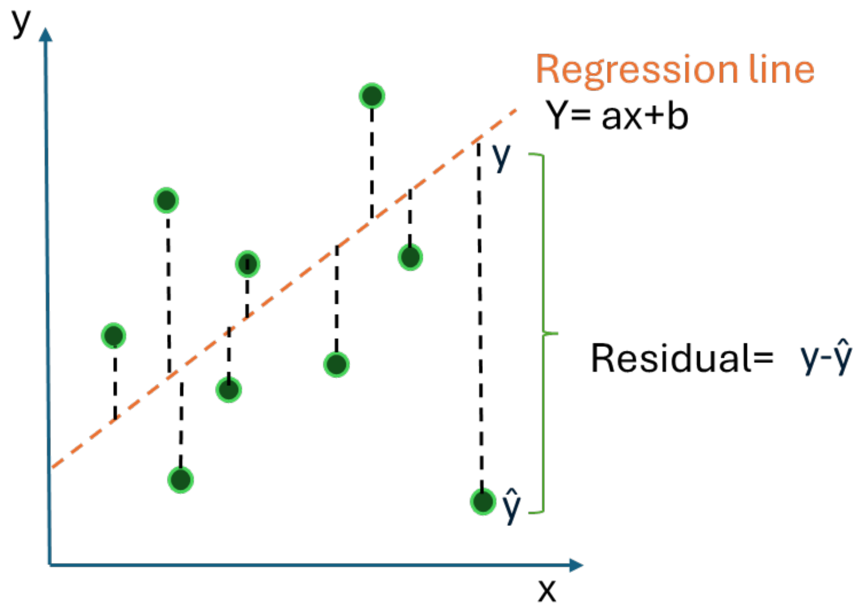

Figure 3-8*: Linear regression, y as the actual value (true value), and ŷ as the predicted value.*

To ensure the evaluation dataset was representative, I applied stratified random sampling following a two-phase data cleaning process; before running the model, to eliminate duplicate addresses, and after running the model, to remove cases with no building detected or high errors. The elimination of duplicate addresses and missing values ensured that only valid building records were included in the validation phase. A critical aspect of this validation strategy was the exclusion of buildings with undetectable WWR values due to image occlusions, tree cover, or missing façade details in Google Maps imagery. By filtering out such cases, the validation dataset contained only buildings where WWR could be meaningfully compared against manually measured values from AutoCAD. This manual verification step was essential in establishing a ground truth benchmark, enabling an accurate evaluation of model performance. As shown in Figure 3-9, I imported selected building images and measured the areas of both the facades and the windows to calculate the ratio of window area to facade area. To minimize selection bias, I used a 10% validation split and set a fixed random state (42) for reproducibility. The final validation sample consisted of approximately 50 buildings, representing a range of WWR values across both neighborhoods. After calculating MSE, MAE, and MRE, I removed the top 10% of data points with the highest residuals to reduce the influence of outliers and improve accuracy.

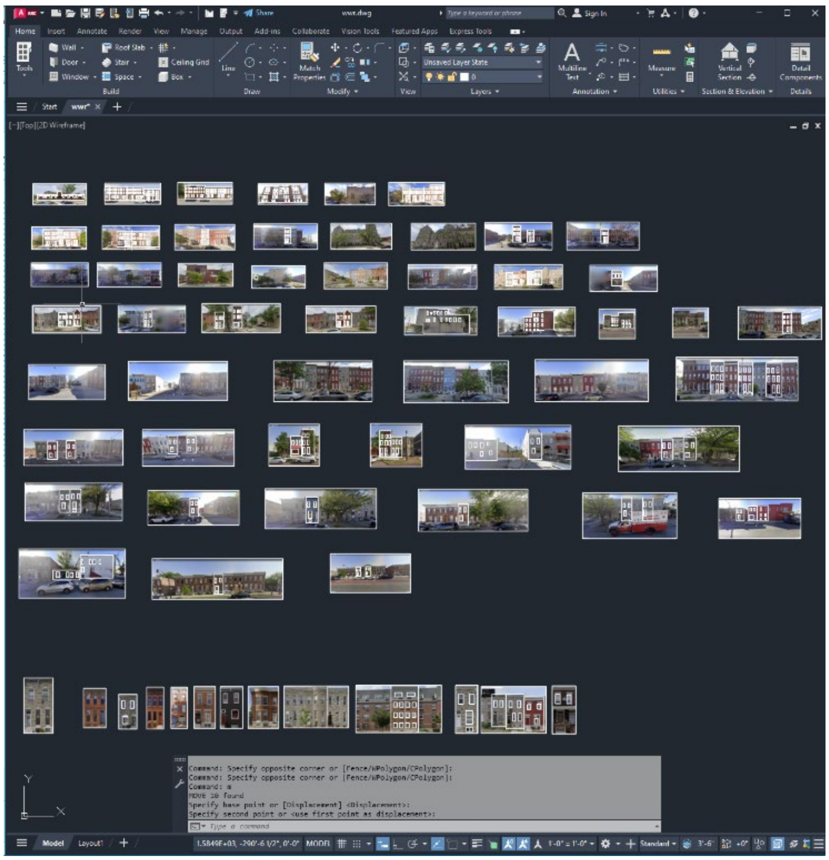

Figure 3-9 *Validation of the data by manually calculating WWRs in AutoCAD.*

MSE measures the average squared difference between predicted and actual values. To guarantee the accuracy of results, minimizing the error is the target and less MSE represents the more reliable model (Harish Babu & Venkatram, 2020). To calculate MSE, I used the following formula (Tiwari, 2022):

$$\mathrm{MSE} = \frac{1}{n}\sum_{i=1}^{n}(y_i - y_p)^2$$

Where y_i is the actual value calculated in Autocad, and y_p is the predicted WWR from the object detection models. Also, n is the number of data points which in this case is the number of calculated WWRs. The range of MSE is between 0, and +∞, which uses L^2 norm, and considers fewer outliers in the error calculation, making it suitable for this research (Chicco et al., 2021; Tyagi et al., 2022). Other metrics I used to analyze the performance of the model were Mean Absolute Error (MAE), and Mean Relative Error (MRE), which I used the following formulas to calculate them:

$$\text{MAE} = \frac{\sum_{i=1}^{n} |y_i - y_p|}{n}$$

$$\text{MRE} = \frac{1}{n}\sum_{i=1}^{n} \frac{|y_i - y_p|}{y_i}$$

Which y_i is the actual value calculated in Autocad, and y_p the WWR calculated using object detection models. Figure 3-8 illustrates the regression model, y predicted, and y actual.

Archetype

Housing Typologies

To perform urban energy modeling, a critical step is the definition of building archetypes with their corresponding physical characteristics. Archetyping simplifies the complexity of a city’s building stock by grouping buildings into representative categories based on attributes such as construction era, form, and material properties (Shen & Wang, 2024). Using extracted building data from Baltimore, I performed an archetyping study on the city's residential buildings. The analysis of Baltimore’s building attributes revealed that more than 50% of the residential structures were constructed before 1940, a period when no formal building codes or insulation requirements were in place. To contribute to this process, I conducted an analysis of grouping extracted WWRs to understand their distribution in different construction times. This study specifically focuses on WWR archetypes within two neighborhoods: Broadway East and Patterson Park.

Chapter 4

Results and analysis

WWR Extraction and Model Performance

In this study, I leveraged machine learning techniques to extract and analyze building characteristics at an urban scale. Specifically, I used object detection techniques of zero-shot learning to collect WWR data from Google Street Images with a high accuracy rate, as demonstrated by an MSE 0f 0.0013 when compared to actual ratios calculated in AutoCAD. The value of MSE should ideally be close to 0 to minimize error, ensuring the reliability of the model's predictions (Harish Babu & Venkatram, 2020). Therefore, the result confirms the reliability of the data-driven approach for use in urban building energy modeling. Table 4-1 represents the total number of buildings in the neighborhood, number of building addresses used as input, and the percentage of successful WWR extractions. Overall, the model extracted WWRs for 52.91% of buildings across both neighborhoods. Some buildings were not processed due to occlusions, poor image quality, or missing Google Street View data.

Table 4-1: Percentage of total data points calculated by the model

Dataset	Percentage of WWR extraction	Number of building addresses	Total number of buildings in the neighborhood
Broadway	49.65%	640	4,629
Patterson	57.94%	991	6,381
Overall across two dataset	52.91%	1831	11,010

The performance of the WWR extraction model, evaluated using regression analysis metrics, is presented in Table 4-2. These results assess the model's accuracy in estimating WWR from Google Maps imagery. The first column shows the initial results obtained without any preprocessing to remove extreme outliers. These outliers are primarily associated with building occlusions in Google Maps imagery, and potential distortions due to variations in perspective and resolution. The presence of such anomalies negatively impacts the model's predictive accuracy, inflating error metrics. To improve the model's robustness, the second column shows results after eliminating the upper 10% of outliers, which correspond to extreme deviations. By filtering out these high-error cases, the refined analysis demonstrates a substantial reduction in error metrics, indicating a more realistic performance of the predictive model.

Table 4-2: Performance metrics of the model

Metric	**Value**	**Value (After removing 10% outliers)**
Mean Absolute Error (MAE)	0.0839	0.0262
Mean Squared Error (MSE)	0.0418	0.0013
Mean relative error	___	16.85%

The predicted values, actual values, and residuals are shown for a total of 50 data points for validation (Removing 10% upper outliers) for both neighborhoods (Figure 4-1). This graph provides a direct comparison between the model's predicted WWRs (blue bars) and the actual WWRs (orange bars). The actual WWRs for Broadway East range from 0.07 to 0.28, as illustrated in the graph. The predictions generally follow the trend of the actual values, indicating that the model effectively captures the variations in WWR. Figure 4-2 visualizes the residual errors for validation sets in both neighborhoods, which are the differences between the actual

WWR values (ground truth from AutoCAD) and the predicted WWR values (model output). Positive residuals indicate overestimation by the model, while negative residuals indicate

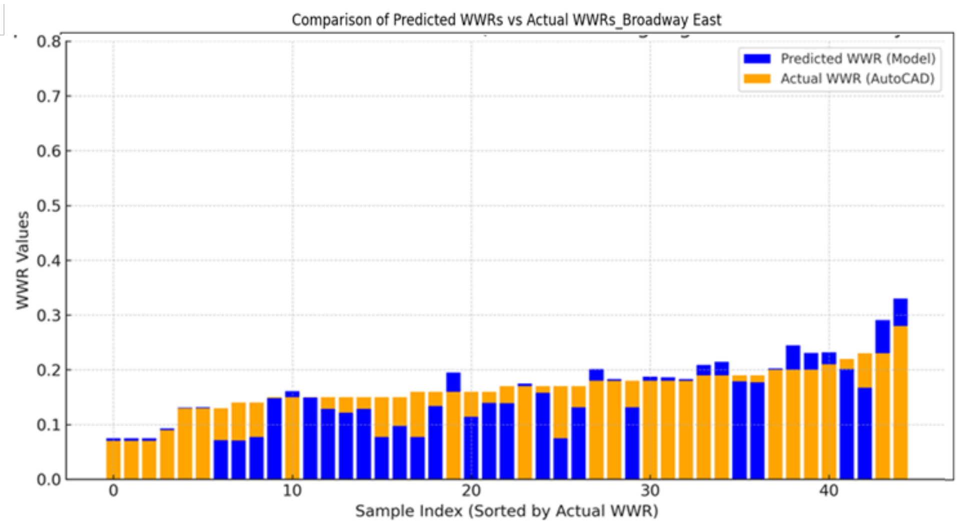

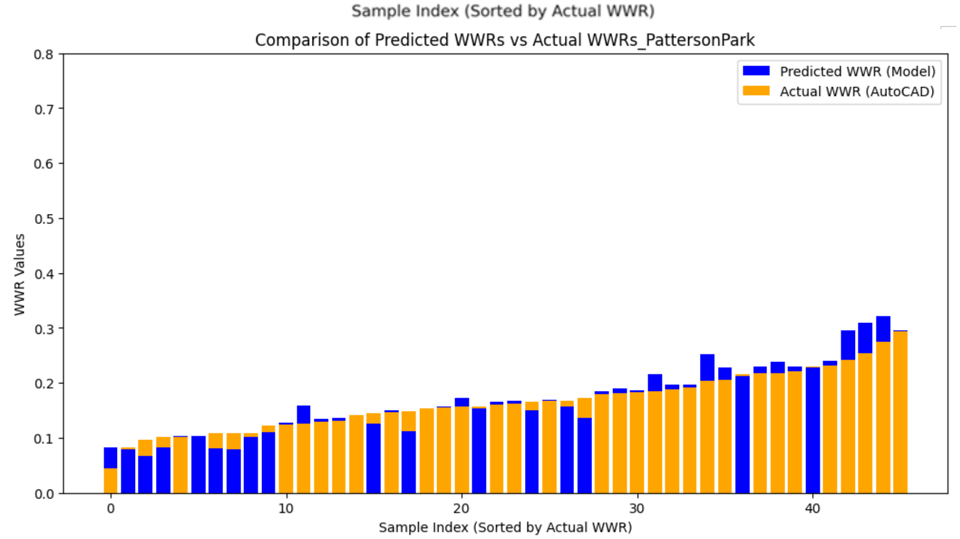

Figure 4-1 *Comparison of predicted WWR vs actual WWRs after removing high errors across the two neighborhoods.*

underestimation. The residual errors appear randomly distributed across the dataset, which is a positive indicator that systematic bias is minimal. Despite some variations, most residuals are centered around zero, implying that removing the high-error cases has improved model stability.

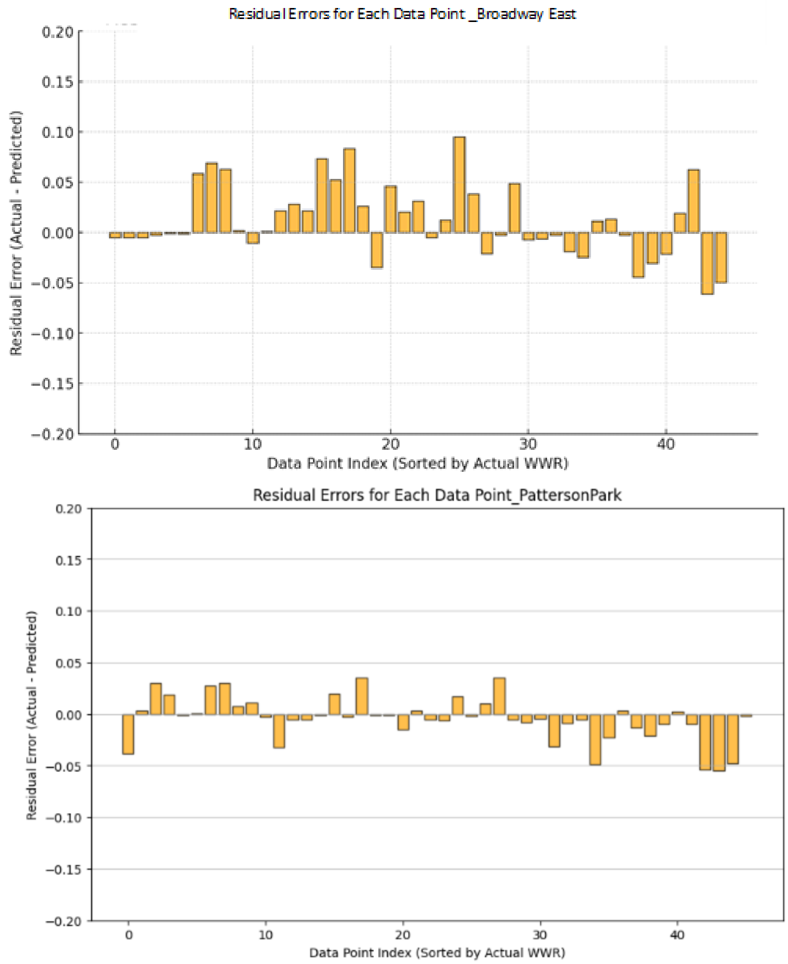

Figure 4-2 *The residual errors shown in the image (difference between predicted, and actual values) for Broadway East, and Patterson Park neighborhoods.*

Figure 4-3 illustrates the buildings in Broadway East, highlighting those with successful versus unsuccessful WWR detections by the model.

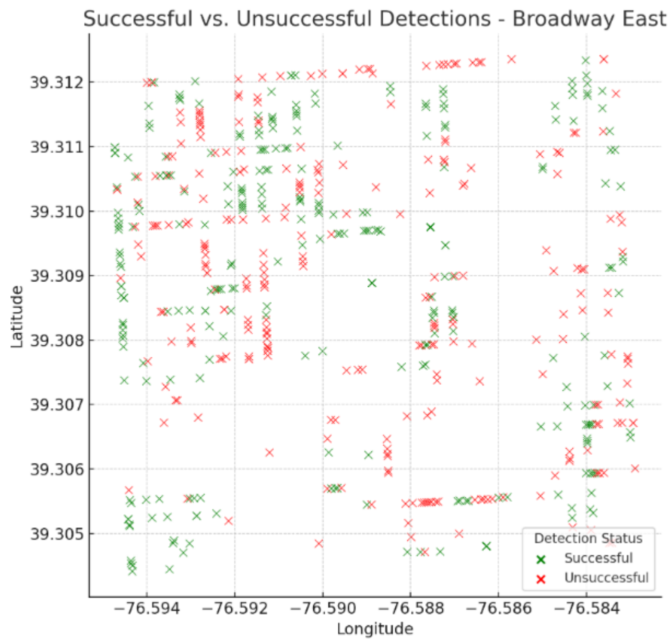

Figure 4-3 *A sample map of one neighborhood with successful vs unsuccessful detections by the model.*

WWR Distribution by Construction Period

In the following analysis, I examine the distribution of WWRs across the two selected neighborhoods, categorized by their respective construction years.

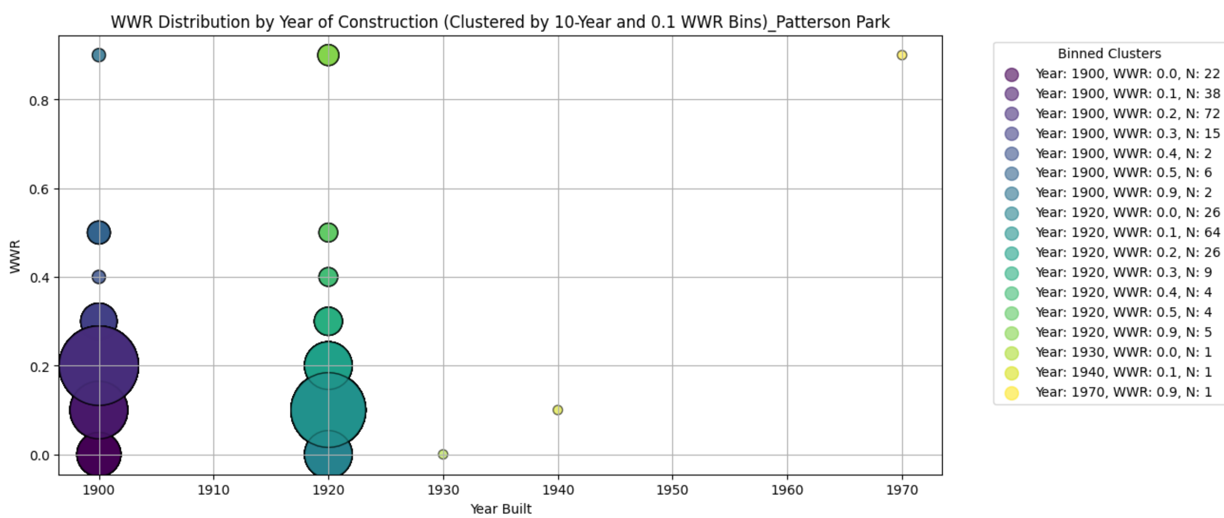

Figure 4-4 *The figures illustrate WWR distribution in the Broadway East neighborhood, and Patterson Park. Data is clustered into 10-year intervals for construction years and .0.1 bins for WWR values, with the size of the bubbles representing the number of buildings within each cluster. The visualization reveals that most buildings in the neighborhoods have a WWR below 0.2 (20%), indicating a predominance of low window-to-wall ratios across different building ages.*

The analysis of WWR distribution in the Broadway East neighborhood provides key insights into the architectural characteristics and energy performance of the area's building stock. The visualization reveals that over 500 building addresses were analyzed, out of which WWRs for approximately 251 buildings were successfully calculated using the designed pipeline in this study. The remaining buildings were either not detected due to the model limitations or were occluded, preventing accurate WWR calculation. The data is clustered into 10-year intervals for construction years and 0.1 bins for WWR values, with bubble sizes representing the number of buildings in each cluster, while color variations distinguish different bins. The most striking observation is that the majority of buildings exhibit a WWR below 0.2 (20%). The results (Figure 4-4) show that most of the studied buildings in this neighborhood, which were constructed prior to 1940, have WWR values below 0.2. The chart further highlights that as construction years increase, WWR values remain predominantly low, with very few buildings exceeding 0.4 (40%) WWR.

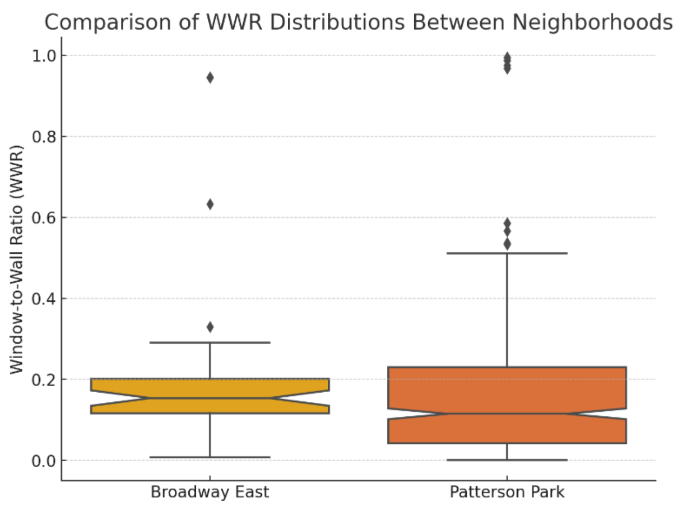

Figure 4-5 *Comparison of WWR distribution between neighborhoods.*

The MAE was calculated to be 0.0839, indicating that, on average, the predicted WWR deviated by approximately 0.08 from the actual values. This level of deviation suggests a reasonable degree of accuracy in the model's estimations. Furthermore, as mentioned earlier, the MSE was determined to be 0.0418 before removing outliers, and after removing 10% of upper high outliers it decreased to 0.0013, which reflects a relatively low level of overall error. Given that MSE penalizes larger errors more heavily than MAE, this result confirms that substantial discrepancies between predicted and actual values were minimal. To assess the variability of errors, the standard deviation of residuals was found to be 0.2003, suggesting a moderate spread in prediction errors. This metric indicates that while most predictions were relatively close to actual values, some outliers or instances of misclassification may have contributed to larger deviations. These variations could be attributed to factors such as occlusions in street-view images, perspective distortions, or challenges in object detection accuracy. For Broadway East, the confidence interval ranged from 0.1480 to 0.2670, while for Patterson Park, it ranged from 0.1483 to 0.1781. The narrower confidence interval for Patterson Park suggests a more consistent distribution of WWR values across the neighborhood, whereas Broadway East exhibits a wider range, potentially reflecting greater architectural variation or inconsistencies in detection performance. This difference is also evident in the boxplot analysis, where Broadway East demonstrated a more dispersed distribution of WWR values compared to Patterson Park, which exhibited a more concentrated clustering. These findings highlight the need for further refinement of the object detection model to improve consistency, particularly in areas with more varied architectural styles or greater image occlusions (Figure 4-5).

Figure 4-6 presents spatial distribution and histogram analysis of WWR values in Patterson Park and Broadway East. The heatmaps illustrate WWR variations across detected buildings, where lighter blue areas indicate higher WWRs, which, upon further analysis, were found to correspond to newer apartment constructions. The histograms show that most buildings have WWRs below 0.2, with a peak around 0.1–0.2.

Figure 4-6 *Distribution of WWRs and heatmap of them across the two neighborhoods*

The analysis of WWR distribution across different construction periods in Patterson Park reveals a significant concentration of buildings constructed in the early 20th century, particularly in 1900 and 1920. These two periods account for most of the dataset, with a combined total of 291 out of 294 buildings (~99%) (Figure 4-4). In contrast, the number of buildings constructed in later years, specifically 1930, 1940, and 1970, is significantly lower, with only one building recorded for each of these decades. A key observation from the dataset is that most buildings exhibit low WWR values (≤0.2). In the 1900 construction period, the most prominent clusters fall within WWR bins of 0.1 (38 buildings), and 0.2 (72 buildings). Similarly, for buildings constructed in 1920, the largest WWR clusters are 0.1 (64 buildings) and 0.2 (26 buildings). This trend suggests that earlier construction practices in the neighborhood had lower WWRs. Higher WWR values (≥0.4) are notably less common. However, a small number of buildings from 1920 exhibit WWR values of 0.4 (4 buildings), 0.5 (5 buildings), and 0.9 (5 buildings), indicating the presence of structures with larger window-to-wall ratios within that period. The only building constructed in 1970 also exhibits a WWR of 0.9, making it an outlier in the dataset (Figure 4-4).

The comparison of the distribution of WWR distribution in 90% sample versus that of 10% for each neighborhood has been represented in Figure 4-7 for the two neighborhoods. In both cases, the distributions are shown after excluding outliers to ensure a more realistic comparison. The Broadway East neighborhood exhibits a broader spread in the sample WWRs, with a noticeable skew toward higher values, while the validation data appears more concentrated

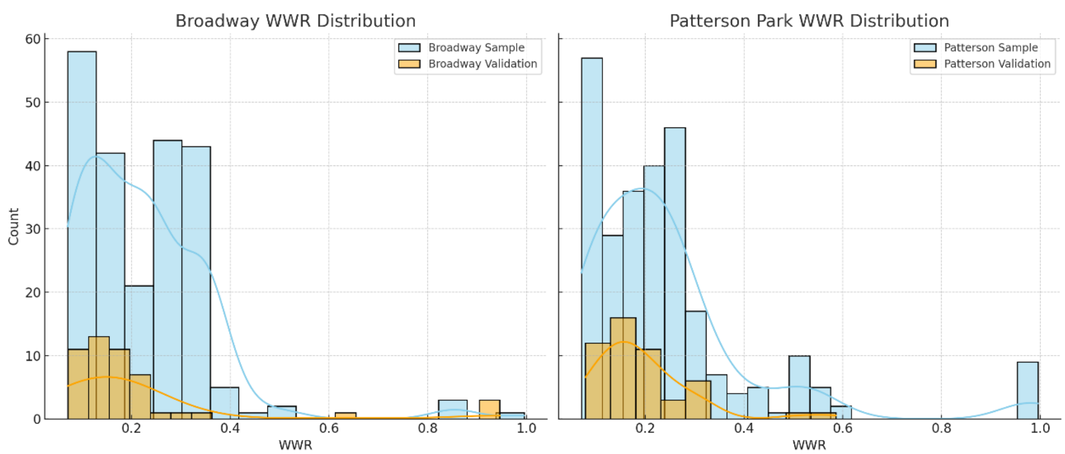

*Figure **3-7** Comparison of WWR distributions between the 90% model-predicted sample and 10% manually validated data for Broadway East and Patterson Park neighborhoods.*

in the mid-range of the distribution. In contrast, the Patterson Park neighborhood shows a more consistent alignment between sample and validation WWRs, with both distributions closely following a similar pattern and range. This alignment indicates that the training data in Patterson Park accurately reflects the underlying characteristics of the buildings used for validation.

Additional Analysis: Height, Age, and WWR

In another analysis, I used the integrated data to compare building height and WWR across Patterson Park and Broadway East. The results show that in both neighborhoods most buildings have two stories with WWR values predominantly below 0.2, with a few outliers.

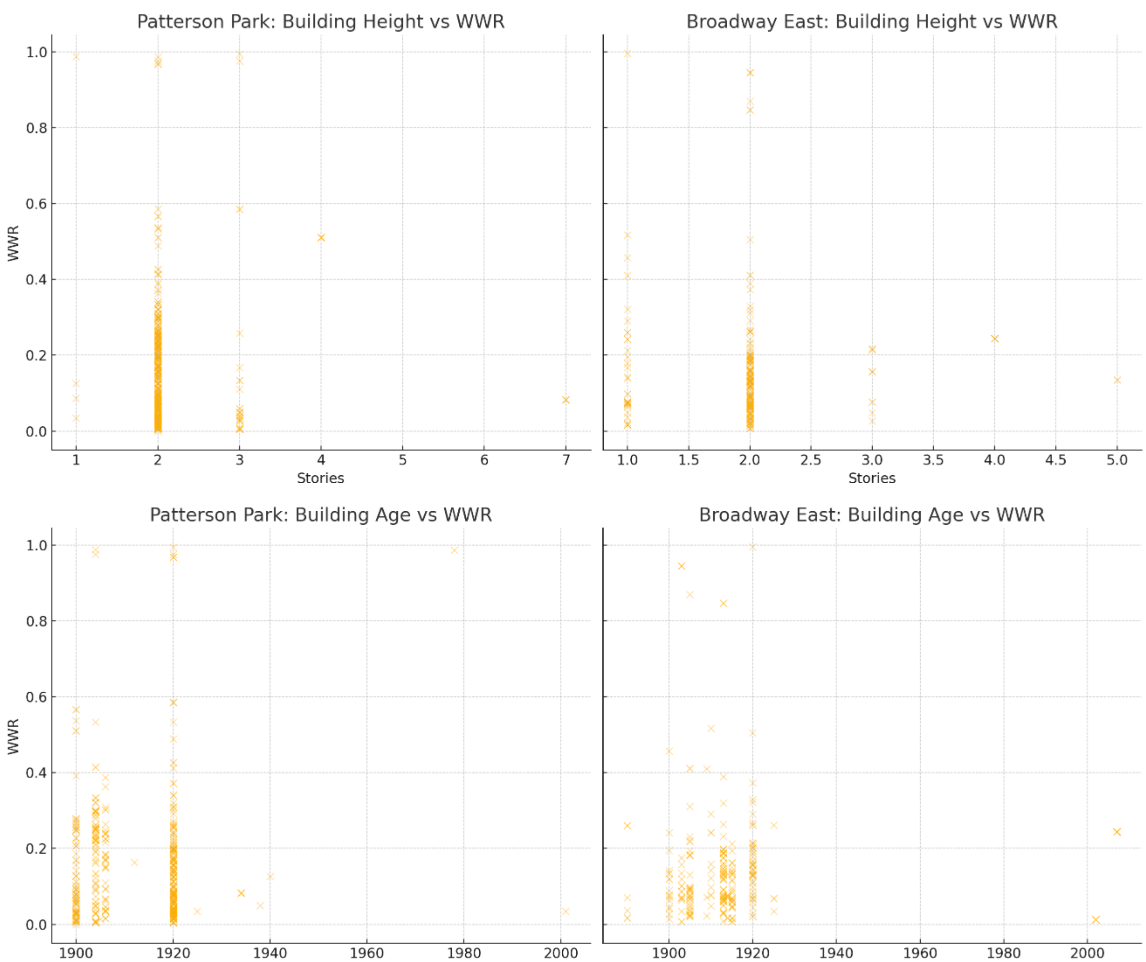

Figure 4-8 *The scatter plots compare WWR against building height (stories) and age (year built) for two Baltimore neighborhoods, Patterson Park and Broadway East.*

Broadway East exhibits a wider range of building heights, but the majority still cluster around two stories, similar to Patterson Park. The building age vs. WWR plots indicate that most buildings in both neighborhoods were built before 1940, with WWR values mostly concentrated between 0.1 and 0.4. A few data points appear beyond the 1980s, likely representing more recent constructions or renovations with different window-to-wall configurations. The overall trend suggests that older buildings tend to have lower WWR values, while some newer structures or modified buildings may incorporate larger window areas, leading to a higher WWR. This analysis highlights that WWR varies with both building height and age, with most buildings maintaining low to moderate WWR values (Figure 4-8).

As shown in Figures 4-4 and 4-8, there are buildings for which the predicted WWR is close to zero. Further investigation revealed that some of these buildings are either damaged structures or vacant buildings lacking windows. Consequently, the amount of glazing relative to the opaque areas of the façade is very low, resulting in a lower WWR. This result also highlights the accuracy of the proposed model in this research, as it successfully identifies buildings with missing or significantly reduced glazing.

Chapter 5

Conclusions

In this study, I present a framework for the automatic calculation of the WWR, an essential metric for various building and urban analyses. One of the key advantages of this workflow is its scalability, enabling the extraction of WWR data across entire cities. This approach enhances data-driven analysis of urban and building-related carbon emissions by leveraging computer vision techniques to enable faster, cost-effective assessments, replacing traditionally labor-intensive, on-site methods (Marasinghe et al., 2024; Whitehurst et al., 2021). I developed a pipeline using two zero-shot object detection models from Hugging Face (An open-vocabulary model capable of recognizing previously unseen objects) and Roboflow for window detection. Unlike typical object detection tasks, the output of this model is a continuous variable, positioning the task as a regression analysis. I evaluated the model's performance using standard regression metrics, including MSE, MAE, and MRE.

Zero shot detection might have accuracy limitations compared to fine-tuned models. However, I selected ZSD for its scalability, generalization across diverse urban environments, and reduced dependency on extensive labeled datasets. Training a fine-tuned model for WWR extraction would require an extensive manually labeled dataset of windows and walls, which is time-intensive and costly. ZSD eliminates this requirement by using large-scale pre-trained multi-modal models, reducing the need for extensive human intervention. Fine-tuned detectors are typically specialized to the data they saw. If a model is trained on facades from one city or a particular style, its performance may decline on a markedly different style unless those were represented in training. Therefore, fine-tuned models deliver customized accuracy and efficiency when sufficient training data is available, whereas zero-shot models unlock quick deployment across diverse cities with minimal preparation. My approach is novel in that it bypasses the need to manually label thousands of images by using pretrained zero-shot object detection models.

The proposed model achieved an MSE of 0.0013, suitable for evaluating continuous predictions. This metric is particularly suited for regression-based tasks where continuous numerical outputs are involved. In contrast, the CNN-based approach previously reported in other paper reports 81.25% accuracy for detecting WWR-Fixed (Ghorbany et al., 2024). This metric measures how often the model correctly classifies fixed windows but does not directly quantify how close the predicted WWR values are to the ground truth on a continuous scale. Since MSE and classification accuracy measure different aspects of performance, direct comparison is difficult. However, I believe that a model validating WWR as a continuous numerical value rather than identifying the bucket of the classifications of windows provides more reliable and precise results for regression-based WWR estimation.

There were also limitations in this work. One limitation encountered in this study relates to the fixed camera headings in Google Street View imagery, which contributed to performance outliers (Figure 5-1). As shown in Figure 5-1, predicted values, actual values, and residuals are presented for 50 validation samples from the Broadway East neighborhood. However, a notable discrepancy between the predicted and actual values is observed for four data points (Figure 5-2). Upon further investigation, it was found that the images for these addresses depicted streets with less visible buildings, leading to the entire image being misclassified as windows. As shown in Table 5-1, the fixed heading angle of the Google Maps camera caused certain images to capture more street elements rather than clear building facades, resulting in outliers, which may not always align with the optimal perspective for capturing building facades. Future Analysis includes addressing the deficiency of this model in the case of fixed angles which capture streets rather than buildings.

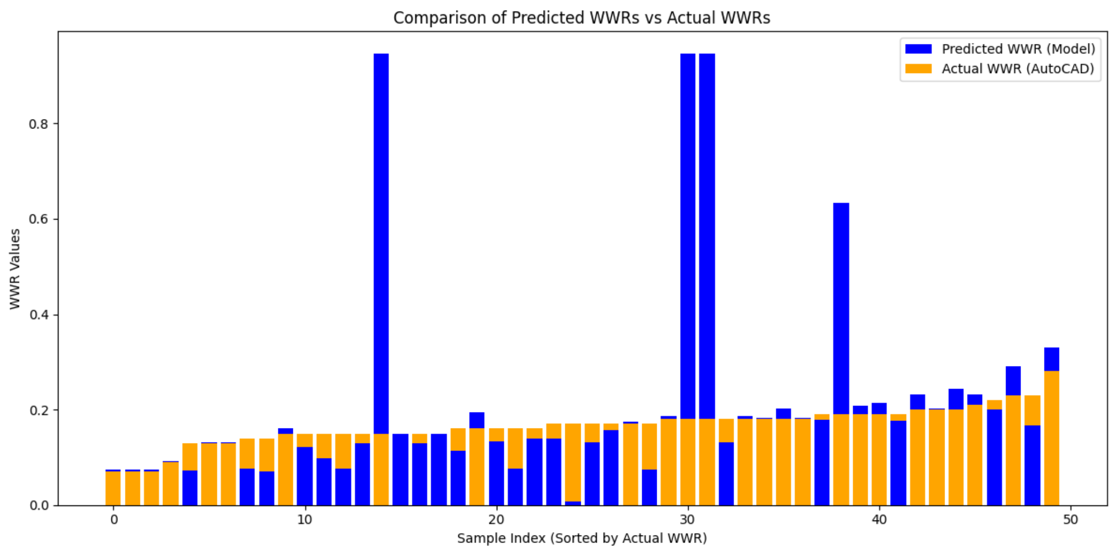

Figure 5-1 *Comparison of Predicted and Actual WWR before removing high errorss: The chart displays the predicted WWR values (blue) generated by the model versus the actual WWR values (orange) calculated in AutoCAD. Discrepancies highlight errors and outliers where the model identifies streets as buildings.*

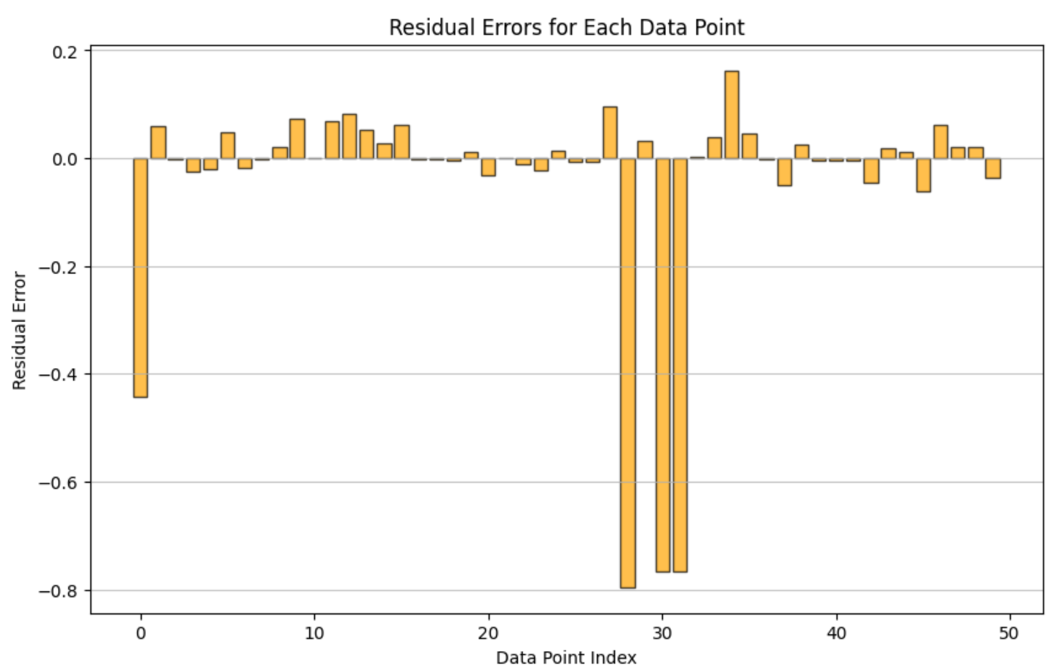

Figure 5-2 *Residual errors between predicted, and actual WWR Values before removing the outliers represent the impact of limitations occurred by fixed angle which led to street capture rather than building.*

Table 5-1: An example of the outliers generated by the model (Up) with the actual building image associated with the address (down)

1812 E Federal St, Baltimore, Maryland	
heading=90	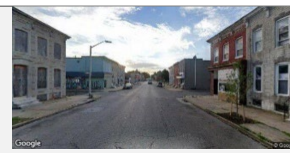
heading=0 *Correct image*	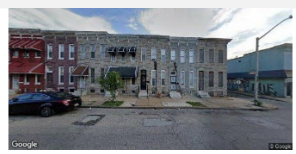

Another challenge was the camera's FOV. I set the FOV to 120 degrees to maximize façade visibility. However, the unique morphology of Baltimore's historic neighborhoods—particularly pre-1940 developments—introduced complications. Narrow streets and minimal setbacks often prevented full façade capture within a single frame, leading to incomplete data and impacting prediction accuracy (Stosur & Pugh, 2017). Additionally, narrow streets increase the likelihood of visual obstructions—such as parked vehicles, street furniture, trees, and awnings—that can block building façades and interfere with detection (Zhang et al., 2024). Since the model relies on image-based feature extraction, these obstructions introduce noise and reduce prediction accuracy. Previous research has shown that occlusion and perspective distortion are significant error sources in architectural feature recognition models (Kortylewski et al., 2021; Santana-Cedrés et al., 2017). Wendel et al. (2010) highlight this limitation, noting that occlusions can disrupt repetitive pattern detection and compromise the accuracy of facade separation (Lian et al., 2018). Addressing occlusions remains an important area for improving automated urban data extraction. Additionally, in some cases (Figure 5-3), the Google Street View images were too blurry to accurately identify buildings or extract WWR (Wang et al., 2022). To address the challenge of detecting occluded areas in façades, studies such as Lian et al. (2018) have leveraged urban building characteristics, particularly regularity, to enhance the detection of occluded elements, making this approach valuable for urban modeling and architectural analysis. However, its effectiveness remains dependent on the quality of the input image and the degree of occlusion, and it struggles with highly irregular façades that lack clear repetitive patterns (Lian et al., 2018).

An additional limitation occurred in segmenting adjacent buildings. My method assumes that neighboring structures belong to the same archetype, a useful simplification for typological generalization. While this assumption was useful for developing a generalized representation of urban residential typologies, it does introduce potential inaccuracies when dealing with areas where adjacent buildings exhibit significant variations in their façades. The pronounced contrast between a detached building and its adjacent open spaces, such as yards or driveways, enhances the segmentation accuracy and reduces the likelihood of misclassification.

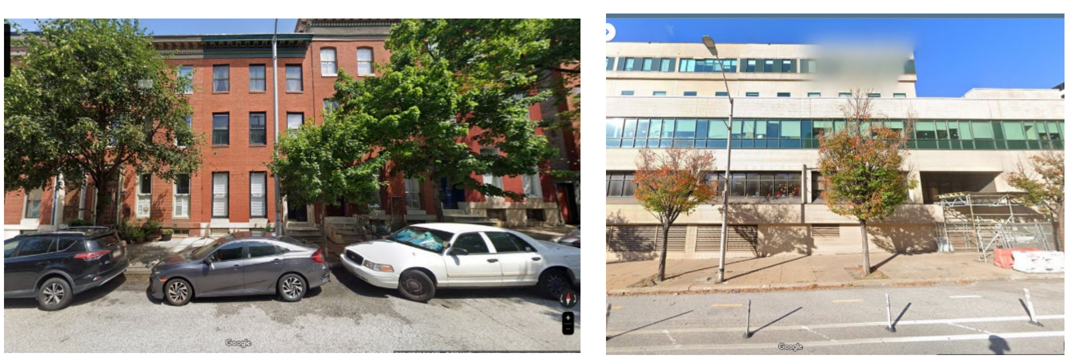

Figure 5-3 *Occlusions occurred in the street images such as tree, car, etc. as a limitation for building detection.*

Extension: Domain knowledge

To address the issue of capturing streets instead of buildings during the building extraction stage, I propose integrating human prior knowledge into the method. According to Liu et al. (2020), in face parsing problems, incorporating prior knowledge is beneficial because human-made structures inherently follow specific patterns. Similarly, applying prior knowledge to urban analysis can enhance the accuracy of building data extraction. In this regard, I suggest capturing images from multiple angles to ensure a reasonable percentage of WWR values falls within an acceptable range. This approach helps mitigate the issue of capturing streets, which leads to outlier WWR values, as seen in Figure 5-1. This problem happens because I initially set the Google Maps camera angle to 90 degrees, aiming to focus primarily on building façades by positioning the camera directly in front of the buildings (Figure3-4) . However, in some cases—especially the outliers—this setting resulted in capturing streets rather than buildings.

From previous knowledge gained during the archetype analysis stage, I know that most buildings in Baltimore, particularly in the selected neighborhoods, were constructed before 1940 and typically have WWRs below 0.5. Given this information, I was able to develop a script to extract images at different angles, such as 90, 120, and 270 degrees, until the captured WWR values fall within a reasonable range of 0.1 to 0.4. This approach ensures more accurate representation of building façades while minimizing errors caused by street captures.

Future iterations of the model could incorporate advanced segmentation techniques, such as detecting repetitive patterns in building facades, and unsupervised segmentation. Additionally, integrating LiDAR data or utilizing 3D point cloud analysis could help refine the detection of individual building boundaries, particularly in mixed-use districts where attached buildings coexist with detached structures and high-rise apartments. Moreover, leveraging multi-angle image capture rather than a single fixed viewpoint could provide a more comprehensive representation of building façades, addressing some of the inaccuracies caused by perspective distortions in Google Street View images. I also plan to explore the development of my framework to detect low-emissivity (Low-E) glass in windows from available street images. This would enhance the precision of energy performance assessments and further contribute to urban sustainability efforts.

References:

Ahmad, T., Chen, H., Guo, Y., & Wang, J. (2018). A comprehensive overview on the data driven and large scale based approaches for forecasting of building energy demand: A review. *Energy and Buildings*, *165*, 301–320.

aldean, A. S. (2023, August 30). Regression Model Performance: Key Metrics and Evaluation Techniques. *Medium*. https://medium.com/@aseafaldean/regression-model-performance-key-metrics-and-evaluation-techniques-db40e63f5fc1

Ali, U., Shamsi, M. H., Bohacek, M., Hoare, C., Purcell, K., Mangina, E., & O'Donnell, J. (2020). A data-driven approach to optimize urban scale energy retrofit decisions for residential buildings. *Applied Energy*, *267*, 114861.

Ali, U., Shamsi, M. H., Hoare, C., Mangina, E., & O'Donnell, J. (2021). Review of urban building energy modeling (UBEM) approaches, methods and tools using qualitative and quantitative analysis. *Energy and Buildings*, *246*, 111073. https://doi.org/10.1016/j.enbuild.2021.111073

Allan, J., Eggimann, S., Wagner, M., Ho, Y. N., Züger, M., Schneider, U., & Orehounig, K. (2022). Operational and embodied emissions associated with urban neighbourhood densification strategies. *Energy and Buildings*, *276*, 112482. https://doi.org/10.1016/j.enbuild.2022.112482

Ang, Y. Q., Berzolla, Z. M., Letellier-Duchesne, S., & Reinhart, C. F. (2023). Carbon reduction technology pathways for existing buildings in eight cities. *Nature Communications*, *14*(1), Article 1. https://doi.org/10.1038/s41467-023-37131-6

Ang, Y. Q., Berzolla, Z. M., & Reinhart, C. F. (2020). From concept to application: A review of use cases in urban building energy modeling. *Applied Energy*, *279*, 115738. https://doi.org/10.1016/j.apenergy.2020.115738

ASHRAE. (2000). *ANSI/ASHRAE/IES Standard 90.1-Energy standard for buildings except low-rise residential buildings* (Vol. 90). ASHRAE.

Balaras, C. A., & Argiriou, A. (2002). Infrared thermography for building diagnostics. *Energy and Buildings*, *34*(2), 171–183.

Balsa-Barreiro, J., & Fritsch, D. (2018). Generation of visually aesthetic and detailed 3D models of historical cities by using laser scanning and digital photogrammetry. *Digital Applications in Archaeology and Cultural Heritage*, *8*, 57–64. https://doi.org/10.1016/j.daach.2017.12.001

Baltimore City Real Property Assessments. (2024). Opendata.Maryland.Gov. https://opendata.maryland.gov/Business-and-Economy/Baltimore-City-Real-Property-Assessments-Hidden-Pr/3x3p-xk2v/about_data

Bansal, A., Sikka, K., Sharma, G., Chellappa, R., & Divakaran, A. (2018). *Zero-shot object detection*. 384–400.

Barns, S. (2018). Smart cities and urban data platforms: Designing interfaces for smart governance. *City, Culture and Society*, *12*, 5–12. https://doi.org/10.1016/j.ccs.2017.09.006

Bishop, D., Gallardo, P., & Williams, B. L. M. (2024). A Review of Multi-Domain Urban Energy Modelling Data. *Clean Energy and Sustainability*, *2*(4), Article 4. https://doi.org/10.70322/ces.2024.10016

Brown, T. B., Mann, B., Ryder, N., Subbiah, M., Kaplan, J., Dhariwal, P., Neelakantan, A., Shyam, P., Sastry, G., Askell, A., Agarwal, S., Herbert-Voss, A., Krueger, G., Henighan, T., Child, R., Ramesh, A., Ziegler, D. M., Wu, J., Winter, C., … Amodei, D. (2020). *Language Models are Few-Shot Learners* (arXiv:2005.14165). arXiv. https://doi.org/10.48550/arXiv.2005.14165

Bureau of the Census. (2023). *Baltimore Metropolitan Council*. https://www.baltometro.org/data/13-residential-units-permitted

Cai, M., Shi, Y., Ren, C., Yoshida, T., Yamagata, Y., Ding, C., & Zhou, N. (2021). The need for urban form data in spatial modeling of urban carbon emissions in China: A critical review. *Journal of Cleaner Production*, *319*, 128792. https://doi.org/10.1016/j.jclepro.2021.128792

Cerezo Davila, C., Reinhart, C. F., & Bemis, J. L. (2016). Modeling Boston: A workflow for the efficient generation and maintenance of urban building energy models from existing geospatial datasets. *Energy*, *117*, 237–250. https://doi.org/10.1016/j.energy.2016.10.057

Chen, L., Zheng, Y., Yu, J., Peng, Y., Li, R., & Han, S. (2024). A GIS-Based Approach for Urban Building Energy Modeling under Climate Change with High Spatial and Temporal Resolution. *Energies*, *17*(17), Article 17. https://doi.org/10.3390/en17174313

Chi, F., Wang, Y., Wang, R., Li, G., & Peng, C. (2020). An investigation of optimal window-to-wall ratio based on changes in building orientations for traditional dwellings. *Solar Energy*, *195*, 64–81. https://doi.org/10.1016/j.solener.2019.11.033

Chicco, D., Warrens, M. J., & Jurman, G. (2021). The coefficient of determination R-squared is more informative than SMAPE, MAE, MAPE, MSE and RMSE in regression analysis evaluation. *PeerJ Computer Science*, *7*, e623. https://doi.org/10.7717/peerj-cs.623

Chundawat, V. S., Tarun, A. K., Mandal, M., & Kankanhalli, M. (2023). Zero-Shot Machine Unlearning. *IEEE Transactions on Information Forensics and Security*, *18*, 2345–2354. https://doi.org/10.1109/TIFS.2023.3265506

Colleto, G. M., & Gomes, V. (2021). Review of archetype development strategies for energy assessment at urban scale. *IOP Conference Series: Earth and Environmental Science*, *855*(1), 012021. https://doi.org/10.1088/1755-1315/855/1/012021

Dabirian, S., Panchabikesan, K., & Eicker, U. (2022). Occupant-centric urban building energy modeling: Approaches, inputs, and data sources—A review. *Energy and Buildings*, *257*, 111809. https://doi.org/10.1016/j.enbuild.2021.111809

Dabirian, S., Saad, M. M., Hussain, S., Peyman, S., Rahimi, N., Monsalvete Alvarez U, P., Yefi, P., & Eicker, U. (2023). Structuring heterogeneous urban data: A framework to develop the data model for energy simulation of cities. *Energy and Buildings*, *296*, 113376. https://doi.org/10.1016/j.enbuild.2023.113376

Dahlström, L., Johari, F., Broström, T., & Widén, J. (2024). Identification of representative building archetypes: A novel approach using multi-parameter cluster analysis applied to the Swedish residential building stock. *Energy and Buildings*, *303*, 113823. https://doi.org/10.1016/j.enbuild.2023.113823

Deng, Z., Javanroodi, K., Nik, V. M., & Chen, Y. (2023). Using urban building energy modeling to quantify the energy performance of residential buildings under climate change. *Building Simulation*, *16*(9), 1629–1643. https://doi.org/10.1007/s12273-023-1032-2

Dino, I. G., Sari, A. E., Iseri, O. K., Akin, S., Kalfaoglu, E., Erdogan, B., Kalkan, S., & Alatan, A. A. (2020). Image-based construction of building energy models using computer vision. *Automation in Construction*, *116*, 103231. https://doi.org/10.1016/j.autcon.2020.103231

Environmental Systems Research Institute. (1998). *ESRI Shapefile Technical Description*.

Evola, G., Costanzo, V., Magrì, C., Margani, G., Marletta, L., & Naboni, E. (2020). A novel comprehensive workflow for modelling outdoor thermal comfort and energy demand in urban canyons: Results and critical issues. *Energy and Buildings*, *216*, 109946. https://doi.org/10.1016/j.enbuild.2020.109946

Excell, L. E., Nutkiewicz, A., & Jain, R. K. (2024). Multi-scale retrofit pathways for improving building performance and energy equity across cities: A UBEM framework. *Energy and Buildings*, *324*, 114931. https://doi.org/10.1016/j.enbuild.2024.114931

Ghorbany, S., & Hu, M. (2024). Urban embodied carbon assessment: Methodology and insights from analyzing over a million buildings in Chicago. *Carbon Management*, *15*(1), 2382993. https://doi.org/10.1080/17583004.2024.2382993

Ghorbany, S., Hu, M., Yao, S., Wang, C., Nguyen, Q. C., Yue, X., Alirezaei, M., Tasdizen, T., & Sisk, M. (2024). Examining the role of passive design indicators in energy burden reduction: Insights from a machine learning and deep learning approach. *Building and Environment*, *250*, 111126. https://doi.org/10.1016/j.buildenv.2023.111126

Harish Babu, G., & Venkatram, N. (2020). A survey on analysis and implementation of state-of-the-art haze removal techniques. *Journal of Visual Communication and Image Representation*, *72*, 102912. https://doi.org/10.1016/j.jvcir.2020.102912

Hecht, R., Kunze, C., & Hahmann, S. (2013). Measuring Completeness of Building Footprints in OpenStreetMap over Space and Time. *ISPRS International Journal of Geo-Information*, *2*(4), Article 4. https://doi.org/10.3390/ijgi2041066

Herfort, B., Lautenbach, S., Porto de Albuquerque, J., Anderson, J., & Zipf, A. (2023a). A spatio-temporal analysis investigating completeness and inequalities of global urban building data in OpenStreetMap. *Nature Communications*, *14*(1), 3985. https://doi.org/10.1038/s41467-023-39698-6

Herfort, B., Lautenbach, S., Porto de Albuquerque, J., Anderson, J., & Zipf, A. (2023b). A spatio-temporal analysis investigating completeness and inequalities of global urban building data in OpenStreetMap. *Nature Communications*, *14*(1), 3985. https://doi.org/10.1038/s41467-023-39698-6

Hoare, C., Aghamolaei, R., Lynch, M., Gaur, A., & O'Donnell, J. (2022). A linked data approach to multi-scale energy modelling. *Advanced Engineering Informatics*, *54*. Scopus. https://doi.org/10.1016/j.aei.2022.101719

Hong, T., Chen, Y., Luo, X., Luo, N., & Lee, S. H. (2020). Ten questions on urban building energy modeling. *Building and Environment*, *168*, 106508. https://doi.org/10.1016/j.buildenv.2019.106508

IEA. (2023). *IEA_Tracking Buildings*. IEA. https://www.iea.org/energy-system/buildings

IEA. (2024). *Empowering Urban Energy Transitions*. IEA. https://www.iea.org/reports/empowering-urban-energy-transitions/executive-summary

IECC & International Code Council. (2021). *International energy conservation code*. International Code Council. (2021). General Requirements. https://codes.iccsafe.org/content/IECC2021P1/chapter-3-ce-general-requirements#IECC2021P1_CE_Ch03_SecC301

Javanroodi, K., Mahdavinejad, M., & Nik, V. M. (2018). Impacts of urban morphology on reducing cooling load and increasing ventilation potential in hot-arid climate. *Applied Energy*, *231*, 714–746. Scopus. https://doi.org/10.1016/j.apenergy.2018.09.116

Javanroodi, K., Perera, A. T. D., Hong, T., & Nik, V. M. (2023). Designing climate resilient energy systems in complex urban areas considering urban morphology: A technical review. *Advances in Applied Energy*, *12*, 100155. https://doi.org/10.1016/j.adapen.2023.100155

Kamal, A., Abidi, S. M. H., Mahfouz, A., Kadam, S., Rahman, A., Hassan, I. G., & Wang, L. L. (2021). Impact of urban morphology on urban microclimate and building energy loads. *Energy and Buildings*, *253*, 111499. https://doi.org/10.1016/j.enbuild.2021.111499

Kim, J., Yeom, S., & Hong, T. (2025). Analyzing the cooling effect, thermal comfort, and energy consumption of integrated arrangement of high-rise buildings and green spaces on urban heat island. *Sustainable Cities and Society*, *119*, 106105. https://doi.org/10.1016/j.scs.2024.106105

Kim, S., Zadeh, P. A., Staub-French, S., Froese, T., & Cavka, B. T. (2016). Assessment of the Impact of Window Size, Position and Orientation on Building Energy Load Using BIM. *Procedia Engineering*, *145*, 1424–1431. https://doi.org/10.1016/j.proeng.2016.04.179

Klimkowska, A., Cavazzi, S., Leach, R., & Grebby, S. (2022). Detailed Three-Dimensional Building Façade Reconstruction: A Review on Applications, Data and Technologies. *Remote Sensing*, *14*(11), Article 11. https://doi.org/10.3390/rs14112579

Klingler, N. (2025, January 16). *N-Shot Learning: Zero vs. Single vs. Two vs. Few (2025)*. Viso.Ai. https://viso.ai/deep-learning/n-shot-learning/

Kortylewski, A., Liu, Q., Wang, A., Sun, Y., & Yuille, A. (2021). Compositional Convolutional Neural Networks: A Robust and Interpretable Model for Object Recognition Under Occlusion. *International Journal of Computer Vision*, *129*(3), 736–760. https://doi.org/10.1007/s11263-020-01401-3

Kropf, K. (2018). *The Handbook of Urban Morphology*. Wiley. https://books.google.com/books?id=Glw6DwAAQBAJ

Li, K., Wan, G., Cheng, G., Meng, L., & Han, J. (2020). Object detection in optical remote sensing images: A survey and a new benchmark. *ISPRS Journal of Photogrammetry and Remote Sensing*, *159*, 296–307. https://doi.org/10.1016/j.isprsjprs.2019.11.023

Li, W., Liu, K., Zhang, L., & Cheng, F. (2020). Object detection based on an adaptive attention mechanism. *Scientific Reports*, *10*(1), 11307. https://doi.org/10.1038/s41598-020-67529-x

Li, Y. (2023). *Developing a GIS-based urban building energy assessment model to support decision making in Richmond*. Sustain.Ubc.Ca. https://sustain.ubc.ca/about/resources/developing-gis-based-urban-building-energy-assessment-model-support-decision-making

Lian, Y., Shen, X., & Hu, Y. (2018). Detecting and inferring repetitive elements with accurate locations and shapes from façades. *The Visual Computer*, *34*(4), 491–506. https://doi.org/10.1007/s00371-017-1355-z

Litjens, G., Kooi, T., Bejnordi, B. E., Setio, A. A. A., Ciompi, F., Ghafoorian, M., van der Laak, J. A. W. M., van Ginneken, B., & Sánchez, C. I. (2017). A survey on deep learning in medical image analysis. *Medical Image Analysis*, *42*, 60–88. https://doi.org/10.1016/j.media.2017.07.005

Liu, H., Li, W., & Zhu, J. (2021). *Translational Symmetry-Aware Facade Parsing for 3D Building Reconstruction* (arXiv:2106.00912). arXiv. https://doi.org/10.48550/arXiv.2106.00912

Luo, H., He, B., Guo, R., Wang, W., Kuai, X., Xia, B., Wan, Y., Ma, D., & Xie, L. (2021). Urban Building Extraction and Modeling Using GF-7 DLC and MUX Images. *Remote Sensing*, *13*(17), Article 17. https://doi.org/10.3390/rs13173414

Ma, R., Fang, D., Chen, J., & Li, X. (2023). A tiled multi-city urban objects dataset for city-scale building energy simulation. *Scientific Data*, *10*(1), Article 1. https://doi.org/10.1038/s41597-023-02261-5

Marasinghe, R., Yigitcanlar, T., Mayere, S., Washington, T., & Limb, M. (2024). Computer vision applications for urban planning: A systematic review of opportunities and constraints. *Sustainable Cities and Society*, *100*, 105047. https://doi.org/10.1016/j.scs.2023.105047

Minderer, M., Gritsenko, A., Stone, A., Neumann, M., Weissenborn, D., Dosovitskiy, A., Mahendran, A., Arnab, A., Dehghani, M., & Shen, Z. (2022). *Simple open-vocabulary object detection*. 728–755.

Model & API. (n.d.). Roboflow. Retrieved February 27, 2025, from https://universe.roboflow.com/yassine-ouardani-i3beo/window-detection-yolo/model/4

Mohammadiziazi, R., Copeland, S., & Bilec, M. M. (2021). Urban building energy model: Database development, validation, and application for commercial building stock. *Energy and Buildings*, *248*, 111175. https://doi.org/10.1016/j.enbuild.2021.111175

Moyano, J., Justo-Estebaranz, Á., Nieto-Julián, J. E., Barrera, A. O., & Fernández-Alconchel, M. (2022). Evaluation of records using terrestrial laser scanner in architectural heritage for information modeling in HBIM construction: The case study of the La Anunciación church (Seville). *Journal of Building Engineering*, *62*, 105190. https://doi.org/10.1016/j.jobe.2022.105190

Mu, X., & Antwi-Afari, M. F. (2024). The applications of Internet of Things (IoT) in industrial management: A science mapping review. *International Journal of Production Research*, *62*(5), 1928–1952. https://doi.org/10.1080/00207543.2023.2290229

Mutani, G., & Todeschi, V. (2021). GIS-based urban energy modelling and energy efficiency scenarios using the energy performance certificate database. *Energy Efficiency*, *14*(5), 47. https://doi.org/10.1007/s12053-021-09962-z

Natanian, J., & Auer, T. (2020). Beyond nearly zero energy urban design: A holistic microclimatic energy and environmental quality evaluation workflow. *Sustainable Cities and Society*, *56*, 102094. https://doi.org/10.1016/j.scs.2020.102094

OpenStreetMap. (n.d.). OpenStreetMap. Retrieved October 31, 2024, from https://www.openstreetmap.org/

Oraiopoulos, A., & Howard, B. (2022). On the accuracy of urban building energy modelling. *Renewable and Sustainable Energy Reviews*, *158*, 111976.

Ouardani, Y. (2023). *Window-detection-yolo Dataset*. Roboflow. https://universe.roboflow.com/yassine-ouardani-i3beo/window-detection-yolo/dataset/4

Philip, A., Pathak, B., Gandhi, S., & Rawal, R. (2023). Developing and Calibrating a Cost-Effective Method to Determine Window-To-Wall Ratio and Air-Conditioning Status of Existing Buildings. In L. L. Wang, H. Ge, Z. J. Zhai, D. Qi, M. Ouf, C. Sun, & D. Wang (Eds.), *Proceedings of the 5th International Conference on Building Energy and Environment* (pp. 2839–2847). Springer Nature. https://doi.org/10.1007/978-981-19-9822-5_303

Phillips, R., Troup, L., Fannon, D., & Eckelman, M. J. (2020). Triple bottom line sustainability assessment of window-to-wall ratio in US office buildings. *Building and Environment*, *182*, 107057. https://doi.org/10.1016/j.buildenv.2020.107057

Pristerà, G., Allacker, K., Rock, M., & Sala, S. (2023). Archetype selection process for the development of a building stock model. *IOP Conference Series: Earth and Environmental Science*, *1196*(1), 012013. https://doi.org/10.1088/1755-1315/1196/1/012013

Qin, R., & Gruen, A. (2014). 3D change detection at street level using mobile laser scanning point clouds and terrestrial images. *ISPRS Journal of Photogrammetry and Remote Sensing*, *90*, 23–35. https://doi.org/10.1016/j.isprsjprs.2014.01.006

Reinhart, C. F., & Davila, C. C. (2016). Urban building energy modeling–A review of a nascent field. *Building and Environment*, *97*, 196–202.

Santana-Cedrés, D., Gomez, L., Alemán-Flores, M., Salgado, A., Esclarín, J., Mazorra, L., & Alvarez, L. (2017). Automatic correction of perspective and optical distortions. *Computer Vision and Image Understanding*, *161*, 1–10. https://doi.org/10.1016/j.cviu.2017.05.016

Shah, D. (2022). *Mean Average Precision (mAP) Explained: Everything You Need to Know*. https://www.v7labs.com/blog/mean-average-precision

Shen, P., & Wang, H. (2024). Archetype building energy modeling approaches and applications: A review. *Renewable and Sustainable Energy Reviews*, *199*, 114478. https://doi.org/10.1016/j.rser.2024.114478

Sherif, T., Katia, R., Nguyen, M., Ma, N., & Rakha, T. (2025). Localizing urban building energy modeling (UBEM) through inclusive microclimate and socioeconomic data. *Applied Energy*, *383*, 125342. https://doi.org/10.1016/j.apenergy.2025.125342

Shi, K., Xu, T., Li, Y., Chen, Z., Gong, W., Wu, J., & Yu, B. (2020). Effects of urban forms on CO2 emissions in China from a multi-perspective analysis. *Journal of Environmental Management*, *262*, 110300. https://doi.org/10.1016/j.jenvman.2020.110300

Simone, Z. D., Biswas, S., & Wu, O. (2024). *Window to Wall Ratio Detection using SegFormer* (arXiv:2406.02706). arXiv. https://doi.org/10.48550/arXiv.2406.02706

Smeriglio, M. (2022). *Opendata.maryland.gov*. https://opendata.maryland.gov/Business-and-Economy/Baltimore-City-Real-Property-Assessments-Hidden-Pr/3x3p-xk2v/about_data

Stosur, T. J., & Pugh, C. E. (2017). *Baltimore City Historic Preservation Design Guidelines*.

Sun, Y., Malihi, S., Li, H., & Maboudi, M. (2022). DeepWindows: Windows Instance Segmentation through an Improved Mask R-CNN Using Spatial Attention and Relation Modules. *ISPRS International Journal of Geo-Information*, *11*(3), Article 3. https://doi.org/10.3390/ijgi11030162

Tiwari, A. (2022). Chapter 2—Supervised learning: From theory to applications. In R. Pandey, S. K. Khatri, N. kumar Singh, & P. Verma (Eds.), *Artificial Intelligence and Machine Learning for EDGE Computing* (pp. 23–32). Academic Press. https://doi.org/10.1016/B978-0-12-824054-0.00026-5

Traore, M. (2022, May 11). *Roboflow's Python Pip Package For Computer Vision*. Roboflow Blog. https://blog.roboflow.com/pip-install-roboflow

Troup, L., Phillips, R., Eckelman, M. J., & Fannon, D. (2019). Effect of window-to-wall ratio on measured energy consumption in US office buildings. *Energy and Buildings*, *203*, 109434. https://doi.org/10.1016/j.enbuild.2019.109434

Tyagi, K., Rane, C., Harshvardhan, & Manry, M. (2022). Chapter 4—Regression analysis. In R. Pandey, S. K. Khatri, N. kumar Singh, & P. Verma (Eds.), *Artificial Intelligence and Machine Learning for EDGE Computing* (pp. 53–63). Academic Press. https://doi.org/10.1016/B978-0-12-824054-0.00007-1

Ultralytics. (2024). *YOLO Performance Metrics*. https://docs.ultralytics.com/guides/yolo-performance-metrics

Valladares-Rendón, L. G., Schmid, G., & Lo, S.-L. (2017). Review on energy savings by solar control techniques and optimal building orientation for the strategic placement of façade shading systems. *Energy and Buildings*, *140*, 458–479. https://doi.org/10.1016/j.enbuild.2016.12.073

von Behren, S., Turek, M., Barthelmes, L., Scholta, H., Hansen, F., Kagerbauer, M., & Eisenmann, C. (2023). Decoding Urban Archetypes: Exploring Mobility-Related Homogeneity among Cities. *Sustainability*, *15*(19), Article 19. https://doi.org/10.3390/su151914231

Wang, J., Jin, L., & Ding, K. (2022). *LiLT: A Simple yet Effective Language-Independent Layout Transformer for Structured Document Understanding* (arXiv:2202.13669). arXiv. https://doi.org/10.48550/arXiv.2202.13669

Wate, P., & Coors, V. (2015). 3D Data Models for Urban Energy Simulation. *Energy Procedia*, *78*, 3372–3377. https://doi.org/10.1016/j.egypro.2015.11.753

Wendel, A., Donoser, M., & Bischof, H. (2010). Unsupervised Facade Segmentation Using Repetitive Patterns. In M. Goesele, S. Roth, A. Kuijper, B. Schiele, & K. Schindler (Eds.), *Pattern Recognition* (pp. 51–60). Springer. https://doi.org/10.1007/978-3-642-15986-2_6

Whitehurst, D., Friedman, B., Kochersberger, K., Sridhar, V., & Weeks, J. (2021). Drone-Based Community Assessment, Planning, and Disaster Risk Management for Sustainable Development. *Remote Sensing*, *13*(9), Article 9. https://doi.org/10.3390/rs13091739

Xu, J., Zhang, Q., Teng, Y., & Pan, W. (2023). Integrating IoT and BIM for tracking and visualising embodied carbon of prefabricated buildings. *Building and Environment*, *242*, 110492. https://doi.org/10.1016/j.buildenv.2023.110492

Xu, Y., Shen, X., & Lim, S. (2021). CorDet: Corner-Aware 3D Object Detection Networks for Automated Scan-to-BIM. *Journal of Computing in Civil Engineering*, *35*(3), 04021002. https://doi.org/10.1061/(ASCE)CP.1943-5487.0000962

Yu, H., Wang, M., Lin, X., Guo, H., Liu, H., Zhao, Y., Wang, H., Li, C., & Jing, R. (2021). Prioritizing urban planning factors on community energy performance based on GIS-informed building energy modeling. *Energy and Buildings*, *249*, 111191. https://doi.org/10.1016/j.enbuild.2021.111191

Yu, X., & Lu, X. (2024). Domain Adaptation of Anchor-Free object detection for urban traffic. *Neurocomputing*, *582*, 127477. https://doi.org/10.1016/j.neucom.2024.127477

Zachariah, A., Rao, P., Corn, B., & Davison, D. (2022). *Zero Shot Learning for Predicting Energy Usage of Buildings in Sustainable Design* (arXiv:2202.05206). arXiv. https://doi.org/10.48550/arXiv.2202.05206

Zalama, E., Gómez-García-Bermejo, J., Llamas, J., & Medina, R. (2011). An Effective Texture Mapping Approach for 3D Models Obtained from Laser Scanner Data to Building Documentation. *Computer-Aided Civil and Infrastructure Engineering*, *26*(5), 381–392. https://doi.org/10.1111/j.1467-8667.2010.00699.x

Zhang, Y., Yue, D., Liu, X., Zou, S., Fan, W., & Liu, Z. (2024). OccFaçade: Enabling precise building façade parsing in large urban scenes with occlusion. *International Journal of Remote Sensing*, *45*(18), 6651–6674. https://doi.org/10.1080/01431161.2024.2391589

Zhao, L., Zhang, H., Wang, Q., & Wang, H. (2021). Digital-Twin-Based Evaluation of Nearly Zero-Energy Building for Existing Buildings Based on Scan-to-BIM. *Advances in Civil Engineering*, *2021*(1), 6638897. https://doi.org/10.1155/2021/6638897

Zhao, Z.-Q., Zheng, P., Xu, S.-T., & Wu, X. (2019). Object Detection With Deep Learning: A Review. *IEEE Transactions on Neural Networks and Learning Systems*, *30*(11), 3212–3232. https://doi.org/10.1109/TNNLS.2018.2876865

Zou, Z., Chen, K., Shi, Z., Guo, Y., & Ye, J. (2023). Object Detection in 20 Years: A Survey. *Proceedings of the IEEE*, *111*(3), 257–276. Proceedings of the IEEE. https://doi.org/10.1109/JPROC.2023.3238524

Appendix A

Code

The code for this research is available at the following GitHub link:

- https://github.com/elnazqasemi/WWR_Extraction
- https://github.com/elnazqasemi/WWR_Extraction/blob/main/WWR_Git.ipynb

---

```
!pip install timm roboflow --quiet
```

```
   ━━━━━━━━━━━━━━━━━━━━━━━━━━━━━━━━━━━━━━━━ 81.5/81.5 kB 887.1 kB/s eta 0:00:00
   ━━━━━━━━━━━━━━━━━━━━━━━━━━━━━━━━━━━━━━━━ 66.8/66.8 kB 2.2 MB/s eta 0:00:00
```

```
#Run these two every time to upload broadway csv from your google drive folder
from google.colab import drive
drive.mount('/content/drive')
```

```
Mounted at /content/drive
```

```
!cp -r /content/drive/MyDrive/DFWWR/Broadway_East_Cad.csv /content
```

```
import pandas as pd
```

```
# !cp -r /content/Broadway /content/drive/MyDrive
```

```
#To not use your API key again and upload images from Drive
#!cp -r /content/drive/MyDrive/Broadway /content
```

```
from tqdm import tqdm
```

Getting the images of each address from CSV file:

```
import requests
from PIL import Image, ImageDraw
from io import BytesIO
import IPython.display as display
import os
import pathlib



def get_street_view_image(api_key, location, size="600x300", fov=120, pitch=0, heading=90):
    base_url = "https://maps.googleapis.com/maps/api/streetview"
    params = {
        "size": size,
        "location": location,
        "fov": fov,
        "pitch": pitch,
        "heading": heading,
        "key": api_key
    }

    response = requests.get(base_url, params=params)
    if response.status_code == 200:
        return Image.open(BytesIO(response.content))
    else:
        raise Exception(f"Error fetching Street View image: {response.status_code}")

# Path to the CSV file
#Copy the csv file in the google colab file section at left bar
```

```
[ ]     if response.status_code == 200:
            with Image.open(image_path) as image:
                # Apply the detector on the image
                predictions = detector(
                    image,
                    candidate_labels=["building"],
                )
                buildings[image_path] = []

                # Extract buildings from each image
                for p in predictions:
                    bb = p["box"]
                    xmin = bb['xmin']
                    ymin = bb['ymin']
                    xmax = bb['xmax']
                    ymax = bb['ymax']
                    buildings[image_path].append(image.crop((xmin, ymin, xmax, ymax)))


    # you can comment following parts in case of large input
    #print(f"number of images: {len(buildings.keys())}")
    #number of buildings detected in each image
    # for image, building in buildings.items():
    #     print(f"{Path(image).stem}: {len(building)}")
```

```
100%|██████████| 960/960 [36:20<00:00,  2.27s/it]
```

```
[ ] # buildings[][0]
```

```
[<PIL.Image.Image image mode=RGB size=278x287>,
 <PIL.Image.Image image mode=RGB size=139x233>]
```

```
[ ]
    # import IPython.display as Display
    # for building in buildings:
    #     Display.display(building)
```

```
#       except Exception as e:
#           print(e)
```

```
!cp -r /content/Patterson_Park /content/drive/MyDrive
```

+ Code   + Text

```
# import cv2
# import numpy as np
```

```
# # Convert the image to binary
# image_bw = cv2.cvtColor(np.array(image), cv2.COLOR_BGR2GRAY)
# _, image_bw = cv2.threshold(image_bw, 127, 255, cv2.THRESH_BINARY)

# # Display the binary image
# display.display(Image.fromarray(image_bw))
```

Detecting Buildings in each address

```
from transformers import pipeline

checkpoint = "google/owlvit-base-patch32"
detector = pipeline(model=checkpoint, task="zero-shot-object-detection")
```

```
Could not find image processor class in the image processor config or the model config. Loading based on pattern matching with the model's feature extractor
```

```
# predictions = detector(
#     image,
#     candidate_labels=["building"],
# )
```

Detecting Windows in Images:

```
from roboflow import Roboflow
rf = Roboflow(api_key="2nDoXqG")#Change it your API key
project = rf.workspace().project("window-detection-xowg3")
model = project.version(1).model
```

```
loading Roboflow workspace...
loading Roboflow project...
```

```
# im = buildings[0]
# im.save('temp_image.jpg')
# result = model.predict('temp_image.jpg', confidence=30, overlap=30).json()
# window_area = sum([int(w['width'])*int(w['height'])for w in result['predictions']], 0)
# total_area = im.width*im.height
# window_area, total_area, window_area/total_area
```

```
(18235, 82008, 0.2223563554775144)
```

```
# buildings_ratio: Dict[str, List[dict]]
from collections import OrderedDict
buildings_ratio = OrderedDict()
for image_path in tqdm(buildings.keys()):
    address = Path(image_path).stem
    total_window_area = 0
    total_facade_area = 0
    for im in buildings[image_path]:
      im.save('temp_image.jpg')
      result = model.predict('temp_image.jpg', confidence=30, overlap=30).json()
      window_area = sum([int(w['width'])*int(w['height']) for w in result['predictions']], 0)
      facade_area = im.width * im.height
      # window_to_total_ratio = window_area / total_area if total_area > 0 else 0

      # ratio_info = {
      #  'total_window_area': total_window_area,
      #  'window_area': window_area,
      #  'total_area': facade_area,
      #   'WWR': window_area/facade_area,
      # }

      # if address not in buildings_ratio:
      #   buildings_ratio[address] = []
      # buildings_ratio[address].append(ratio_info)
      # buildings_ratio[address] = window_area/total_area

      total_window_area += window_area
      total_facade_area += facade_area


    # if total_facade_area > 0:
    #     buildings_ratio[address] = {
    #         'window_area': total_window_area,
    #         'facade_area': total_facade_area,
    #         'WWR': total_window_area / total_facade_area,
```

```
[ ] # If you want separate columns for 'Group_E' and 'Group_N'
    df['Group_E'] = df['Address'].apply(lambda x: 'E' if ' E ' in x else 'Other')
    df['Group_N'] = df['Address'].apply(lambda x: 'N' if ' N ' in x else 'Other')
```

```
[ ] # Save the EN separated to a new CSV file
    df.to_csv('/content/dfEN.csv', index=False)
```

```
[ ] !cp -r /content/drive/MyDrive/DFWWR/dfEN.csv /content
```

```
[ ] #Is it really necessary to do this?
    df = pd.read_csv('/content/dfEN.csv')

    # Function to replace values
    def replace_values(row):
        if row['Group_E'] == ' E ':
            return row['replacement_column']
        else:
            return row['column_to_replace']

    # Apply the function to create a new column or overwrite the existing one
    df['new_column'] = df.apply(replace_values, axis=1)

    # Display the updated DataFrame
    print(df)
```

```
[ ] !cp -r //content/dfEN.csv /content/drive/MyDrive/DFWWR
```

Getting the Latitude, and longitude of each address:

```
[ ]

    df = pd.read_csv('/content/dfEN.csv')

    df['Address'] = df['Address'].str.replace(", Baltimore, Maryland", "")


    df.to_csv('/content/dfEN.csv', index=False)
```

```
[ ] !cp -r //content/dfENlonlat.csv /content/drive/MyDrive/DFWWR
```

residual graph:

```
[ ] import pandas as pd
    import matplotlib.pyplot as plt
```

```python
import pandas as pd
import matplotlib.pyplot as plt

# Load the CSV data
df = pd.read_csv('/content/Broadway_East_Cad50smpl.csv')

df = df.dropna(subset=['Cad_WWR'])
df = df[df['Cad_WWR'] != ' ']

df['Cad_WWR'] = pd.to_numeric(df['Cad_WWR'], errors='coerce')
df['WWR'] = pd.to_numeric(df['WWR'], errors='coerce')

df = df.dropna(subset=['Cad_WWR', 'WWR'])
df = df[df['Cad_WWR'] > 0]

df['Residual'] = df['Cad_WWR'] - df['WWR']

df_sorted = df.sort_values(by='WWR').reset_index(drop=True)

fig, ax = plt.subplots(figsize=(12, 6))

bar_width = 0.8

ax.bar(
    df_sorted.index,
    df_sorted['WWR'],
    color='blue',
    width=bar_width,
    label='Predicted WWR (Model)'
)

ax.bar(
    df_sorted.index,
    df_sorted['Cad_WWR'],
    color='orange',
    width=bar_width,
    alpha=0.7,
    label='Actual WWR (AutoCAD)'
)


for i in range(len(df_sorted)):
    x = df_sorted.index[i]
    predicted = df_sorted['WWR'].iloc[i]
    actual = df_sorted['Cad_WWR'].iloc[i]
    ax.plot([x, x], [predicted, actual], color='red', linewidth=1.5, label='Error' if i == 0 else "")

ax.set_xlabel("Sample Index (Sorted by Predicted WWR)")
ax.set_ylabel("WWR Values")
ax.set_title("Comparison of Predicted WWRs vs Actual WWRs with Residuals")
ax.legend()

# Display the plot
plt.tight_layout()
plt.show()
```

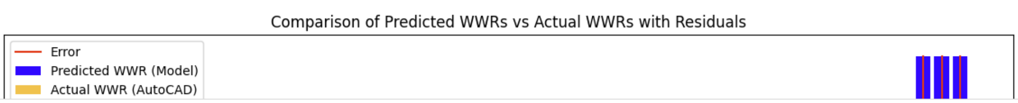

```
[ ] import pandas as pd
    import matplotlib.pyplot as plt

    # Load the CSV data
    df = pd.read_csv('/content/Broadway_East_Cad50smpl.csv')

    df = df.dropna(subset=['Cad_WWR'])
    df = df[df['Cad_WWR'] != ' ']

    df['Cad_WWR'] = pd.to_numeric(df['Cad_WWR'], errors='coerce')
    df['WWR'] = pd.to_numeric(df['WWR'], errors='coerce')

    df = df.dropna(subset=['Cad_WWR', 'WWR'])
    df = df[df['Cad_WWR'] > 0]

    df['Residual'] = df['Cad_WWR'] - df['WWR']

    df_sorted = df.sort_values(by='Cad_WWR').reset_index(drop=True)

    fig, ax = plt.subplots(figsize=(12, 6))

    bar_width = 0.8

    ax.bar(
        df_sorted.index,
        df_sorted['Residual'],
        color='blue',
        width=bar_width,
        label='Residuals'
    )

    ax.bar(
        df_sorted.index,
        df_sorted['Cad_WWR'],
        color='orange',
        width=bar_width,
        alpha=0.7,
        label='Actual (CAD) WWR'
    )

    ax.set_xlabel("Sample Index (Sorted by Cad_WWR)")
    ax.set_ylabel("WWR / Residual Values")
    ax.set_title("Residuals of the model WWRs vs Actual WWR calculated by AutoCad")
    ax.legend()

    plt.tight_layout()
    plt.show()
```

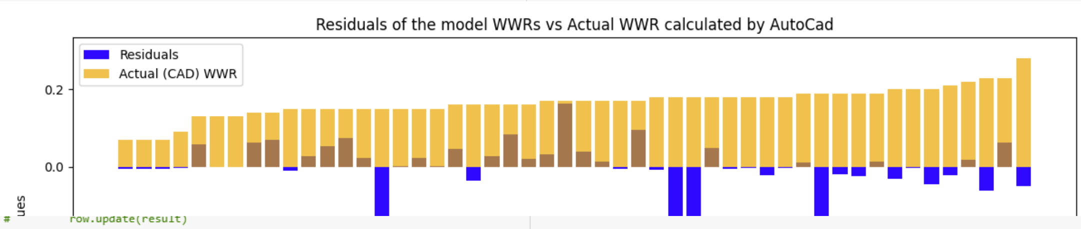


```
#       row.update(result)
#       writer.writerow(row)
```

residual graph:

```
[ ] import pandas as pd
    import matplotlib.pyplot as plt
```

```
[ ] df = pd.read_csv('/content/Broadway_East_Cad.csv')

    df = df.dropna(subset=['Cad_WWR'])
    # Remove rows with empty strings in the 'Cad_WWR' column
    df = df[df['Cad_WWR'] != ' ']
    # Convert the 'Cad_WWR' column to float
    df['Cad_WWR'] = df['Cad_WWR'].astype(float)
```

```
[ ] df.shape
```

```
(25, 15)
```

```
[ ] # Convert 'Cad_WWR' and 'WWR' to numeric, coercing errors to NaN
    df['Cad_WWR'] = pd.to_numeric(df['Cad_WWR'], errors='coerce')
    df['WWR'] = pd.to_numeric(df['WWR'], errors='coerce')

    df = df.dropna(subset=['Cad_WWR', 'WWR'])

    df["Residual"] = df["Cad_WWR"] - df["WWR"]

    df_sorted = df.sort_values(by="Cad_WWR")

    fig, ax = plt.subplots(figsize=(12, 6))

    ax.bar(
        df_sorted.index,
        df_sorted["Residual"],
        color="blue",
        label="Residuals"
    )

    ax.bar(
        df_sorted.index,
        df_sorted["Cad_WWR"],
        color="orange",
        alpha=0.7,
        label="Actual (CAD) WWR"
    )

    ax.set_xlabel("Sample Index (Sorted by Cad_WWR)")
    ax.set_ylabel("WWR / Residual Values")
    ax.set_title("Residuals of Predicted WWRs vs Actual WWR (CAD)")
    ax.legend()

    plt.tight_layout()
    plt.show()
```

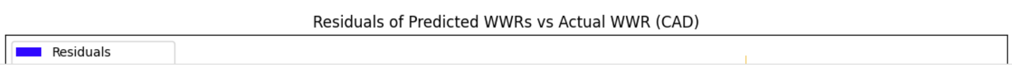

```
# 	row.update(result)
# 	writer.writerow(row)
# df_out
```

In case of "No Building detected":

```
!cp -r /content/drive/MyDrive/DFWWR/Broadway_East.csv /content
```

```
import pandas as pd

df = pd.read_csv('/content/Broadway_East.csv')


column_name = 'WWR'

# Replace 0
df[column_name] = df[column_name].replace(0, 'No building detected or tree in front of the building')

df.to_csv('/content/Broadway_East.csv', index=False)
```

Move to your Drive:

```
!cp -r //content/Broadway_East.csv /content/drive/MyDrive/DFWWR
```

Total Broadway Buildings:640 / Total Patterson Park Neighborhood: 960

```
Start coding or generate with AI.
```

```
!cp -r //content/df.csv /content/drive/MyDrive/DFWWR
```

Four facade WWR(Dividing addresses into East, and North groups)

```
df = pd.read_csv('/content/Broadway_East_Cad.csv')

# Function to assign groups based on 'E' or 'N'
def assign_group(address):
    if ' E ' in address:
        return 'E'
    elif ' N ' in address:
        return 'N'
    else:
        return 'Other'


# If you want separate columns for 'Group_E' and 'Group_N'
df['Group_E'] = df['Address'].apply(lambda x: 'E' if ' E ' in x else 'Other')
df['Group_N'] = df['Address'].apply(lambda x: 'N' if ' N ' in x else 'Other')
```

```
[ ] import pandas as pd
    import matplotlib.pyplot as plt

    # Load the CSV data
    df = pd.read_csv('/content/Broadway_East_Cad50smpl.csv')

    # Drop rows where 'Cad_WWR' is NaN or empty strings
    df = df.dropna(subset=['Cad_WWR'])
    df = df[df['Cad_WWR'] != ' ']

    df['Cad_WWR'] = pd.to_numeric(df['Cad_WWR'], errors='coerce')
    df['WWR'] = pd.to_numeric(df['WWR'], errors='coerce')

    df = df.dropna(subset=['Cad_WWR', 'WWR'])
    df = df[df['Cad_WWR'] > 0]

    df_sorted = df.sort_values(by='Cad_WWR').reset_index(drop=True)

    # Plotting
    fig, ax = plt.subplots(figsize=(12, 6))

    # Set bar width
    bar_width = 0.8

    for i in range(len(df_sorted)):
        x = df_sorted.index[i]
        predicted = df_sorted['WWR'].iloc[i]
        actual = df_sorted['Cad_WWR'].iloc[i]

        # Plot the shorter bar first
        if predicted >= actual:
            ax.bar(x, predicted, color='blue', width=bar_width, label='Predicted WWR (Model)' if i == 0 else "")
            ax.bar(x, actual, color='orange', width=bar_width, label='Actual WWR (AutoCAD)' if i == 0 else "")
        else:
            ax.bar(x, actual, color='orange', width=bar_width, label='Actual WWR (AutoCAD)' if i == 0 else "")
            ax.bar(x, predicted, color='blue', width=bar_width, label='Predicted WWR (Model)' if i == 0 else "")

    # Customize the plot
    ax.set_xlabel("Sample Index (Sorted by Actual WWR)")
    ax.set_ylabel("WWR Values")
    ax.set_title("Comparison of Predicted WWRs vs Actual WWRs")
    ax.legend()

    # Display the plot
    plt.tight_layout()
    plt.show()
```

```
import pandas as pd
import matplotlib.pyplot as plt

# Load the CSV data
df = pd.read_csv('/content/Broadway_East_Cad50smpl.csv')

# Drop rows where 'Cad_WWR' is NaN or empty strings
df = df.dropna(subset=['Cad_WWR'])
df = df[df['Cad_WWR'] != ' ']

# Convert 'Cad_WWR' and 'WWR' to numeric, coercing errors to NaN
df['Cad_WWR'] = pd.to_numeric(df['Cad_WWR'], errors='coerce')
df['WWR'] = pd.to_numeric(df['WWR'], errors='coerce')

# Drop rows where conversion failed or where Cad_WWR is not available
df = df.dropna(subset=['Cad_WWR', 'WWR'])
df = df[df['Cad_WWR'] > 0]

# Calculate residuals
df['Error'] = df['Cad_WWR'] - df['WWR']

# Plotting Residual Errors for Each Point
plt.figure(figsize=(10, 6))
plt.bar(range(len(df['Error'])), df['Error'], color='orange', alpha=0.7, edgecolor='black')
plt.xlabel("Data Point Index")
plt.ylabel("Residual Error")
plt.title("Residual Errors for Each Data Point")
plt.grid(axis='y', alpha=0.75)
plt.show()
```

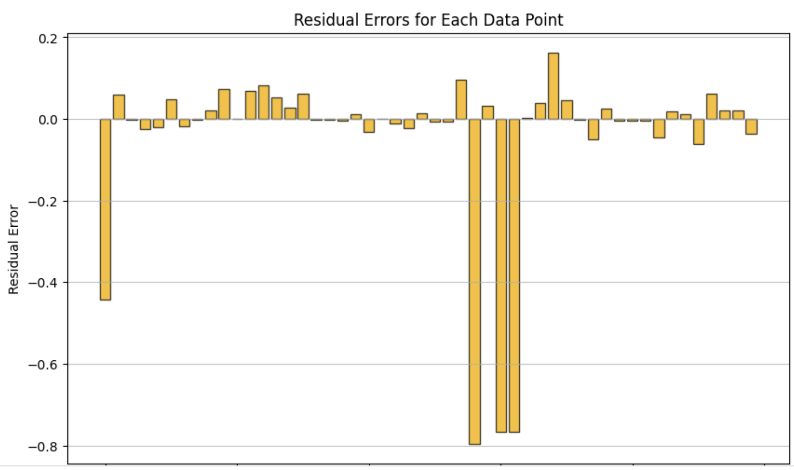

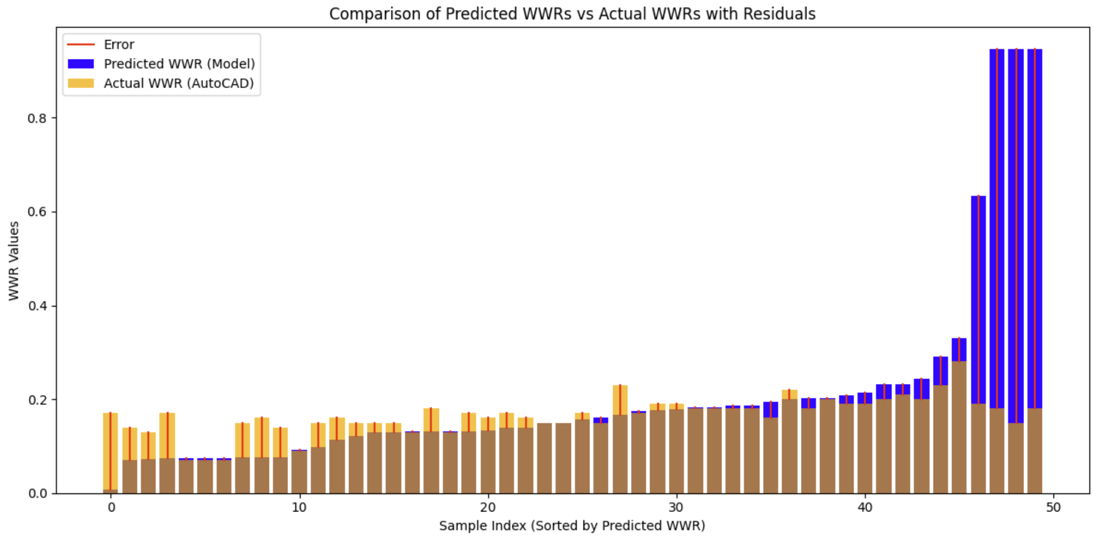


```
import pandas as pd
import matplotlib.pyplot as plt

df = pd.read_csv('/content/Broadway_East_Cad50smpl.csv')

df = df.dropna(subset=['Cad_WWR'])
df = df[df['Cad_WWR'] != ' ']

# Convert 'Cad_WWR' and 'WWR' to numeric, coercing errors to NaN
df['Cad_WWR'] = pd.to_numeric(df['Cad_WWR'], errors='coerce')
df['WWR'] = pd.to_numeric(df['WWR'], errors='coerce')

# Drop rows where conversion failed or where Cad_WWR is not available
df = df.dropna(subset=['Cad_WWR', 'WWR'])
df = df[df['Cad_WWR'] > 0]

# Calculate residuals
df['Residual'] = df['Cad_WWR'] - df['WWR']

# Sort by 'Cad_WWR' (Actual WWR) and reset index to ensure no gaps
df_sorted = df.sort_values(by='Cad_WWR').reset_index(drop=True)

# Plotting
fig, ax = plt.subplots(figsize=(12, 6))

# Set bar width
bar_width = 0.8
```

Calculate Mean realtive error elimianting 10%upper outliers

```
[ ]
threshold = df_clean["Relative Error"].quantile(0.90)

df_filtered = df_clean[df_clean["Relative Error"] <= threshold]

mean_relative_error_filtered = df_filtered["Relative Error"].mean()
median_relative_error_filtered = df_filtered["Relative Error"].median()

tools.display_dataframe_to_user(name="Filtered Relative Error Analysis", dataframe=df_filtered)

mean_relative_error_filtered, median_relative_error_filtered
```

```
[ ] df["WWR"] = pd.to_numeric(df["WWR"], errors="coerce")
df["Cad_WWR"] = pd.to_numeric(df["Cad_WWR"], errors="coerce")

df_clean = df.dropna(subset=["WWR", "Cad_WWR"])

df_clean["Relative Error"] = abs(df_clean["Cad_WWR"] - df_clean["WWR"]) / df_clean["Cad_WWR"]

mean_relative_error = df_clean["Relative Error"].mean()
median_relative_error = df_clean["Relative Error"].median()

import ace_tools as tools
tools.display_dataframe_to_user(name="Relative Error Analysis", dataframe=df_clean)

mean_relative_error, median_relative_error
```

Selecting 10% of datapoints for validation

```
[ ]
import pandas as pd

file_path = "/mnt/data/Broadway_East_Cad - Broadway_East_Cad.csv"
df = pd.read_csv(file_path)

df_unique = df.drop_duplicates(subset=["Address"])

df_unique["WWR"] = pd.to_numeric(df_unique["WWR"], errors="coerce")

df_detected = df_unique.dropna(subset=["WWR"])

sample_size = int(len(df_detected) * 0.10)
df_validation_sample = df_detected.sample(n=sample_size, random_state=42)  # Set random_state for reproducibility

import ace_tools as tools
tools.display_dataframe_to_user(name="Randomly Selected Validation Sample", dataframe=df_validation_sample)
```

```python
import matplotlib.pyplot as plt
import os
from PIL import Image, ImageDraw
from roboflow import Roboflow
from pathlib import Path

# Initialize Roboflow model
rf = Roboflow(api_key="2nDoXqGj")#Replace it with your API key
project = rf.workspace().project("window-detection-xowg3")
model = project.version(1).model

# Single building image analysis from Google Drive
image_path = '/content/drive/MyDrive/Broadway/1812 E Lafayette Ave, Baltimore, Maryland.jpg'  # Path to the single building image

if os.path.exists(image_path):
    with Image.open(image_path) as image:
        # Apply the window detection model
        result = model.predict(image_path, confidence=30, overlap=30).json()

        # Draw bounding boxes on the image
        draw = ImageDraw.Draw(image)
        for prediction in result['predictions']:
            bb = prediction['x'], prediction['y'], prediction['width'], prediction['height']
            x1 = int(bb[0] - bb[2] / 2)
            y1 = int(bb[1] - bb[3] / 2)
            x2 = int(bb[0] + bb[2] / 2)
            y2 = int(bb[1] + bb[3] / 2)
            draw.rectangle([x1, y1, x2, y2], outline="blue", width=3)

        # Display the image inline using Matplotlib
        plt.figure(figsize=(10, 8))
        plt.imshow(image)
        plt.title("Detected Windows for Single Building")
        plt.axis('off')
        plt.show()
else:
    print(f"Image not found at {image_path}")
```

```
loading Roboflow workspace...
loading Roboflow project...
```

Detected Windows for Single Building

Appendix B

Presentation Slides

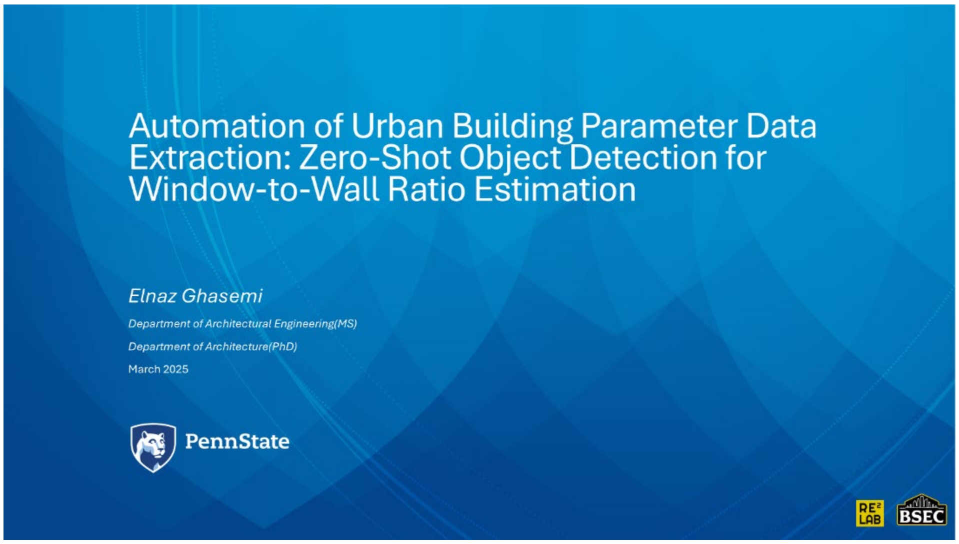

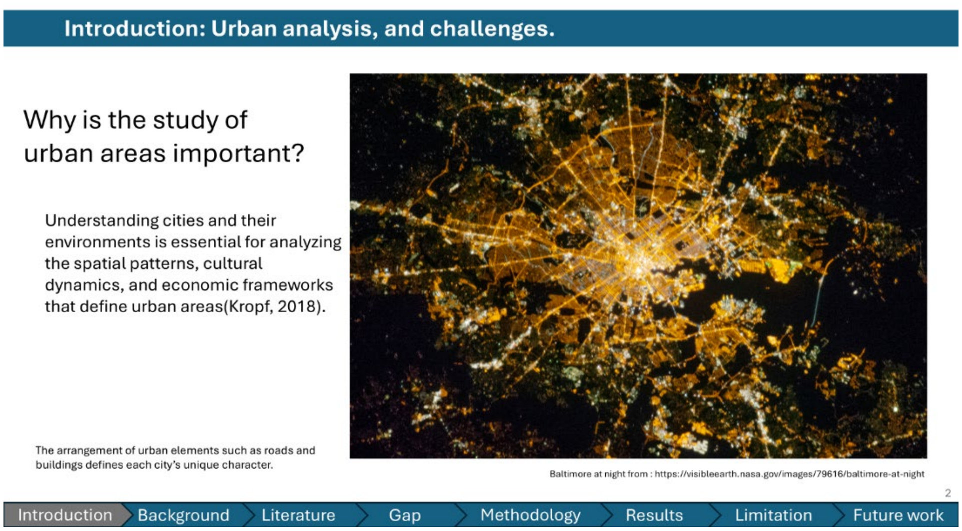

Introduction: Environmental issues

Cities are responsible for consuming a significant portion of global energy in different sectors, accounting for approximately 75% of primary energy use and 70% of greenhouse gas emissions(IEA, 2024).

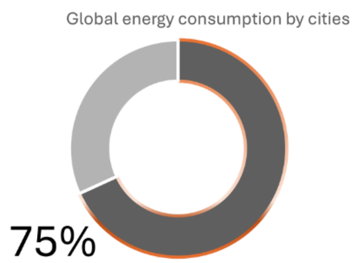

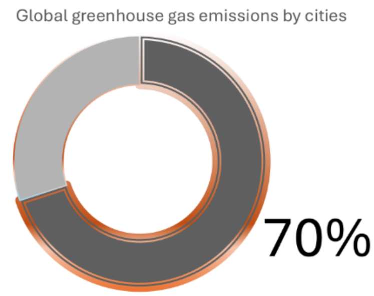

Introduction

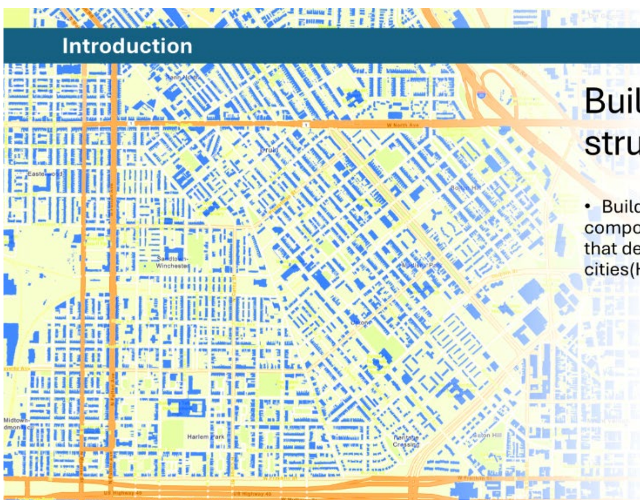

Buildings in urban structure

- Buildings are an essential physical component of urban settlements that define the structure of the cities(Hecht et al., 2013).

Energy and process-related CO2 emissions by buildings.

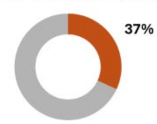

Introduction

Why do we need existing building geometric data?

To create a digital representation of buildings for the following purposes:

- Energy modeling and efficiency to support environmental goals (Herfort et al., 2023)
- Renovation and historical preservation

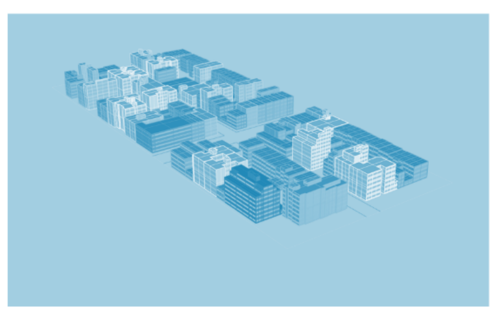

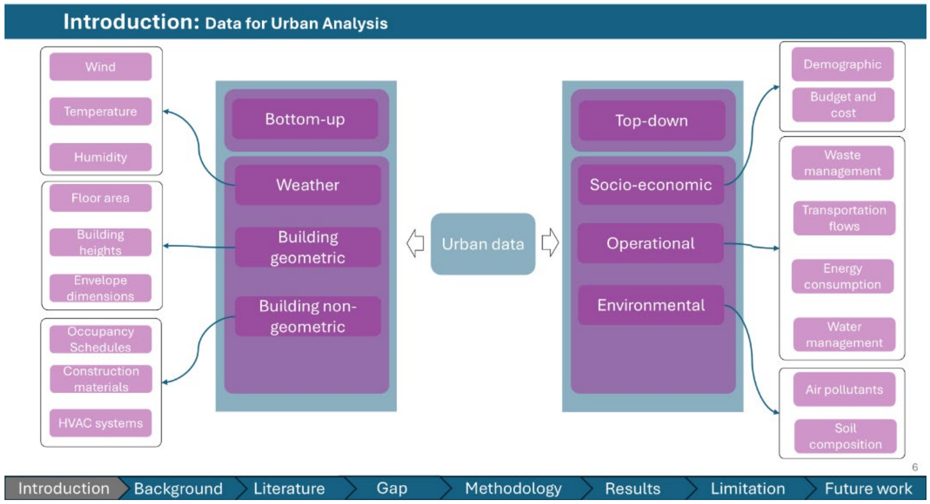
Introduction: Data for Urban Analysis
Wind
Temperature
Humidity
Floor area
Building heights
Envelope dimensions
Occupancy Schedules
Construction materials
HVAC systems
Bottom-up
Weather
Building geometric
Building non-geometric
Urban data
Top-down
Socio-economic
Operational
Environmental
Demographic
Budget and cost
Waste management
Transportation flows
Energy consumption
Water management
Air pollutants
Soil composition
Introduction
Background
Literature
Gap
Methodology
Results
Limitation
Future work

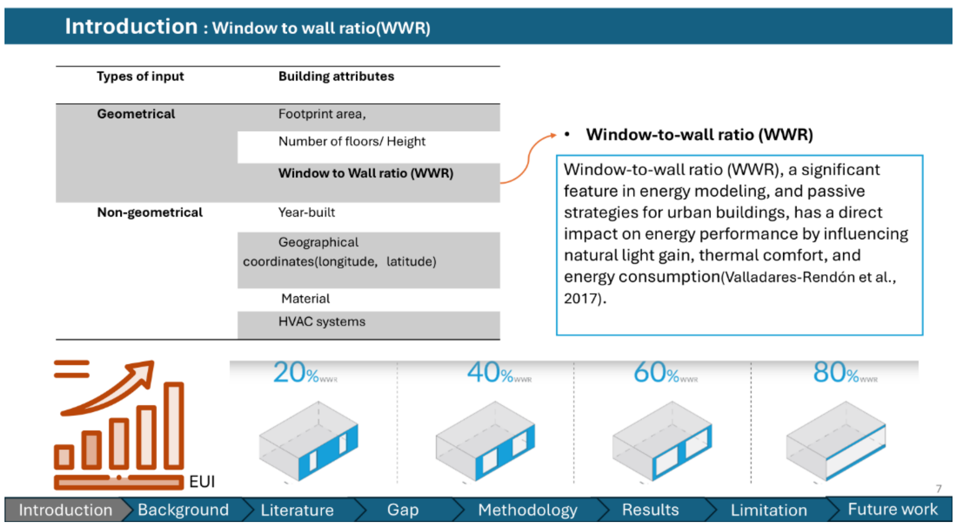
Introduction : Window to wall ratio(WWR)
Types of input
Building attributes
Geometrical
Footprint area,
Number of floors/ Height
Window to Wall ratio (WWR)
Non-geometrical
Year-built
Geographical coordinates(longitude, latitude)
Material
HVAC systems
• Window-to-wall ratio (WWR)
Window-to-wall ratio (WWR), a significant feature in energy modeling, and passive strategies for urban buildings, has a direct impact on energy performance by influencing natural light gain, thermal comfort, and energy consumption(Valladares-Rendón et al., 2017).
EUI
20%
40%
60%
80%
Introduction
Background
Literature
Gap
Methodology
Results
Limitation
Future work

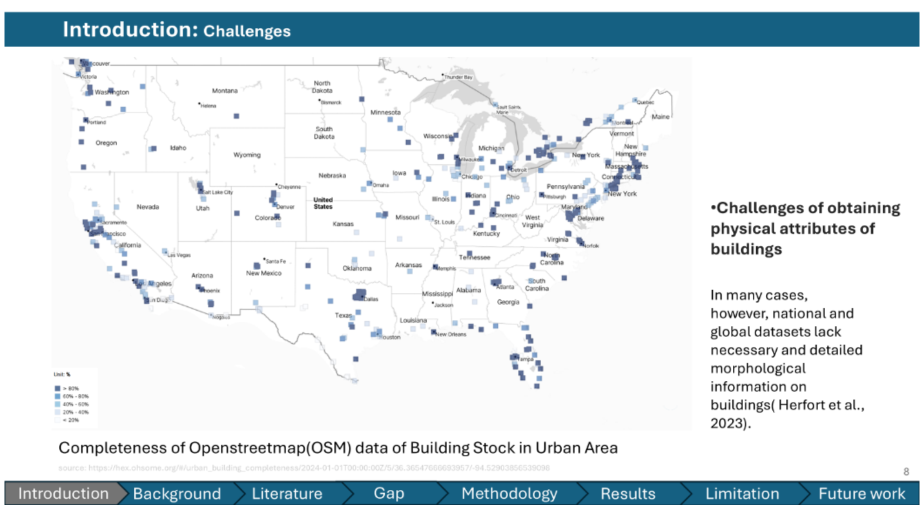
Introduction: Challenges
•Challenges of obtaining physical attributes of buildings
In many cases, however, national and global datasets lack necessary and detailed morphological information on buildings(Herfort et al., 2023).
Completeness of Openstreetmap(OSM) data of Building Stock in Urban Area
Introduction
Background
Literature
Gap
Methodology
Results
Limitation
Future work

Introduction: Problem statement

Problem statement

- There is no comprehensive and integrated urban-scale building geometric dataset, including WWR, in Baltimore, which is essential for urban building energy analysis.

Introduction | Background | Literature | Gap | Methodology | Results | Limitation | Future work

Introduction: Research Objectives

Main Research Objective: Developing a framework for extracting comprehensive urban geometrical data

Sub-Objectives:

Objective 1: Review object detection methods for urban building energy modeling.
Objective 2: Develop a framework for WWR extraction.
Objective 3: Integrate data to analyze the distribution of WWRs across construction periods in two studied neighborhoods.

10

Introduction | Background | Literature | Gap | Methodology | Results | Limitation | Future work

Background: Object detection

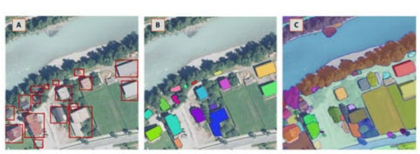

Shengzi Gui, 2023

- **Object Detection:**

•A computer vision technique used to **identify and locate objects** in images.

- **Zero-Shot Object Detection (ZSD):**

Unsupervised object detection method that identifies unseen object classes (Bansal et al., 2018).

•Unlike supervised learning, it does **not require labeled training data** for every class.

- **Advantages of ZSD in Urban Analysis:**

•**Bypasses the need for large labeled datasets**, reducing **time and resource constraints** (Brown et al., 2020).

•**Scalable and adaptable** for large-scale **urban energy modeling** and analysis.

11

Introduction | Background | Literature | Gap | Methodology | Results | Limitation | Future work

Literature Review

Object Detection in Urban Analysis: Applications and advancements.

Healthcare and medical scans

Agriculture, and monitor crop health

Urban planning and urban morphology monitoring

Literature review:

Extracting **single building façade dimensions** using 3d scanning, and Lidar to create a virtual representation of the building.

(Balsa-Barreiro & Fritsch, 2018; Moyano et al., 2022; Zalama et al., 2011)

Source of the image: https://lanmarservices.com/3d-laser-scanning-basics/

light detection and ranging(lidar)

Both produce point clouds, but LiDAR systems generally capture larger areas at lower resolution compared to laser scanning.

Literature review:

Summary of **urban-scale** building geometric characteristics extraction

Detection of thermal insulation damages, and analyze thermal performance of buildings (Balaras & Argiriou, 2002).

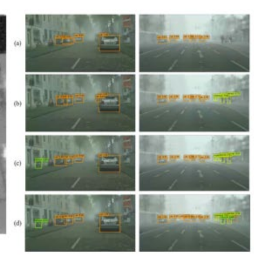

Improving object detection performance in real-world weather conditions for urban traffic analysis(X. Yu & Lu, 2024).

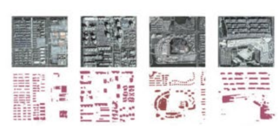

Building extraction for mid-rise, to high-rise buildings.

Building footprint identification, and extraction using satellite imagery(Luo et al., 2021).

Literature review:

Urban scale building characteristic extraction

- Combining RGB and thermal aerial images enables the construction of 3D geometries and thermal maps.
- Machine learning approach to extract building footprints, and window to wall ratio using aerial drone images of 45 degree.

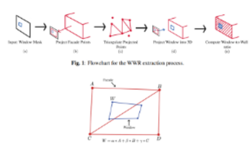

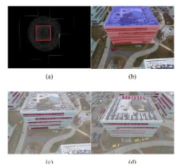

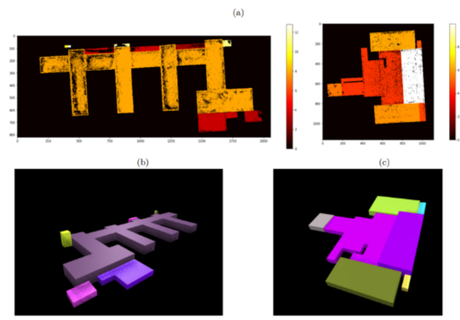

Samir Touzani, 2020, 2021.

15

Introduction | Background | Literature | Gap | Methodology | Results | Limitation | Future work

Previous studies:

Object detection methods to extract **window-to-wall ratio**

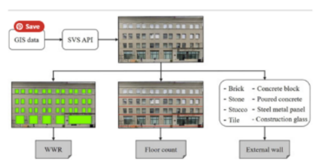

https://cocodataset.org/#home

Machine learning approach to extract building window to wall ratio using Google map Application programming interface.

Trained their model from scratch on curated datasets (unrealistic, idealized images) such as COCO(Ghorbany et al., 2024).

Data-driven models to calculate window-to-wall ratio, and number of floors for commercial buildings in a neighborhood scale of Pittsburgh city using Street View Statics (SVS) and Google images application programming interface (API). (Mohammadiziazi et al., 2021)

Uses semantic segmentation (Fully Convolutional Networks and SegFormer) to classify windows and façades in images, requiring explicit pixel-level labeling but do not propose a scalable method for city-wide WWR extraction(De Simone et al. 2023).

16

Introduction | Background | Literature | Gap | Methodology | Results | Limitation | Future work

Gap:

Gap

- Working on a small area of a block which is not scalable to a city
- Not applicable to other cities and building images since they have been trained on curated datasets (unrealistic, idealized images).
  - Creating curated datasets is costly and time consuming. Models that are trained purely on curated datasets are prune to learn spurious correlations of data (shortcuts in the data, e.g. special colors) instead of the actual task and they are difficult to generalize to other domains (e.g. other cities)
- Working on a single building
- Working on axonometric images, decreasing the accuracy of the results.

17

Introduction | Background | Literature | Gap | Methodology | Results | Limitation | Future work

State Of Art:

•**Introduction of a new pipeline** integrating **zero-shot object detection** into urban energy modeling workflows.

- The proposed approach is **highly scalable**, enabling the **automatic extraction of WWR** across **Baltimore and other urban environments**. Traditional methods rely on **supervised object detection models** that require **fine-tuning on large labeled datasets**, making them less adaptable to diverse building typologies.
- This research leverages the **zero-shot learning capability of multi-modal transformer-based models**, allowing **generalization across different urban settings** without additional training. Compared to previous studies, this method is **more adaptable and practical for large-scale urban energy modeling** (Chundawat et al., 2023).

Methodology:

1. **Data Collection:** Sources and types of data (Existing, and generated data).

   -**Building Detection:** Using Google Street View images and object detection models.

2. **Data Integration:** Spatial join techniques for combining data.

Required data for building energy modeling, and sources to obtain

Types of attributes	Building attributes	Sources	Type of source data
Geometrical	Footprint area	OpenStreetMap building footprint data(OpenStreetMap, n.d.)	GIS base data
	Number of floors	Real Property Information of Baltimore(Smeriglio, 2022)	Text
	Window to Wall ratio (WWR)	Street Images from Google Map API	Image
	Building orientation	Real Property Information of Baltimore(Smeriglio, 2022)	Text
Non-geometrical	Year-built, material, zone code, block, parcel, ward, address, direction, longitude, latitude,	Real Property Information of Baltimore(Baltimore City Real Property Assessments, 2024)	Text

Methodology:

- **Data Collection**

  Selected two neighborhoods with R-8 zone code(medium density) to develop the methodology:

  -Patterson Park,
  -And Broadway East

Google street image

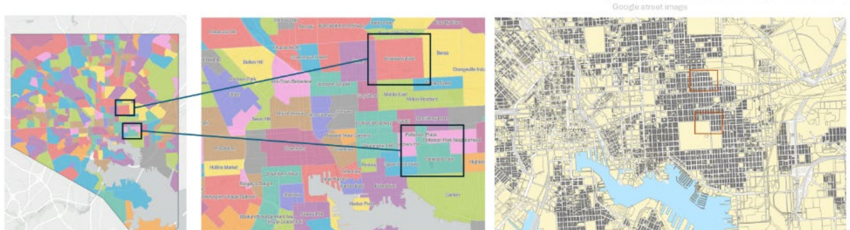

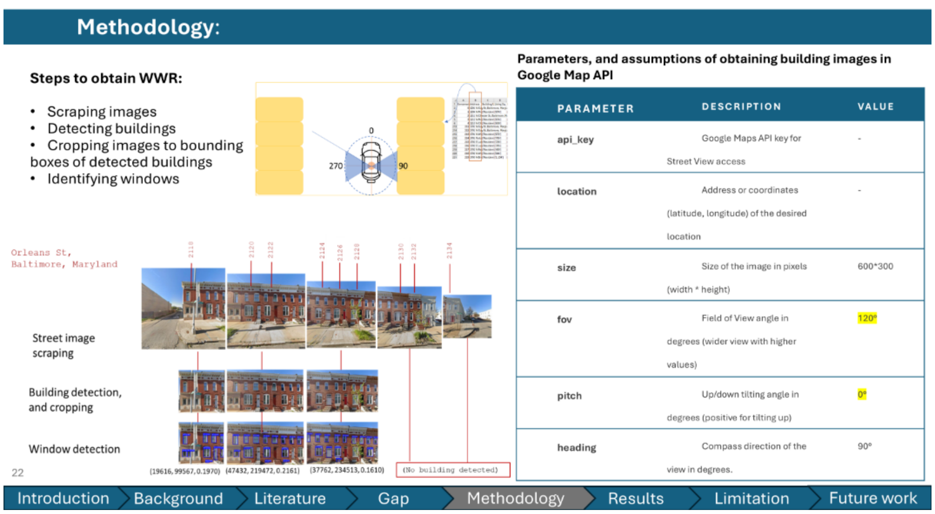

Parameters, and assumptions of obtaining building images in Google Map API

PARAMETER	DESCRIPTION	VALUE
api_key	Google Maps API key for Street View access	-
location	Address or coordinates (latitude, longitude) of the desired location	-
size	Size of the image in pixels (width * height)	600*300
fov	Field of View angle in degrees (wider view with higher values)	120°
pitch	Up/down tilting angle in degrees (positive for tilting up)	0°
heading	Compass direction of the view in degrees.	90°

Methodology:

- **Validation:**

Manually annotating the data by measuring window to wall ratio in AutoCad for 10% of the datapoints(addresses).

$$\mathrm{MSE} = \frac{1}{n}\sum_{i=1}^{n}(Y_i - \hat{Y}_i)^2$$

MSE = mean squared error
n = number of data points
Y_i = observed values
$\hat{Y}_i$ = predicted values

$$\mathrm{MAE} = \frac{\sum_{i=1}^{n}|y_i - x_i|}{n}$$

MAE = mean absolute error
y_i = prediction
x_i = true value
n = total number of data points

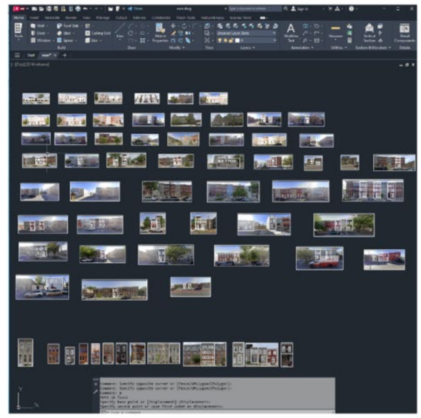

24

Methodology:

- **Applying the WWR extraction methodology to the four sides of a building**

WWR for four sides:

Addresses including " E "	Addresses including " N "
E = 0	E = Calculated via WWR extraction
W = 0	W = Calculated via WWR extraction*
N = Calculated via WWR extraction	N = 0
S = Calculated via WWR extraction*	S = 0

*Backyard façade WWR has been considered the same as the front.

$$WWR_i = \sum_{i=1}^{n}\frac{(Total\ detected\ glazing\ area)_i}{(Total\ detected\ building\ area)_i}$$

25

Methodology:

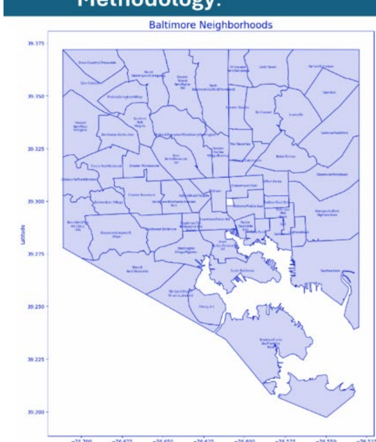

Data integration

- **Spatial Join:** Combining geometrical and non-geometrical data. Using longitude, and latitude of the buildings in ArcGIS.

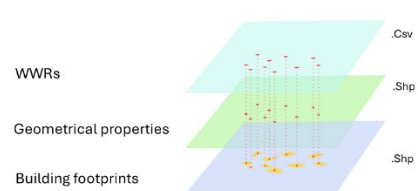

26

Results:

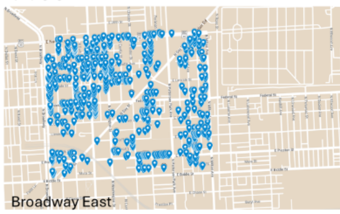

Geographical scope of WWR extraction

•Maps show the **distribution of datapoints and buildings** used as input for the model in **Broadway East** and **Patterson Park**.

•Percentage of calculated buildings by the model is displayed in the table.

Some buildings **were not processed** due to **occlusions, poor image quality, or missing Google Street View data**.

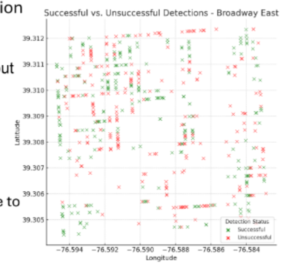

Percentage of total datapoints calculated by the model

Dataset	Percentage of WWR extraction	Number of building addresses	Total number of buildings in the neighborhood
Broadway	49.65%	640	4,629
Patterson	57.94%	991	6,381
Overall across two dataset	52.91%	1831	11,010

27

Introduction | Background | Literature | Gap | Methodology | Results | Limitation | Future work

Results:

- The predicted values, actual values, and residuals are shown for a total of 50 datapoints for validation(Removing 10% upper outliers).
- The actual WWRs range from 0.07 to 0.28, as illustrated in the graph.

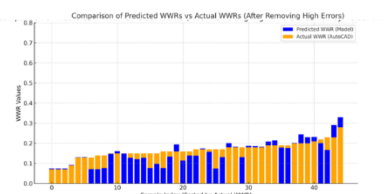

- Residual Errors for Predicted WWR Values, which range from ≈-0.06 to +0.9

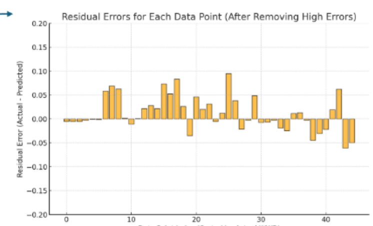

Performance metrics

Metric	Value	Value(After removing 10% outliers)
Mean Absolute Error (MAE)	0.0839	0.0262
Mean Squared Error (MSE)	0.0418	0.0013

28

Introduction | Background | Literature | Gap | Methodology | Results | Limitation | Future work

Results:

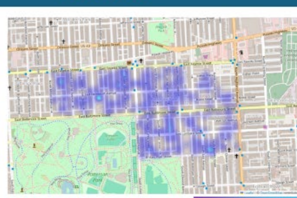

Patterson Park

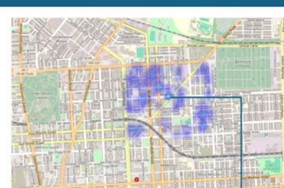

Broadway East

Distribution of WWR Values in Patterson Park

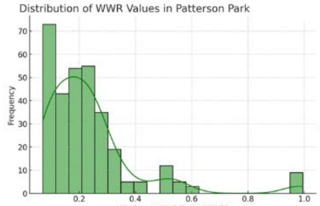

Distribution of WWR Values in Broadway East

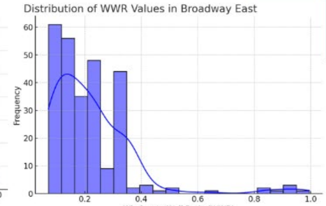

- Heatmap of the value of WWRs across the two neighborhoods

-An example of an apartment with higher WWR in comparison to rowhouse attached buildings:

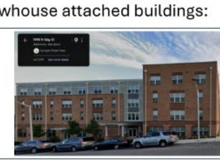

- Histogram distribution of WWRs across the two neighborhooods:

-The highest frequency of WWR values is in the **0.1-0.2** range.

29

Introduction | Background | Literature | Gap | Methodology | Results | Limitation | Future work

Results:

WWR Distribution by Year of Construction

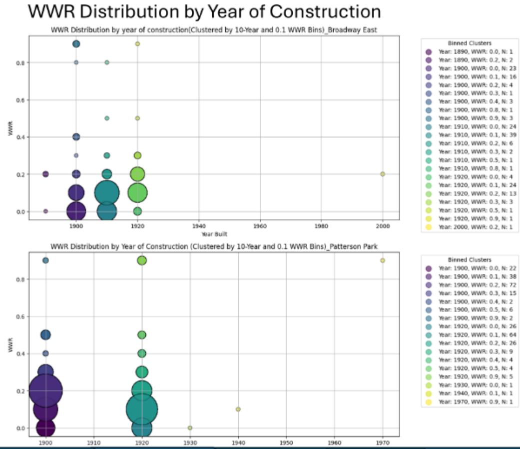

-Broadway East: Most of the buildings were constructed before 1920, with the majority having WWR values in the range of 0.1–0.15.

-Patterson Park: The majority of buildings have a WWR of 0.2 and were primarily built around 1900.

-The results of this analysis are particularly important for energy and carbon modeling of these neighborhoods.

The wider distribution range of WWR values in Patterson Park suggests a greater variety of building archetypes for modeling phase.

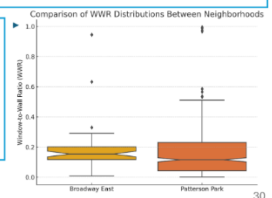

Results:

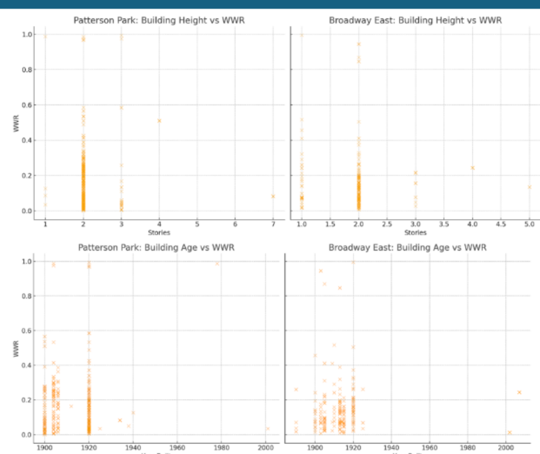

- Scatterplot of building age vs WWR, and Building height vs WWR

-Percentage of buildings with two stories:
•**Patterson Park**: **89.53%**
•**Broadway East**: **62.46%**

-Both neighborhoods have **most buildings constructed before 1920**, with very few structures built after this period.

- More variation in WWR in Patterson Park suggests a greater variety of building typologies.

• Limitations:

Occlusion Challenges:

- Buildings may be partially obscured by trees, vehicles, or people, leading to incomplete or inaccurate WWR extraction. Occlusions disrupt façade segmentation and pattern detection (Wendel et al., 2010; Lian et al., 2018).

Architectural Variability:

- Model applied to historical neighborhoods with multifamily attached buildings, limiting WWR extraction for all four sides of single-family homes due to missing Google Maps images.

Image Quality Issues:

- Some Google Street View images were too blurry, affecting building and window detection accuracy (J. Wang et al., 2022).

a. Occluded building

b. Image Quality Issues

Future Works: Integrating Domain Knowledge

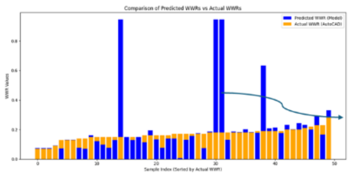

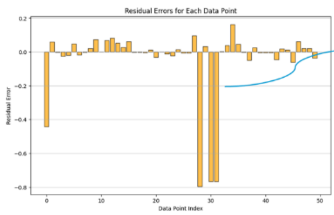

•Issue: Initial 90-degree camera angle led to capturing streets instead of buildings, in some cases, causing outlier WWR values.

•Proposed Solution: Incorporate human prior knowledge to refine building extraction.

- Inspired by Liu et al. (2020) on prior knowledge in face parsing.

Outlier: 0.8

An example of the outliers generated by the model (Up) with the actual building image associated with the address (down)

1812 E Federal St, Baltimore, Maryland

heading=90

heading=0

Correct image

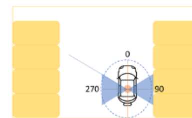

•Improvement Strategy: Adjust image capture angles dynamically.

- Continue capturing until WWR values fall within a **reasonable range (0.1–0.4)**.

33

Introduction | Background | Literature | Gap | Methodology | Results | Limitation | Future work

Future Works:

•Addressing Occlusions:

- Leverage urban building characteristics, such as **regularity, to enhance occlusion detection** (Lian et al., 2018).
- Improve segmentation accuracy for obstructed façades.

•Other Assessments:

- Develop a framework to detect **low-emissivity (Low-E) glass** in windows from street images.
- Improve energy modeling precision and contribute to urban sustainability analysis.

- **Acknowledgments**
  - **Funding:** U.S. Department of Energy.
    Baltimore Social Environmental Collaboration (BSEC) project.

- **Publication**
  - The full paper of this analysis has been accepted by ARCC conference, Washington DC, April 2025.

34

Introduction | Background | Literature | Gap | Methodology | Results | Limitation | Future work

References

- -Delmastro, C., & Chen, O. (2023). IEA_Tracking Buildings. IEA. https://www.iea.org/energy-system/buildings
- -Barns, S. (2018). Smart cities and urban data platforms: Designing interfaces for smart governance. *City, Culture and Society*, *12*, 5–12. https://doi.org/10.1016/j.ccs.2017.09.006
- -Ali, U., Shamsi, M. H., Hoare, C., Mangina, E., & O'Donnell, J. (2021). Review of urban building energy modeling (UBEM) approaches, methods and tools using qualitative and quantitative analysis. *Energy and Buildings*, *246*, 111073. https://doi.org/10.1016/j.enbuild.2021.111073
- -Luo, H., He, B., Guo, R., Wang, W., Kuai, X., Xia, B., Wan, Y., Ma, D., & Xie, L. (2021). Urban Building Extraction and Modeling Using GF-7 DLC and MUX Images. *Remote Sensing*, *13*(17), Article 17. https://doi.org/10.3390/rs13173414
- Building footprint and height extraction from RGB drone imagery (Conference Presentation) Conference Paper , Samir Touzani, Jessica Granderson, April 2020 .
- A machine learning approach to estimate windows-to-wall ratio using drone imagery, Samir Touzani, Marc Wudunn, Samuel Fernandes, Avideh Zakhor, Rohullah Najibi, and Jessica Granderson, 2021.
- Gui, S., Song, S., Qin, R., & Tang, Y. (2024). Remote Sensing Object Detection in the Deep Learning Era—A Review. *Remote Sensing*, *16*(2), 327. https://doi.org/10.3390/rs16020327
- Liu, H., Xu, Y., Zhang, J., Zhu, J., Li, Y., & Hoi, S. C. H. (2020). DeepFacade: A Deep Learning Approach to Facade Parsing With Symmetric Loss. IEEE Transactions on Multimedia, 22(12), 3153–3165. IEEE Transactions on Multimedia. https://doi.org/10.1109/TMM.2020.2971431
- Lian, Y., Shen, X., & Hu, Y. (2018). Detecting and inferring repetitive elements with accurate locations and shapes from façades. The Visual Computer, 34(4), 491–506. https://doi.org/10.1007/s00371-017-1355-z
- Wang, J., Jin, L., & Ding, K. (2022). LiLT: A Simple yet Effective Language-Independent Layout Transformer for Structured Document Understanding (arXiv:2202.13669). arXiv. https://doi.org/10.48550/arXiv.2202.13669
- Wendel, A., Donoser, M., & Bischof, H. (2010). Unsupervised Facade Segmentation Using Repetitive Patterns. In M. Goesele, S. Roth, A. Kuijper, B. Schiele, & K. Schindler (Eds.), Pattern Recognition (pp. 51–60). Springer. https://doi.org/10.1007/978-3-642-15986-2_6

35

References

- IEA. (2023). IEA_Tracking Buildings. IEA. https://www.iea.org/energy-system/buildings
- IEA. (2024). Empowering Urban Energy Transitions. IEA. https://www.iea.org/reports/empowering-urban-energy-transitions/executive-summary
- IECC & International Code Council. (2021). International energy conservation code. International Code Council. (2021). General Requirements. https://codes.iccsafe.org/content/IECC2021P1/chapter-3-ce-general-requirements#IECC2021P1_CE_Ch03_SecC301
- Ghorbany, S., Hu, M., Yao, S., Wang, C., Nguyen, Q. C., Yue, X., Alirezaei, M., Tasdizen, T., & Sisk, M. (2024). Examining the role of passive design indicators in energy burden reduction: Insights from a machine learning and deep learning approach. Building and Environment, 250, 111126. https://doi.org/10.1016/j.buildenv.2023.111126
- Dabirian, S., Saad, M. M., Hussain, S., Peyman, S., Rahimi, N., Monsalvete Alvarez U, P., Yefi, P., & Eicker, U. (2023). Structuring heterogeneous urban data: A framework to develop the data model for energy simulation of cities. Energy and Buildings, 296, 113376. https://doi.org/10.1016/j.enbuild.2023.113376
- Bureau of the Census. (2023). Baltimore Metropolitan Council. https://www.baltometro.org/data/13-residential-units-permitted
- Baltimore City Real Property Assessments. (2024). Opendata.Maryland.Gov. https://opendata.maryland.gov/Business-and-Economy/Baltimore-City-Real-Property-Assessments-Hidden-Pr/3x3p-xk2v/about_data
- Simone, Z. D., Biswas, S., & Wu, O. (2024). Window to Wall Ratio Detection using SegFormer (arXiv:2406.02706). arXiv. https://doi.org/10.48550/arXiv.2406.02706

36

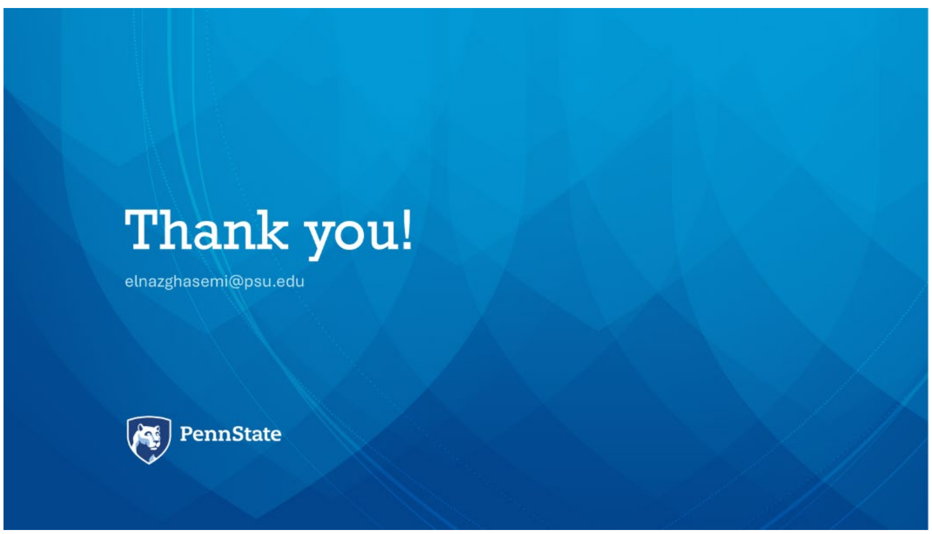

Appendix C

Addresses

The list of addresses has been shown below. The rows without a WWR number indicate buildings which are not detected in the image.

Address	WWR	Address	WWR
1 N Curley St, Baltimore, Maryland	0.2617099	1201 N Gay St, Baltimore, Maryland	0.633147
1 N Glover St, Baltimore, Maryland		1204 N Montford Ave, Baltimore, Maryland	
1 N Kenwood Ave, Baltimore, Maryland	0.0067164	1211 N Chester St, Baltimore, Maryland	
1 N Linwood Ave, Baltimore, Maryland	0.0175161	1212 N Montford Ave, Baltimore, Maryland	0.071535
1 N Luzerne Ave, Baltimore, Maryland		1213 N Chester St, Baltimore, Maryland	
1 N Milton Ave, Baltimore, Maryland		1213 N Montford Ave, Baltimore, Maryland	
1 S Ellwood Ave, Baltimore, Maryland	0.006167	1217 N Broadway, Baltimore, Maryland	0.04591
1 S Linwood Ave, Baltimore, Maryland	0.0481644	1219 N Gay St, Baltimore, Maryland	0.131402
10 N Clinton St, Baltimore, Maryland		1220 N Montford Ave, Baltimore, Maryland	0.022335
10 N Highland Ave, Baltimore, Maryland		1221 N Broadway, Baltimore, Maryland	0.214462
10 N Lakewood Ave, Baltimore, Maryland	0.0270666	1223 N Broadway, Baltimore, Maryland	0.214462
10 N Linwood Ave, Baltimore, Maryland		1223 N Montford Ave, Baltimore, Maryland	0.071535
10 N Potomac St, Baltimore, Maryland		1224 N Washington St, Baltimore, Maryland	
10 S Decker Ave, Baltimore, Maryland	0.2236563	1225 N Broadway, Baltimore, Maryland	0.214462
100 N Decker Ave, Baltimore, Maryland	0.216636	1225 N Montford Ave, Baltimore, Maryland	0.212785
100 N Ellwood Ave, Baltimore, Maryland	0.2238837	1229 N Gay St, Baltimore, Maryland	0.201314
100 S Clinton St, Baltimore, Maryland	0.0148718	1238 N Gay St, Baltimore, Maryland	0.131402
100 S Potomac St, Baltimore, Maryland		1240 N Gay St, Baltimore, Maryland	0.131402
101 N Belnord Ave, Baltimore, Maryland		1253 N Broadway, Baltimore, Maryland	0.208776
101 N Curley St, Baltimore, Maryland	0.9678322	1255 N Broadway, Baltimore, Maryland	0.156461
101 N Linwood Ave, Baltimore, Maryland		1257 N Broadway, Baltimore, Maryland	0.156461
101 N Luzerne Ave, Baltimore, Maryland		1257 N Broadway, Baltimore, Maryland	0.156461
101 N Rose St, Baltimore, Maryland		1257 N Broadway, Baltimore, Maryland	0.156461
101 Rochester Pl, Baltimore, Maryland	0.168448	1301 N Broadway, Baltimore, Maryland	0.202668
101 S Linwood Ave, Baltimore, Maryland	0.0596131	1302 N Montford Ave, Baltimore, Maryland	
101 S Robinson St, Baltimore, Maryland		1303 N Broadway, Baltimore, Maryland	0.139627
102 N Clinton St, Baltimore, Maryland		1304 N Montford Ave, Baltimore, Maryland	
102 N Decker Ave, Baltimore, Maryland	0.216636	1310 N Montford Ave, Baltimore, Maryland	
102 N Kenwood Ave, Baltimore, Maryland		1311 N Broadway, Baltimore, Maryland	
102 N Lakewood Ave, Baltimore, Maryland	0.0861933	1311 N Montford Ave, Baltimore, Maryland	
102 N Luzerne Ave, Baltimore, Maryland		1312 N Chester St, Baltimore, Maryland	
102 N Potomac St, Baltimore, Maryland	0.5372421	1314 N Chester St, Baltimore, Maryland	

102 N Streeper St, Baltimore, Maryland	0.1140205	1317 N Montford Ave, Baltimore, Maryland	0.076958
102 Rochester Pl, Baltimore, Maryland	0.168448	1317 N Washington St, Baltimore, Maryland	0.149162
102 S East Ave, Baltimore, Maryland		1318 N Milton Ave, Baltimore, Maryland	0.070886
102 S Ellwood Ave, Baltimore, Maryland	0.2407612	1319 N Montford Ave, Baltimore, Maryland	0.076958
102 S Potomac St, Baltimore, Maryland		1320 N Chester St, Baltimore, Maryland	
103 N Ellwood Ave, Baltimore, Maryland	0.2238837	1321 N Montford Ave, Baltimore, Maryland	0.09767
103 N Glover St, Baltimore, Maryland		1322 N Chester St, Baltimore, Maryland	
103 S Clinton St, Baltimore, Maryland	0.0147302	1322 N Milton Ave, Baltimore, Maryland	0.037013
103 S Curley St, Baltimore, Maryland	0.2562298	1326 N Chester St, Baltimore, Maryland	
103 S Linwood Ave, Baltimore, Maryland	0.0596131	1327 N Wolfe St, Baltimore, Maryland	
103 S Potomac St, Baltimore, Maryland		1334 N Chester St, Baltimore, Maryland	
103 S Potomac St, Baltimore, Maryland		1402 N Milton Ave, Baltimore, Maryland	0.014318
104 N Curley St, Baltimore, Maryland	0.9678322	1406 N Montford Ave, Baltimore, Maryland	0.121832
104 N East Ave, Baltimore, Maryland		1409 N Collington Ave, Baltimore, Maryland	
104 N Lakewood Ave, Baltimore, Maryland	0.0193289	1416 N Collington Ave, Baltimore, Maryland	
104 N Potomac St, Baltimore, Maryland		1418 N Milton Ave, Baltimore, Maryland	
104 Rochester Pl, Baltimore, Maryland	0.1494198	1422 N Collington Ave, Baltimore, Maryland	
104 S Bouldin St, Baltimore, Maryland		1428 N Milton Ave, Baltimore, Maryland	
104 S East Ave, Baltimore, Maryland		1432 N Milton Ave, Baltimore, Maryland	
104 S Ellwood Ave, Baltimore, Maryland		1434 N Milton Ave, Baltimore, Maryland	
104 S Highland Ave, Baltimore, Maryland		1435 N Broadway, Baltimore, Maryland	0.021143
104 S Potomac St, Baltimore, Maryland		1500 N Collington Ave, Baltimore, Maryland	0.070947
105 N Belnord Ave, Baltimore, Maryland	0.3093659	1500 N Washington St, Baltimore, Maryland	0.097854
105 N Clinton St, Baltimore, Maryland		1500 N Wolfe St, Baltimore, Maryland	
105 N Curley St, Baltimore, Maryland	0.9678322	1500 N Wolfe St, Baltimore, Maryland	
105 N Glover St, Baltimore, Maryland	0.2279161	1501 N Collington Ave, Baltimore, Maryland	0.070947
105 N Lakewood Ave, Baltimore, Maryland		1502 N Wolfe St, Baltimore, Maryland	
105 N Luzerne Ave, Baltimore, Maryland		1503 N Wolfe St, Baltimore, Maryland	
105 N Rose St, Baltimore, Maryland	0.2711301	1504 N Collington Ave, Baltimore, Maryland	
105 Rochester Pl, Baltimore, Maryland	0.1494198	1504 Rutland Ave, Baltimore, Maryland	
106 N Belnord Ave, Baltimore, Maryland	0.3094145	1506 N Collington Ave, Baltimore, Maryland	
106 N Kenwood Ave, Baltimore, Maryland	0.0385129	1506 Rutland Ave, Baltimore, Maryland	
106 N Linwood Ave, Baltimore, Maryland		1507 N Collington Ave, Baltimore, Maryland	
106 N Luzerne Ave, Baltimore, Maryland	0.0785754	1507 N Wolfe St, Baltimore, Maryland	
106 N Potomac St, Baltimore, Maryland		1508 N Collington Ave, Baltimore, Maryland	
106 N Streeper St, Baltimore, Maryland		1509 N Port St, Baltimore, Maryland	
106 Rochester Pl, Baltimore, Maryland	0.1494198	1509 N Wolfe St, Baltimore, Maryland	
106 Rochester Pl, Baltimore, Maryland	0.1494198	1510 N Durham St, Baltimore, Maryland	0.221718
106 S Clinton St, Baltimore, Maryland		1510 N Montford Ave, Baltimore, Maryland	
107 N Clinton St, Baltimore, Maryland		1511 N Collington Ave, Baltimore, Maryland	
107 N Ellwood Ave, Baltimore, Maryland		1511 N Wolfe St, Baltimore, Maryland	
107 N Luzerne Ave, Baltimore, Maryland	0.0785754	1512 N Collington Ave, Baltimore, Maryland	0.017059
107 N Streeper St, Baltimore, Maryland	0.1125042	1513 N Collington Ave, Baltimore, Maryland	0.017059

107 S Bouldin St, Baltimore, Maryland		1513 N Montford Ave, Baltimore, Maryland	
107 S Clinton St, Baltimore, Maryland	0.0337216	1514 Rutland Ave, Baltimore, Maryland	
107 S Curley St, Baltimore, Maryland	0.2562298	1515 N Broadway, Baltimore, Maryland	0.218242
107 S Linwood Ave, Baltimore, Maryland	0.0509226	1516 N Collington Ave, Baltimore, Maryland	0.07681
107 S Robinson St, Baltimore, Maryland	0.2171593	1517 N Collington Ave, Baltimore, Maryland	0.017059
108 N Belnord Ave, Baltimore, Maryland	0.3094145	1517 N Wolfe St, Baltimore, Maryland	
108 N Curley St, Baltimore, Maryland	0.1366638	1518 N Collington Ave, Baltimore, Maryland	0.07681
108 N Decker Ave, Baltimore, Maryland	0.1543647	1519 N Collington Ave, Baltimore, Maryland	0.07681
108 N East Ave, Baltimore, Maryland		1519 Rutland Ave, Baltimore, Maryland	0.057578
108 N Glover St, Baltimore, Maryland	0.2279161	1521 N Broadway, Baltimore, Maryland	0.077087
108 N Lakewood Ave, Baltimore, Maryland		1521 N Wolfe St, Baltimore, Maryland	
108 N Rose St, Baltimore, Maryland	0.2663524	1523 N Broadway, Baltimore, Maryland	0.077087
108 N Streeper St, Baltimore, Maryland	0.0259897	1523 N Wolfe St, Baltimore, Maryland	
108 Rochester Pl, Baltimore, Maryland	0.067295	1524 N Wolfe St, Baltimore, Maryland	
108 S Bouldin St, Baltimore, Maryland		1527 N Broadway, Baltimore, Maryland	0.048943
108 S Curley St, Baltimore, Maryland	0.2885112	1527 N Wolfe St, Baltimore, Maryland	
109 N Clinton St, Baltimore, Maryland		1528 N Wolfe St, Baltimore, Maryland	
109 N Decker Ave, Baltimore, Maryland	0.1543647	1531 N Broadway, Baltimore, Maryland	0.067343
109 N East Ave, Baltimore, Maryland		1532 N Wolfe St, Baltimore, Maryland	
109 N Kenwood Ave, Baltimore, Maryland	0.0385129	1533 N Broadway, Baltimore, Maryland	0.067343
109 N Lakewood Ave, Baltimore, Maryland	0.0193289	1533 N Wolfe St, Baltimore, Maryland	
109 N Linwood Ave, Baltimore, Maryland		1537 N Wolfe St, Baltimore, Maryland	0.091014
109 N Luzerne Ave, Baltimore, Maryland	0.0785754	1600 N Chester St, Baltimore, Maryland	0.347557
109 N Milton Ave, Baltimore, Maryland	0.0418993	1600 N Chester St, Baltimore, Maryland	0.347557
109 S Bouldin St, Baltimore, Maryland		1600 N Chester St, Baltimore, Maryland	0.347557
109 S Linwood Ave, Baltimore, Maryland		1600 N Chester St, Baltimore, Maryland	0.347557
11 N Curley St, Baltimore, Maryland	0.2018005	1600 N Chester St, Baltimore, Maryland	0.347557
11 N Decker Ave, Baltimore, Maryland	0.3025894	1600 N Chester St, Baltimore, Maryland	0.347557
11 N Ellwood Ave, Baltimore, Maryland	0.1760974	1600 N Chester St, Baltimore, Maryland	0.347557
11 N Kenwood Ave, Baltimore, Maryland	0.0330408	1600 N Chester St, Baltimore, Maryland	0.347557
11 N Luzerne Ave, Baltimore, Maryland	0.0288422	1600 N Chester St, Baltimore, Maryland	0.347557
11 N Potomac St, Baltimore, Maryland	0.0146383	1600 N Chester St, Baltimore, Maryland	0.347557
11 S Curley St, Baltimore, Maryland	0.2230103	1600 N Chester St, Baltimore, Maryland	0.347557
11 S Ellwood Ave, Baltimore, Maryland		1600 N Chester St, Baltimore, Maryland	0.347557
11 S Linwood Ave, Baltimore, Maryland	0.0060962	1600 N Chester St, Baltimore, Maryland	0.347557
110 N Belnord Ave, Baltimore, Maryland	0.1897453	1600 N Chester St, Baltimore, Maryland	0.347557
110 N Decker Ave, Baltimore, Maryland	0.1543647	1600 N Chester St, Baltimore, Maryland	0.347557
110 N East Ave, Baltimore, Maryland		1600 N Chester St, Baltimore, Maryland	0.347557
110 N Highland Ave, Baltimore, Maryland		1600 N Chester St, Baltimore, Maryland	0.347557
110 N Kenwood Ave, Baltimore, Maryland		1600 N Chester St, Baltimore, Maryland	0.347557
110 N Lakewood Ave, Baltimore, Maryland		1600 N Chester St, Baltimore, Maryland	0.347557
110 N Linwood Ave, Baltimore, Maryland		1600 N Chester St, Baltimore, Maryland	0.347557
110 N Luzerne Ave, Baltimore, Maryland	0.0341939	1600 N Chester St, Baltimore, Maryland	0.347557

110 Rochester Pl, Baltimore, Maryland	0.067295	1600 N Chester St, Baltimore, Maryland	0.347557
110 S Clinton St, Baltimore, Maryland		1600 N Chester St, Baltimore, Maryland	0.347557
110 S Curley St, Baltimore, Maryland	0.2885112	1600 N Chester St, Baltimore, Maryland	0.347557
110 S East Ave, Baltimore, Maryland		1600 N Chester St, Baltimore, Maryland	0.347557
110 S Ellwood Ave, Baltimore, Maryland		1600 N Chester St, Baltimore, Maryland	0.347557
111 N Clinton St, Baltimore, Maryland		1600 N Chester St, Baltimore, Maryland	0.347557
111 N Decker Ave, Baltimore, Maryland	0.1543647	1600 N Chester St, Baltimore, Maryland	0.347557
111 N East Ave, Baltimore, Maryland		1600 N Chester St, Baltimore, Maryland	0.347557
111 N Kenwood Ave, Baltimore, Maryland		1600 N Chester St, Baltimore, Maryland	0.347557
111 N Linwood Ave, Baltimore, Maryland		1600 N Chester St, Baltimore, Maryland	0.347557
111 N Streeper St, Baltimore, Maryland	0.1140205	1600 N Chester St, Baltimore, Maryland	0.347557
111 Rochester Pl, Baltimore, Maryland	0.067295	1600 N Chester St, Baltimore, Maryland	0.347557
111 S Linwood Ave, Baltimore, Maryland		1600 N Chester St, Baltimore, Maryland	0.347557
112 N Decker Ave, Baltimore, Maryland	0.037103	1600 N Chester St, Baltimore, Maryland	0.347557
112 N Ellwood Ave, Baltimore, Maryland	0.0357214	1600 N Chester St, Baltimore, Maryland	0.347557
112 N Highland Ave, Baltimore, Maryland		1600 N Chester St, Baltimore, Maryland	0.347557
112 N Linwood Ave, Baltimore, Maryland		1600 N Chester St, Baltimore, Maryland	0.347557
112 N Streeper St, Baltimore, Maryland		1600 N Chester St, Baltimore, Maryland	0.347557
112 S Clinton St, Baltimore, Maryland		1601 N Broadway, Baltimore, Maryland	0.182582
112 S Highland Ave, Baltimore, Maryland		1601 N Broadway, Baltimore, Maryland	0.182582
112 S Potomac St, Baltimore, Maryland		1601 N Broadway, Baltimore, Maryland	0.182582
101 N Clinton St, Baltimore, Maryland	0.0138664	1601 N Broadway, Baltimore, Maryland	0.182582
101 N Lakewood Ave, Baltimore, Maryland	0.0861933	1601 Rutland Ave, Baltimore, Maryland	
101 S East Ave, Baltimore, Maryland		1601 Rutland Ave, Baltimore, Maryland	
101 S Ellwood Ave, Baltimore, Maryland	0.0829734	1602 N Wolfe St, Baltimore, Maryland	
101 S Ellwood Ave, Baltimore, Maryland	0.0829734	1603 N Broadway, Baltimore, Maryland	0.182582
101 S Ellwood Ave, Baltimore, Maryland	0.0829734	1603 N Wolfe St, Baltimore, Maryland	
101 S Ellwood Ave, Baltimore, Maryland	0.0829734	1604 N Wolfe St, Baltimore, Maryland	
101 S Ellwood Ave, Baltimore, Maryland	0.0829734	1605 N Wolfe St, Baltimore, Maryland	
101 S Ellwood Ave, Baltimore, Maryland	0.0829734	1606 N Milton Ave, Baltimore, Maryland	0.077118
113 N Ellwood Ave, Baltimore, Maryland	0.0357214	1607 Rutland Ave, Baltimore, Maryland	
113 N Kenwood Ave, Baltimore, Maryland		1609 N Bradford St, Baltimore, Maryland	
113 N Lakewood Ave, Baltimore, Maryland		1609 N Broadway, Baltimore, Maryland	0.02258
113 N Luzerne Ave, Baltimore, Maryland	0.0341939	1609 N Broadway, Baltimore, Maryland	0.02258
113 N Potomac St, Baltimore, Maryland		1609 N Wolfe St, Baltimore, Maryland	
113 N Rose St, Baltimore, Maryland	0.2491543	1609 Rutland Ave, Baltimore, Maryland	
113 Rochester Pl, Baltimore, Maryland		1610 N Milton Ave, Baltimore, Maryland	0.077118
113 S Bouldin St, Baltimore, Maryland		1610 N Wolfe St, Baltimore, Maryland	
113 S Clinton St, Baltimore, Maryland	0.0148718	1612 N Chapel St, Baltimore, Maryland	0.071887
113 S Linwood Ave, Baltimore, Maryland		1613 N Durham St, Baltimore, Maryland	0.175021
113 S Robinson St, Baltimore, Maryland	0.1856458	1614 N Milton Ave, Baltimore, Maryland	
103 N Milton Ave, Baltimore, Maryland		1615 N Broadway, Baltimore, Maryland	
105 N Ellwood Ave, Baltimore, Maryland		1615 N Durham St, Baltimore, Maryland	0.157881

114 N Curley St, Baltimore, Maryland	0.426901	1615 N Wolfe St, Baltimore, Maryland	
114 N Kenwood Ave, Baltimore, Maryland	0.0812464	1617 Rutland Ave, Baltimore, Maryland	
114 N Rose St, Baltimore, Maryland	0.2491543	1618 N Washington St, Baltimore, Maryland	
114 N Streeper St, Baltimore, Maryland		1621 N Wolfe St, Baltimore, Maryland	
114 S Bouldin St, Baltimore, Maryland		1621 Rutland Ave, Baltimore, Maryland	
114 S Clinton St, Baltimore, Maryland		1622 N Washington St, Baltimore, Maryland	
114 S Curley St, Baltimore, Maryland	0.2556908	1623 N Broadway, Baltimore, Maryland	0.230871
114 S Ellwood Ave, Baltimore, Maryland	0.302462	1623 Rutland Ave, Baltimore, Maryland	
109 N Potomac St, Baltimore, Maryland		1624 N Regester St, Baltimore, Maryland	
115 N Belnord Ave, Baltimore, Maryland	0.2608696	1625 N Broadway, Baltimore, Maryland	0.04846
115 N Curley St, Baltimore, Maryland	0.426901	1625 Rutland Ave, Baltimore, Maryland	
115 N East Ave, Baltimore, Maryland		1626 N Washington St, Baltimore, Maryland	
115 N Kenwood Ave, Baltimore, Maryland	0.0812464	1631 N Broadway, Baltimore, Maryland	0.130812
115 N Linwood Ave, Baltimore, Maryland		1631 N Wolfe St, Baltimore, Maryland	
115 N Luzerne Ave, Baltimore, Maryland		1633 N Broadway, Baltimore, Maryland	0.193487
115 N Rose St, Baltimore, Maryland	0.2491543	1633 N Washington St, Baltimore, Maryland	0.06975
115 Rochester Pl, Baltimore, Maryland		1636 N Washington St, Baltimore, Maryland	0.040636
115 S Clinton St, Baltimore, Maryland		1638 N Milton Ave, Baltimore, Maryland	
115 S Linwood Ave, Baltimore, Maryland	0.0050789	1644 N Milton Ave, Baltimore, Maryland	
115 S Linwood Ave, Baltimore, Maryland	0.0050789	1644 N Washington St, Baltimore, Maryland	
115 S Potomac St, Baltimore, Maryland		1700 N Gay St, Baltimore, Maryland	0.012739
115 S Robinson St, Baltimore, Maryland	0.1856458	1700 N Gay St, Baltimore, Maryland	0.012739
116 N Clinton St, Baltimore, Maryland	0.1858445	1700 N Gay St, Baltimore, Maryland	0.012739
116 N Kenwood Ave, Baltimore, Maryland	0.0812464	1700 N Gay St, Baltimore, Maryland	0.012739
116 N Lakewood Ave, Baltimore, Maryland		1700 N Gay St, Baltimore, Maryland	0.012739
116 N Linwood Ave, Baltimore, Maryland	0.0229251	1700 N Gay St, Baltimore, Maryland	0.012739
116 N Luzerne Ave, Baltimore, Maryland		1700 N Gay St, Baltimore, Maryland	0.012739
116 N Rose St, Baltimore, Maryland	0.2491543	1700 N Gay St, Baltimore, Maryland	0.012739
116 S Ellwood Ave, Baltimore, Maryland	0.302462	1700 N Gay St, Baltimore, Maryland	0.012739
116 S Potomac St, Baltimore, Maryland		1700 N Gay St, Baltimore, Maryland	0.012739
111 N Glover St, Baltimore, Maryland	0.214452	1700 N Gay St, Baltimore, Maryland	0.012739
117 N Curley St, Baltimore, Maryland	0.0557532	1700 N Gay St, Baltimore, Maryland	0.012739
117 N East Ave, Baltimore, Maryland		1700 N Gay St, Baltimore, Maryland	0.012739
117 N Kenwood Ave, Baltimore, Maryland	0.0812464	1700 N Gay St, Baltimore, Maryland	0.012739
117 N Lakewood Ave, Baltimore, Maryland		1700 N Gay St, Baltimore, Maryland	0.012739
117 N Linwood Ave, Baltimore, Maryland	0.0229251	1700 N Gay St, Baltimore, Maryland	0.012739
117 N Milton Ave, Baltimore, Maryland		1700 N Gay St, Baltimore, Maryland	0.012739
117 N Streeper St, Baltimore, Maryland		1700 N Gay St, Baltimore, Maryland	0.012739
117 S Bouldin St, Baltimore, Maryland	0.0109526	1700 N Gay St, Baltimore, Maryland	0.012739
117 S Clinton St, Baltimore, Maryland		1700 N Gay St, Baltimore, Maryland	0.012739
117 S Linwood Ave, Baltimore, Maryland	0.0050789	1700 N Gay St, Baltimore, Maryland	0.012739
117 S Potomac St, Baltimore, Maryland		1700 N Gay St, Baltimore, Maryland	0.012739
117 S Robinson St, Baltimore, Maryland		1700 N Gay St, Baltimore, Maryland	0.012739

114 N Decker Ave, Baltimore, Maryland	0.037103
118 N Clinton St, Baltimore, Maryland	
118 N Glover St, Baltimore, Maryland	0.2272721
118 N Linwood Ave, Baltimore, Maryland	0.0229251
118 N Streeper St, Baltimore, Maryland	0.1347463
118 Rochester Pl, Baltimore, Maryland	
118 S Bouldin St, Baltimore, Maryland	0.0109526
118 S East Ave, Baltimore, Maryland	0.0344784
118 S Highland Ave, Baltimore, Maryland	
119 N Curley St, Baltimore, Maryland	0.0557532
119 N Lakewood Ave, Baltimore, Maryland	
119 N Linwood Ave, Baltimore, Maryland	0.0229251
119 N Luzerne Ave, Baltimore, Maryland	0.0654264
119 N Potomac St, Baltimore, Maryland	
119 Rochester Pl, Baltimore, Maryland	
119 S Bouldin St, Baltimore, Maryland	0.0109526
119 S East Ave, Baltimore, Maryland	0.0344784
12 N Ellwood Ave, Baltimore, Maryland	0.1760974
12 N Kenwood Ave, Baltimore, Maryland	0.0330408
12 N Potomac St, Baltimore, Maryland	0.0146383
12 S Decker Ave, Baltimore, Maryland	0.2236563
120 N East Ave, Baltimore, Maryland	
120 N Ellwood Ave, Baltimore, Maryland	0.080655
120 N Linwood Ave, Baltimore, Maryland	
120 N Rose St, Baltimore, Maryland	
120 S Clinton St, Baltimore, Maryland	0
120 S East Ave, Baltimore, Maryland	0.0344784
121 N Belnord Ave, Baltimore, Maryland	
121 N Ellwood Ave, Baltimore, Maryland	0.080655
121 N Kenwood Ave, Baltimore, Maryland	0.0183012
121 N Linwood Ave, Baltimore, Maryland	
121 N Rose St, Baltimore, Maryland	0.1025555
121 Rochester Pl, Baltimore, Maryland	
121 S Bouldin St, Baltimore, Maryland	0.0066269
121 S Linwood Ave, Baltimore, Maryland	0.0394007
121 S Potomac St, Baltimore, Maryland	
122 N Belnord Ave, Baltimore, Maryland	0.1721714
122 N Clinton St, Baltimore, Maryland	
122 N Decker Ave, Baltimore, Maryland	
122 N East Ave, Baltimore, Maryland	
122 N Kenwood Ave, Baltimore, Maryland	0.0317076
122 S Bouldin St, Baltimore, Maryland	0.0066269
122 S Clinton St, Baltimore, Maryland	0.0068762
1700 N Gay St, Baltimore, Maryland	0.012739
1700 N Gay St, Baltimore, Maryland	0.012739
1700 N Gay St, Baltimore, Maryland	0.012739
1700 N Washington St, Baltimore, Maryland	0.135482
1701 N Broadway, Baltimore, Maryland	0.117707
1701 N Chapel St, Baltimore, Maryland	
1701 N Chester St, Baltimore, Maryland	
1701 N Gay St, Baltimore, Maryland	0.135329
1701 N Gay St, Baltimore, Maryland	0.135329
1701 N Wolfe St, Baltimore, Maryland	0.094215
1701 Rutland Ave, Baltimore, Maryland	0.870149
1702 E Lafayette Ave, Baltimore, Maryland	0.160939
1702 E Lanvale St, Baltimore, Maryland	0.145749
1702 N Regester St, Baltimore, Maryland	0.231626
1702 N Wolfe St, Baltimore, Maryland	
1703 N Broadway, Baltimore, Maryland	0.176986
1704 E Lanvale St, Baltimore, Maryland	
1704 N Collington Ave, Baltimore, Maryland	
1705 N Broadway, Baltimore, Maryland	0.186337
1705 N Durham St, Baltimore, Maryland	0.182402
1705 N Port St, Baltimore, Maryland	0.187176
1705 N Washington St, Baltimore, Maryland	0.101508
1705 N Wolfe St, Baltimore, Maryland	0.094215
1706 E Oliver St, Baltimore, Maryland	0.158849
1706 E Preston St, Baltimore, Maryland	0.163571
1707 Crystal Ave, Baltimore, Maryland	
1707 E Lafayette Ave, Baltimore, Maryland	0.160939
1707 E Lanvale St, Baltimore, Maryland	
1707 N Washington St, Baltimore, Maryland	0.101508
1708 N Regester St, Baltimore, Maryland	0.187667
1709 E Lafayette Ave, Baltimore, Maryland	
1709 N Broadway, Baltimore, Maryland	0.075611
1710 E Oliver St, Baltimore, Maryland	
1710 N Regester St, Baltimore, Maryland	
1710 N Wolfe St, Baltimore, Maryland	0.094215
1711 N Washington St, Baltimore, Maryland	0.070817
1712 N Milton Ave, Baltimore, Maryland	0.201943
1712 N Wolfe St, Baltimore, Maryland	0.094215
1713 E Oliver St, Baltimore, Maryland	0.158849
1713 N Broadway, Baltimore, Maryland	0.033147
1713 N Washington St, Baltimore, Maryland	0.070817
1713 N Wolfe St, Baltimore, Maryland	0.024386
1714 E Lanvale St, Baltimore, Maryland	

122 S Curley St, Baltimore, Maryland	0.3218988	1714 N Washington St, Baltimore, Maryland	0.070817
123 N Curley St, Baltimore, Maryland	0.0290926	1714 N Wolfe St, Baltimore, Maryland	0.094215
123 N Glover St, Baltimore, Maryland	0.2759185	1716 E Lanvale St, Baltimore, Maryland	
123 N Lakewood Ave, Baltimore, Maryland		1716 N Washington St, Baltimore, Maryland	0.006968
123 N Luzerne Ave, Baltimore, Maryland	0.0654264	1716 N Wolfe St, Baltimore, Maryland	0.028934
123 N Milton Ave, Baltimore, Maryland		1717 N Collington Ave, Baltimore, Maryland	0.049166
123 N Potomac St, Baltimore, Maryland		1718 E Lanvale St, Baltimore, Maryland	
123 Rochester Pl, Baltimore, Maryland		1718 E Preston St, Baltimore, Maryland	0.163571
123 S Clinton St, Baltimore, Maryland		1718 N Washington St, Baltimore, Maryland	0.006968
123 S Linwood Ave, Baltimore, Maryland	0.1107086	1718 Rutland Ave, Baltimore, Maryland	0.008716
124 N Belnord Ave, Baltimore, Maryland	0.1909635	1719 E Federal St, Baltimore, Maryland	
124 N Clinton St, Baltimore, Maryland		1719 E Lafayette Ave, Baltimore, Maryland	
124 N Ellwood Ave, Baltimore, Maryland	0.0829606	1719 E Oliver St, Baltimore, Maryland	
124 N Luzerne Ave, Baltimore, Maryland		1719 E Preston St, Baltimore, Maryland	0.291481
124 N Potomac St, Baltimore, Maryland	0.2388457	1719 N Wolfe St, Baltimore, Maryland	0.035248
124 Rochester Pl, Baltimore, Maryland		1720 Rutland Ave, Baltimore, Maryland	
124 S Clinton St, Baltimore, Maryland	0.0068762	1721 E Federal St, Baltimore, Maryland	
124 S Curley St, Baltimore, Maryland	0.3218988	1721 N Collington Ave, Baltimore, Maryland	
124 S East Ave, Baltimore, Maryland	0.0344784	1721 N Durham St, Baltimore, Maryland	0.071526
125 N Belnord Ave, Baltimore, Maryland	0.1721714	1721 N Washington St, Baltimore, Maryland	
125 N Ellwood Ave, Baltimore, Maryland	0.0829606	1721 Rutland Ave, Baltimore, Maryland	
125 N Linwood Ave, Baltimore, Maryland		1722 N Washington St, Baltimore, Maryland	
125 N Rose St, Baltimore, Maryland	0.1117395	1723 E Lafayette Ave, Baltimore, Maryland	0.135167
125 N Streeper St, Baltimore, Maryland		1723 E Oliver St, Baltimore, Maryland	0.143198
125 S Bouldin St, Baltimore, Maryland	0.0066269	1723 N Collington Ave, Baltimore, Maryland	
125 S Robinson St, Baltimore, Maryland	0.2261093	1724 N Wolfe St, Baltimore, Maryland	0.024386
126 N Decker Ave, Baltimore, Maryland		1725 E Federal St, Baltimore, Maryland	0.075019
126 N East Ave, Baltimore, Maryland		1726 N Montford Ave, Baltimore, Maryland	
126 N Lakewood Ave, Baltimore, Maryland		1726 N Washington St, Baltimore, Maryland	
126 N Linwood Ave, Baltimore, Maryland		1726 N Wolfe St, Baltimore, Maryland	0.035248
126 N Luzerne Ave, Baltimore, Maryland		1727 Llewelyn Ave, Baltimore, Maryland	
126 N Rose St, Baltimore, Maryland	0.1117395	1728 E Lafayette Ave, Baltimore, Maryland	0.120535
126 S Bouldin St, Baltimore, Maryland	0.0556321	1728 E Lanvale St, Baltimore, Maryland	
126 S Curley St, Baltimore, Maryland	0.3218988	1728 N Collington Ave, Baltimore, Maryland	
126 S East Ave, Baltimore, Maryland	0.0344784	1728 N Washington St, Baltimore, Maryland	
126 S Ellwood Ave, Baltimore, Maryland	0.308705	1728 N Wolfe St, Baltimore, Maryland	0.035248
126 S Potomac St, Baltimore, Maryland		1729 E Lafayette Ave, Baltimore, Maryland	0.120535
127 N Curley St, Baltimore, Maryland	0.1231932	1729 E Lafayette Ave, Baltimore, Maryland	0.120535
127 N Decker Ave, Baltimore, Maryland		1729 N Broadway, Baltimore, Maryland	
127 N Ellwood Ave, Baltimore, Maryland		1729 N Broadway, Baltimore, Maryland	
127 N Lakewood Ave, Baltimore, Maryland		1729 N Washington St, Baltimore, Maryland	
127 N Linwood Ave, Baltimore, Maryland		1730 E Lafayette Ave, Baltimore, Maryland	
127 N Milton Ave, Baltimore, Maryland		1730 N Washington St, Baltimore, Maryland	

127 N Rose St, Baltimore, Maryland	0.2073917	1731 E Lafayette Ave, Baltimore, Maryland	
127 S Clinton St, Baltimore, Maryland		1731 Llewelyn Ave, Baltimore, Maryland	
127 S Curley St, Baltimore, Maryland	0.3218988	1731 N Broadway, Baltimore, Maryland	0.028585
127 S Linwood Ave, Baltimore, Maryland	0.0284525	1732 N Chester St, Baltimore, Maryland	
127 S Potomac St, Baltimore, Maryland		1733 E Lafayette Ave, Baltimore, Maryland	0.028585
128 N Decker Ave, Baltimore, Maryland		1733 E Preston St, Baltimore, Maryland	0.114817
128 N Kenwood Ave, Baltimore, Maryland	0.0297207	1734 E Lafayette Ave, Baltimore, Maryland	
128 N Lakewood Ave, Baltimore, Maryland		1735 E Federal St, Baltimore, Maryland	0.019989
128 N Luzerne Ave, Baltimore, Maryland	0.0305585	1735 N Bradford St, Baltimore, Maryland	0.109601
128 N Streeper St, Baltimore, Maryland	0.1588706	1737 N Bradford St, Baltimore, Maryland	0.109601
128 Rochester Pl, Baltimore, Maryland		1737 N Washington St, Baltimore, Maryland	
129 N Linwood Ave, Baltimore, Maryland		1738 E Lanvale St, Baltimore, Maryland	0.31992
129 N Potomac St, Baltimore, Maryland		1738 Llewelyn Ave, Baltimore, Maryland	
129 N Streeper St, Baltimore, Maryland		1738 N Gay St, Baltimore, Maryland	
129 Rochester Pl, Baltimore, Maryland		1739 E North Ave, Baltimore, Maryland	
129 S Bouldin St, Baltimore, Maryland	0.0556321	1739 N Washington St, Baltimore, Maryland	
129 S Curley St, Baltimore, Maryland	0.2983741	1740 Llewelyn Ave, Baltimore, Maryland	
129 S Linwood Ave, Baltimore, Maryland	0.0284525	1740 N Gay St, Baltimore, Maryland	
129 S Robinson St, Baltimore, Maryland	0.2390838	1742 E Preston St, Baltimore, Maryland	
13 N Belnord Ave, Baltimore, Maryland		1743 E North Ave, Baltimore, Maryland	
13 N Clinton St, Baltimore, Maryland	0.4120353	1743 E North Ave, Baltimore, Maryland	
13 N Decker Ave, Baltimore, Maryland		1743 N Washington St, Baltimore, Maryland	
13 N Rose St, Baltimore, Maryland	0.1753469	1744 E Lanvale St, Baltimore, Maryland	
13 S Curley St, Baltimore, Maryland	0.1917264	1744 E Preston St, Baltimore, Maryland	0.187552
13 S East Ave, Baltimore, Maryland		1745 E Federal St, Baltimore, Maryland	0.31097
13 S Linwood Ave, Baltimore, Maryland	0.0060962	1745 E North Ave, Baltimore, Maryland	0.263441
13 S Potomac St, Baltimore, Maryland		1746 E Lanvale St, Baltimore, Maryland	
130 N Curley St, Baltimore, Maryland	0.1231932	1748 E Preston St, Baltimore, Maryland	0.132795
130 N Decker Ave, Baltimore, Maryland		1749 E Oliver St, Baltimore, Maryland	0.058299
130 N East Ave, Baltimore, Maryland		1752 N Gay St, Baltimore, Maryland	
130 N Ellwood Ave, Baltimore, Maryland		1754 E Preston St, Baltimore, Maryland	0.155613
130 N Luzerne Ave, Baltimore, Maryland	0.0305585	1759 E Preston St, Baltimore, Maryland	0.155613
130 Rochester Pl, Baltimore, Maryland		1759 E Preston St, Baltimore, Maryland	0.155613
130 S Clinton St, Baltimore, Maryland	0.0643687	1800 Rutland Ave, Baltimore, Maryland	
130 S Ellwood Ave, Baltimore, Maryland	0.3870116	1801 E Federal St, Baltimore, Maryland	0.411643
130 S Potomac St, Baltimore, Maryland		1801 E Federal St, Baltimore, Maryland	0.411643
131 N Belnord Ave, Baltimore, Maryland	0.2075731	1801 E Lafayette Ave, Baltimore, Maryland	
131 N Decker Ave, Baltimore, Maryland		1801 E North Ave, Baltimore, Maryland	0.095024
131 N Milton Ave, Baltimore, Maryland		1801 E Preston St, Baltimore, Maryland	0.244885
131 N Potomac St, Baltimore, Maryland		1802 E Oliver St, Baltimore, Maryland	0.268294
131 N Rose St, Baltimore, Maryland	0.2073917	1802 N Montford Ave, Baltimore, Maryland	0.01623
131 S East Ave, Baltimore, Maryland	0.0344784	1802 N Wolfe St, Baltimore, Maryland	0.075354
131 S Potomac St, Baltimore, Maryland		1803 N Wolfe St, Baltimore, Maryland	0.075354

131 S Robinson St, Baltimore, Maryland	0.2390838	1804 N Washington St, Baltimore, Maryland	0.029054
132 N Kenwood Ave, Baltimore, Maryland		1804 N Wolfe St, Baltimore, Maryland	0.075354
132 N Lakewood Ave, Baltimore, Maryland		1805 N Montford Ave, Baltimore, Maryland	0.01623
132 N Rose St, Baltimore, Maryland	0.2073917	1805 Rutland Ave, Baltimore, Maryland	
132 N Streeper St, Baltimore, Maryland	0.078604	1806 E Federal St, Baltimore, Maryland	0.063782
132 Rochester Pl, Baltimore, Maryland	0.0159734	1806 N Collington Ave, Baltimore, Maryland	0.194453
132 S Clinton St, Baltimore, Maryland		1807 E Preston St, Baltimore, Maryland	
132 S East Ave, Baltimore, Maryland	0.0344784	1807 N Broadway, Baltimore, Maryland	0.189872
133 N Belnord Ave, Baltimore, Maryland	0.2075731	1807 N Broadway, Baltimore, Maryland	0.189872
133 N Ellwood Ave, Baltimore, Maryland		1807 N Broadway, Baltimore, Maryland	0.189872
133 N Kenwood Ave, Baltimore, Maryland	0.0297207	1807 N Collington Ave, Baltimore, Maryland	
133 N Luzerne Ave, Baltimore, Maryland	0.0305585	1807 N Wolfe St, Baltimore, Maryland	0.062597
133 N Rose St, Baltimore, Maryland	0.2567117	1808 E Lanvale St, Baltimore, Maryland	
133 N Streeper St, Baltimore, Maryland	0.1347463	1808 N Chapel St, Baltimore, Maryland	0.197079
133 Rochester Pl, Baltimore, Maryland	0.0159734	1809 N Collington Ave, Baltimore, Maryland	
133 S Bouldin St, Baltimore, Maryland		1810 E Federal St, Baltimore, Maryland	
133 S Linwood Ave, Baltimore, Maryland	0.0050251	1811 N Broadway, Baltimore, Maryland	0.175137
133 S Potomac St, Baltimore, Maryland		1811 N Broadway, Baltimore, Maryland	0.175137
133 S Robinson St, Baltimore, Maryland	0.1818601	1811 N Port St, Baltimore, Maryland	0.139443
134 N East Ave, Baltimore, Maryland		1811 Rutland Ave, Baltimore, Maryland	
134 N Luzerne Ave, Baltimore, Maryland		1812 E Federal St, Baltimore, Maryland	0.945701
134 N Potomac St, Baltimore, Maryland		1812 E Lafayette Ave, Baltimore, Maryland	0.138811
134 Rochester Pl, Baltimore, Maryland	0.0159734	1812 E Lanvale St, Baltimore, Maryland	
134 S Clinton St, Baltimore, Maryland		1812 E Oliver St, Baltimore, Maryland	
134 S Ellwood Ave, Baltimore, Maryland	0.363205	1813 N Wolfe St, Baltimore, Maryland	
134 S Highland Ave, Baltimore, Maryland	0.0063621	1814 E Federal St, Baltimore, Maryland	0.945701
135 N Kenwood Ave, Baltimore, Maryland		1814 E Oliver St, Baltimore, Maryland	
135 N Lakewood Ave, Baltimore, Maryland		1814 N Chapel St, Baltimore, Maryland	0.198013
135 N Linwood Ave, Baltimore, Maryland		1814 N Montford Ave, Baltimore, Maryland	0.117343
135 N Milton Ave, Baltimore, Maryland		1814 N Wolfe St, Baltimore, Maryland	
135 Rochester Pl, Baltimore, Maryland	0.0159734	1815 N Wolfe St, Baltimore, Maryland	
135 S Bouldin St, Baltimore, Maryland	0.031485	1815 Rutland Ave, Baltimore, Maryland	
135 S Curley St, Baltimore, Maryland	0.3337342	1816 E Federal St, Baltimore, Maryland	0.945701
135 S East Ave, Baltimore, Maryland	0.0344784	1816 E Lafayette Ave, Baltimore, Maryland	
135 S Potomac St, Baltimore, Maryland		1816 N Chapel St, Baltimore, Maryland	0.198013
136 N Decker Ave, Baltimore, Maryland	0.0636086	1816 N Washington St, Baltimore, Maryland	0.148339
136 N East Ave, Baltimore, Maryland		1817 N Regester St, Baltimore, Maryland	0.13274
136 N Ellwood Ave, Baltimore, Maryland		1817 Rutland Ave, Baltimore, Maryland	
136 N Kenwood Ave, Baltimore, Maryland		1818 E Oliver St, Baltimore, Maryland	
136 N Luzerne Ave, Baltimore, Maryland		1818 N Chapel St, Baltimore, Maryland	0.198013
136 N Rose St, Baltimore, Maryland	0.2567117	1818 N Washington St, Baltimore, Maryland	0.128353
136 Rochester Pl, Baltimore, Maryland	0.0464072	1818 Rutland Ave, Baltimore, Maryland	
136 S Bouldin St, Baltimore, Maryland	0.031485	1819 E Federal St, Baltimore, Maryland	

136 S Curley St, Baltimore, Maryland	0.3337342	1819 E Federal St, Baltimore, Maryland	
136 S East Ave, Baltimore, Maryland	0.0940084	1819 N Collington Ave, Baltimore, Maryland	0.163556
136 S Ellwood Ave, Baltimore, Maryland	0.2254989	1819 N Wolfe St, Baltimore, Maryland	0.04965
137 N Ellwood Ave, Baltimore, Maryland	0.1687877	1819 Rutland Ave, Baltimore, Maryland	
137 N Luzerne Ave, Baltimore, Maryland		1820 N Milton Ave, Baltimore, Maryland	
137 N Potomac St, Baltimore, Maryland	0.0756693	1820 N Port St, Baltimore, Maryland	0.134055
137 Rochester Pl, Baltimore, Maryland	0.0464072	1820 N Washington St, Baltimore, Maryland	0.128353
137 S Curley St, Baltimore, Maryland	0.3337342	1821 E Federal St, Baltimore, Maryland	0.087209
137 S East Ave, Baltimore, Maryland	0.0940084	1821 N Collington Ave, Baltimore, Maryland	0.095566
137 S Linwood Ave, Baltimore, Maryland		1821 N Regester St, Baltimore, Maryland	0.13274
138 N East Ave, Baltimore, Maryland		1822 E Federal St, Baltimore, Maryland	0.087209
138 N Glover St, Baltimore, Maryland	0.5666225	1822 E Lafayette Ave, Baltimore, Maryland	
138 N Kenwood Ave, Baltimore, Maryland	0.0400714	1822 N Port St, Baltimore, Maryland	0.134055
138 N Linwood Ave, Baltimore, Maryland		1822 N Washington St, Baltimore, Maryland	0.065241
138 Rochester Pl, Baltimore, Maryland	0.038063	1823 N Washington St, Baltimore, Maryland	0.065241
138 S Bouldin St, Baltimore, Maryland		1823 Rutland Ave, Baltimore, Maryland	
138 S Clinton St, Baltimore, Maryland		1824 E Federal St, Baltimore, Maryland	0.087209
138 S Ellwood Ave, Baltimore, Maryland	0.2254989	1825 Rutland Ave, Baltimore, Maryland	
139 N Curley St, Baltimore, Maryland	0.0632578	1826 Rutland Ave, Baltimore, Maryland	
139 N Glover St, Baltimore, Maryland	0.5666225	1827 N Port St, Baltimore, Maryland	0.140354
139 N Lakewood Ave, Baltimore, Maryland		1827 N Wolfe St, Baltimore, Maryland	
139 N Linwood Ave, Baltimore, Maryland		1827 Rutland Ave, Baltimore, Maryland	
139 N Luzerne Ave, Baltimore, Maryland		1829 E Lafayette Ave, Baltimore, Maryland	0.04107
139 Rochester Pl, Baltimore, Maryland		1829 N Montford Ave, Baltimore, Maryland	0.071036
139 S Curley St, Baltimore, Maryland	0.4140176	1830 N Collington Ave, Baltimore, Maryland	0.066941
139 S East Ave, Baltimore, Maryland	0.0940084	1830 N Port St, Baltimore, Maryland	0.160712
139 S Robinson St, Baltimore, Maryland	0.1540496	1831 N Washington St, Baltimore, Maryland	0.155006
14 N Curley St, Baltimore, Maryland	0.1972542	1831 N Wolfe St, Baltimore, Maryland	
14 N East Ave, Baltimore, Maryland	0.0418774	1832 N Collington Ave, Baltimore, Maryland	0.066941
14 N Ellwood Ave, Baltimore, Maryland		1833 N Chester St, Baltimore, Maryland	
14 N Glover St, Baltimore, Maryland	0.2666357	1833 Rutland Ave, Baltimore, Maryland	0.051121
14 N Kenwood Ave, Baltimore, Maryland	0.0163672	1834 N Port St, Baltimore, Maryland	0.040082
14 N Lakewood Ave, Baltimore, Maryland	0.0270666	1835 E Lafayette Ave, Baltimore, Maryland	
14 S Highland Ave, Baltimore, Maryland	0.0137234	1835 N Collington Ave, Baltimore, Maryland	0.131656
14 S Robinson St, Baltimore, Maryland	0.2208194	1835 N Montford Ave, Baltimore, Maryland	0.007081
140 N East Ave, Baltimore, Maryland		1836 E Lafayette Ave, Baltimore, Maryland	
140 N Ellwood Ave, Baltimore, Maryland	0.1687877	1836 Rutland Ave, Baltimore, Maryland	0.051121
140 S Bouldin St, Baltimore, Maryland		1837 E North Ave, Baltimore, Maryland	
140 S East Ave, Baltimore, Maryland	0.0940084	1837 N Regester St, Baltimore, Maryland	0.0306
140 S Highland Ave, Baltimore, Maryland		1838 N Chapel St, Baltimore, Maryland	0.139945
141 N Curley St, Baltimore, Maryland	0.0632578	1838 Rutland Ave, Baltimore, Maryland	0.07029
141 N Ellwood Ave, Baltimore, Maryland	0.1687877	1839 E Lafayette Ave, Baltimore, Maryland	
141 N Milton Ave, Baltimore, Maryland		1839 N Collington Ave, Baltimore, Maryland	0.066941

141 N Potomac St, Baltimore, Maryland	0.0756693	1840 Rutland Ave, Baltimore, Maryland	0.07029
141 N Streeper St, Baltimore, Maryland	0.1588706	1841 N Montford Ave, Baltimore, Maryland	0.007081
141 S Curley St, Baltimore, Maryland	0.4140176	1843 N Chester St, Baltimore, Maryland	0.061119
141 S Linwood Ave, Baltimore, Maryland	0.0095488	1845 N Chester St, Baltimore, Maryland	0.061119
142 N Curley St, Baltimore, Maryland		1847 N Collington Ave, Baltimore, Maryland	0.046355
142 N Decker Ave, Baltimore, Maryland		1848 N Wolfe St, Baltimore, Maryland	
142 N Luzerne Ave, Baltimore, Maryland	0.0401127	1850 N Wolfe St, Baltimore, Maryland	
142 S Bouldin St, Baltimore, Maryland		1851 N Collington Ave, Baltimore, Maryland	0.113878
143 N Decker Ave, Baltimore, Maryland		1873 N Gay St, Baltimore, Maryland	0.080239
143 N Ellwood Ave, Baltimore, Maryland		1901 E Federal St, Baltimore, Maryland	0.318451
143 N Luzerne Ave, Baltimore, Maryland		1903 E Lafayette Ave, Baltimore, Maryland	0.067174
143 S East Ave, Baltimore, Maryland		1904 E Lafayette Ave, Baltimore, Maryland	0.067174
144 N Curley St, Baltimore, Maryland	0.0352417	1906 E Lafayette Ave, Baltimore, Maryland	0.091186
144 N East Ave, Baltimore, Maryland		1906 E Lanvale St, Baltimore, Maryland	
144 N Ellwood Ave, Baltimore, Maryland		1908 E Lafayette Ave, Baltimore, Maryland	0.091186
144 N Linwood Ave, Baltimore, Maryland		1909 E Lafayette Ave, Baltimore, Maryland	0.088289
144 N Potomac St, Baltimore, Maryland	0.072099	1909 E North Ave, Baltimore, Maryland	
144 N Streeper St, Baltimore, Maryland	0.2553112	1911 E Lafayette Ave, Baltimore, Maryland	0.088289
144 S Bouldin St, Baltimore, Maryland	0.1284853	1918 E Lafayette Ave, Baltimore, Maryland	0.092599
144 S East Ave, Baltimore, Maryland	0.0940084	1920 E Lanvale St, Baltimore, Maryland	
144 S Ellwood Ave, Baltimore, Maryland	0.2642729	1923 E North Ave, Baltimore, Maryland	
145 N Curley St, Baltimore, Maryland	0.0352417	1924 E Lafayette Ave, Baltimore, Maryland	0.059709
145 N Ellwood Ave, Baltimore, Maryland		1925 E Lafayette Ave, Baltimore, Maryland	
145 N Linwood Ave, Baltimore, Maryland		1926 E Lafayette Ave, Baltimore, Maryland	0.059709
145 N Milton Ave, Baltimore, Maryland		1933 E North Ave, Baltimore, Maryland	0.84659
145 S Linwood Ave, Baltimore, Maryland	0.1334021	1933 E North Ave, Baltimore, Maryland	0.84659
145 S Robinson St, Baltimore, Maryland	0.1721861	1937 E North Ave, Baltimore, Maryland	0.389113
146 N Curley St, Baltimore, Maryland	0.0352417	1938 E Lafayette Ave, Baltimore, Maryland	
146 N Decker Ave, Baltimore, Maryland		1939 E Lafayette Ave, Baltimore, Maryland	0.098976
146 N Kenwood Ave, Baltimore, Maryland	0.060061	2000 E Oliver St, Baltimore, Maryland	0.026753
146 N Streeper St, Baltimore, Maryland	0.2553112	2000 E Preston St, Baltimore, Maryland	
146 S Bouldin St, Baltimore, Maryland	0.1284853	2001 E Lanvale St, Baltimore, Maryland	
147 N Ellwood Ave, Baltimore, Maryland		2001 E North Ave, Baltimore, Maryland	
147 N Kenwood Ave, Baltimore, Maryland	0.0331371	2003 E Hoffman St, Baltimore, Maryland	
147 N Lakewood Ave, Baltimore, Maryland		2004 E Lanvale St, Baltimore, Maryland	0.120068
147 S East Ave, Baltimore, Maryland	0.0940084	2004 E Preston St, Baltimore, Maryland	0.089323
147 S Linwood Ave, Baltimore, Maryland	0.1334021	2006 E Hoffman St, Baltimore, Maryland	
147 S Robinson St, Baltimore, Maryland	0.1721861	2007 E Lanvale St, Baltimore, Maryland	0.120068
148 N Lakewood Ave, Baltimore, Maryland		2008 E Preston St, Baltimore, Maryland	0.044011
148 N Linwood Ave, Baltimore, Maryland		2009 E Lanvale St, Baltimore, Maryland	0.120068
148 N Streeper St, Baltimore, Maryland	0.0138338	2010 E Hoffman St, Baltimore, Maryland	
148 S Highland Ave, Baltimore, Maryland		2010 E Preston St, Baltimore, Maryland	0.044011
148 S Highland Ave, Baltimore, Maryland		2011 E North Ave, Baltimore, Maryland	

149 N Ellwood Ave, Baltimore, Maryland		2013 E Lanvale St, Baltimore, Maryland	0.372798
149 N Lakewood Ave, Baltimore, Maryland		2014 E Preston St, Baltimore, Maryland	
149 N Milton Ave, Baltimore, Maryland		2015 E Lafayette Ave, Baltimore, Maryland	
15 N Curley St, Baltimore, Maryland	0.1972542	2015 E Oliver St, Baltimore, Maryland	
15 N Decker Ave, Baltimore, Maryland		2016 E Lanvale St, Baltimore, Maryland	
15 N Glover St, Baltimore, Maryland		2023 E Preston St, Baltimore, Maryland	0.058241
15 N Kenwood Ave, Baltimore, Maryland	0.0163672	2024 E Lafayette Ave, Baltimore, Maryland	0.081989
15 N Luzerne Ave, Baltimore, Maryland	0.0288422	2024 E Lanvale St, Baltimore, Maryland	0.034393
15 N Potomac St, Baltimore, Maryland	0.0146383	2025 E Lanvale St, Baltimore, Maryland	0.034393
15 N Rose St, Baltimore, Maryland	0.1753469	2025 E Oliver St, Baltimore, Maryland	
15 S Curley St, Baltimore, Maryland	0.1917264	2027 E Lanvale St, Baltimore, Maryland	0.068806
15 S Ellwood Ave, Baltimore, Maryland		2027 E Preston St, Baltimore, Maryland	
15 S Robinson St, Baltimore, Maryland	0.2208194	2028 E Lanvale St, Baltimore, Maryland	0.068806
150 N Decker Ave, Baltimore, Maryland		2029 E Lanvale St, Baltimore, Maryland	0.068806
150 N East Ave, Baltimore, Maryland		2029 E North Ave, Baltimore, Maryland	
150 N Ellwood Ave, Baltimore, Maryland	0.0426192	2029 E North Ave, Baltimore, Maryland	
150 N Lakewood Ave, Baltimore, Maryland		2029 E Oliver St, Baltimore, Maryland	
150 N Linwood Ave, Baltimore, Maryland		2032 Ellsworth St, Baltimore, Maryland	0.08335
150 S Bouldin St, Baltimore, Maryland	0.4884618	2035 E Lanvale St, Baltimore, Maryland	0.261899
151 N Curley St, Baltimore, Maryland	0.0243152	2037 E Lanvale St, Baltimore, Maryland	0.261899
151 N Decker Ave, Baltimore, Maryland		2037 E North Ave, Baltimore, Maryland	
151 N Ellwood Ave, Baltimore, Maryland	0.1949708	2039 E Lanvale St, Baltimore, Maryland	0.261899
151 N Streeper St, Baltimore, Maryland	0.078604	2045 E North Ave, Baltimore, Maryland	
151 S Robinson St, Baltimore, Maryland	0.2399522	2047 E North Ave, Baltimore, Maryland	
152 N Curley St, Baltimore, Maryland		2049 E North Ave, Baltimore, Maryland	
152 N Ellwood Ave, Baltimore, Maryland	0.0426192	2100 E Biddle St, Baltimore, Maryland	0.329766
152 N Lakewood Ave, Baltimore, Maryland		2101 E Preston St, Baltimore, Maryland	
152 N Luzerne Ave, Baltimore, Maryland	0.1692708	2103 E Oliver St, Baltimore, Maryland	0.133853
153 N Curley St, Baltimore, Maryland	0.0243152	2106 E Hoffman St, Baltimore, Maryland	
153 N Ellwood Ave, Baltimore, Maryland	0.1949708	2107 E Preston St, Baltimore, Maryland	
153 N Milton Ave, Baltimore, Maryland		2108 E Federal St, Baltimore, Maryland	
153 N Streeper St, Baltimore, Maryland	0.0956107	2112 E Biddle St, Baltimore, Maryland	0.067817
153 S Robinson St, Baltimore, Maryland	0.1101576	2115 E Preston St, Baltimore, Maryland	
154 N Curley St, Baltimore, Maryland		2116 E Biddle St, Baltimore, Maryland	
154 N East Ave, Baltimore, Maryland		2117 E Preston St, Baltimore, Maryland	
154 N Ellwood Ave, Baltimore, Maryland	0.0426192	2118 E Federal St, Baltimore, Maryland	0.021389
155 N Kenwood Ave, Baltimore, Maryland		2119 E Preston St, Baltimore, Maryland	
155 N Linwood Ave, Baltimore, Maryland		2121 E Preston St, Baltimore, Maryland	
155 N Potomac St, Baltimore, Maryland		2123 E Oliver St, Baltimore, Maryland	0.075062
155 S Robinson St, Baltimore, Maryland	0.2399522	2123 E Preston St, Baltimore, Maryland	
156 N Ellwood Ave, Baltimore, Maryland	0.1949708	2124 E Oliver St, Baltimore, Maryland	
156 N Linwood Ave, Baltimore, Maryland		2125 E Oliver St, Baltimore, Maryland	0.075062
156 N Potomac St, Baltimore, Maryland		2126 E Federal St, Baltimore, Maryland	0.504842

157 N Ellwood Ave, Baltimore, Maryland	0.1949708	2126 E Hoffman St, Baltimore, Maryland	
157 N Linwood Ave, Baltimore, Maryland		2126 E Oliver St, Baltimore, Maryland	
157 N Milton Ave, Baltimore, Maryland	0.029724	2127 E Preston St, Baltimore, Maryland	
158 N Curley St, Baltimore, Maryland		2128 E Federal St, Baltimore, Maryland	
158 N Decker Ave, Baltimore, Maryland	0.0383017	2129 E Federal St, Baltimore, Maryland	
159 N Decker Ave, Baltimore, Maryland	0.0383017	2129 E Preston St, Baltimore, Maryland	
159 N Potomac St, Baltimore, Maryland		2130 E Biddle St, Baltimore, Maryland	0.321697
16 N Clinton St, Baltimore, Maryland		2130 E Hoffman St, Baltimore, Maryland	
16 N Curley St, Baltimore, Maryland		2130 E Oliver St, Baltimore, Maryland	0.075062
16 N Ellwood Ave, Baltimore, Maryland		2132 E Oliver St, Baltimore, Maryland	0.075062
16 N Lakewood Ave, Baltimore, Maryland		2133 E Federal St, Baltimore, Maryland	
16 N Luzerne Ave, Baltimore, Maryland	0.0288422	2135 E Federal St, Baltimore, Maryland	0.063907
16 N Potomac St, Baltimore, Maryland		2135 E North Ave, Baltimore, Maryland	
16 N Streeper St, Baltimore, Maryland		2136 E Federal St, Baltimore, Maryland	
16 S Curley St, Baltimore, Maryland	0.1917264	2136 E Oliver St, Baltimore, Maryland	
16 S Ellwood Ave, Baltimore, Maryland		2138 E Oliver St, Baltimore, Maryland	
16 S Robinson St, Baltimore, Maryland		2200 E Biddle St, Baltimore, Maryland	0.244427
161 N Streeper St, Baltimore, Maryland	0.0138338	2200 E Biddle St, Baltimore, Maryland	0.244427
162 N Decker Ave, Baltimore, Maryland		2200 E Biddle St, Baltimore, Maryland	0.244427
163 N Decker Ave, Baltimore, Maryland		2200 E Biddle St, Baltimore, Maryland	0.244427
164 N Potomac St, Baltimore, Maryland		2200 E Biddle St, Baltimore, Maryland	0.244427
165 N Curley St, Baltimore, Maryland	0.0882404	2200 E Biddle St, Baltimore, Maryland	0.244427
17 N Belnord Ave, Baltimore, Maryland	0.2720101	2200 E Biddle St, Baltimore, Maryland	0.244427
17 N Decker Ave, Baltimore, Maryland	0.2577035	2200 E Biddle St, Baltimore, Maryland	0.244427
17 N Luzerne Ave, Baltimore, Maryland	0.0071006	2200 E Biddle St, Baltimore, Maryland	0.244427
17 N Milton Ave, Baltimore, Maryland		2200 E Biddle St, Baltimore, Maryland	0.244427
17 N Rose St, Baltimore, Maryland	0.1753469	2200 E Biddle St, Baltimore, Maryland	0.244427
17 N Streeper St, Baltimore, Maryland		2200 E Biddle St, Baltimore, Maryland	0.244427
17 S Decker Ave, Baltimore, Maryland	0.2800436	2200 E Biddle St, Baltimore, Maryland	0.244427
17 S East Ave, Baltimore, Maryland		2200 E Biddle St, Baltimore, Maryland	0.244427
17 S Robinson St, Baltimore, Maryland	0.2484881	2200 E Biddle St, Baltimore, Maryland	0.244427
18 N Decker Ave, Baltimore, Maryland	0.2577035	2200 E Biddle St, Baltimore, Maryland	0.244427
18 N Ellwood Ave, Baltimore, Maryland	0.142036	2200 E Biddle St, Baltimore, Maryland	0.244427
18 S Decker Ave, Baltimore, Maryland	0.2800436	2200 E Biddle St, Baltimore, Maryland	0.244427
18 S East Ave, Baltimore, Maryland		2200 E Biddle St, Baltimore, Maryland	0.244427
18 S Ellwood Ave, Baltimore, Maryland		2200 E Biddle St, Baltimore, Maryland	0.244427
18 S Robinson St, Baltimore, Maryland	0.2484881	2200 E Biddle St, Baltimore, Maryland	0.244427
19 N Curley St, Baltimore, Maryland	0.1987069	2200 E Biddle St, Baltimore, Maryland	0.244427
19 N Luzerne Ave, Baltimore, Maryland	0.0071006	2200 E Biddle St, Baltimore, Maryland	0.244427
19 N Potomac St, Baltimore, Maryland		2200 E Biddle St, Baltimore, Maryland	0.244427
19 S Ellwood Ave, Baltimore, Maryland		2200 E Biddle St, Baltimore, Maryland	0.244427
19 S Linwood Ave, Baltimore, Maryland		2200 E Biddle St, Baltimore, Maryland	0.244427
2 N Clinton St, Baltimore, Maryland		2200 E Biddle St, Baltimore, Maryland	0.244427

2 N East Ave, Baltimore, Maryland	
2 S Decker Ave, Baltimore, Maryland	0.0954007
2 S East Ave, Baltimore, Maryland	
2 S Potomac St, Baltimore, Maryland	
20 N East Ave, Baltimore, Maryland	0.0363722
20 N Kenwood Ave, Baltimore, Maryland	
20 N Lakewood Ave, Baltimore, Maryland	
20 N Linwood Ave, Baltimore, Maryland	
20 N Luzerne Ave, Baltimore, Maryland	
20 N Streeper St, Baltimore, Maryland	0.200662
20 S Curley St, Baltimore, Maryland	0.209219
20 S Ellwood Ave, Baltimore, Maryland	
20 S Highland Ave, Baltimore, Maryland	
20 S Potomac St, Baltimore, Maryland	
21 N Belnord Ave, Baltimore, Maryland	0.049454
21 N Curley St, Baltimore, Maryland	0.1987069
21 N East Ave, Baltimore, Maryland	0.0039217
21 N Ellwood Ave, Baltimore, Maryland	0.1702786
21 N Kenwood Ave, Baltimore, Maryland	
21 N Luzerne Ave, Baltimore, Maryland	
21 N Milton Ave, Baltimore, Maryland	
21 S East Ave, Baltimore, Maryland	
21 S Linwood Ave, Baltimore, Maryland	
22 N Lakewood Ave, Baltimore, Maryland	0.0121313
22 N Potomac St, Baltimore, Maryland	
22 N Streeper St, Baltimore, Maryland	0.200662
22 S Curley St, Baltimore, Maryland	0.2216212
22 S East Ave, Baltimore, Maryland	
22 S Ellwood Ave, Baltimore, Maryland	
22 S Potomac St, Baltimore, Maryland	
22 S Robinson St, Baltimore, Maryland	0.2484881
23 N Clinton St, Baltimore, Maryland	
23 N Kenwood Ave, Baltimore, Maryland	
23 N Linwood Ave, Baltimore, Maryland	
23 S East Ave, Baltimore, Maryland	
23 S Ellwood Ave, Baltimore, Maryland	
23 S Linwood Ave, Baltimore, Maryland	
23 S Potomac St, Baltimore, Maryland	
24 N East Ave, Baltimore, Maryland	0.0039217
24 N Potomac St, Baltimore, Maryland	
24 S Curley St, Baltimore, Maryland	0.2216212
24 S Ellwood Ave, Baltimore, Maryland	
24 S Highland Ave, Baltimore, Maryland	
2200 E Biddle St, Baltimore, Maryland	0.244427
2200 E Biddle St, Baltimore, Maryland	0.244427
2200 E Biddle St, Baltimore, Maryland	0.244427
2200 E Biddle St, Baltimore, Maryland	0.244427
2200 E Biddle St, Baltimore, Maryland	0.244427
2200 E Biddle St, Baltimore, Maryland	0.244427
2200 E Biddle St, Baltimore, Maryland	0.244427
2200 E Biddle St, Baltimore, Maryland	0.244427
2200 E Biddle St, Baltimore, Maryland	0.244427
2200 E Oliver St, Baltimore, Maryland	
2201 E North Ave, Baltimore, Maryland	
2201 E Preston St, Baltimore, Maryland	0.144415
2201 Mura St, Baltimore, Maryland	
2203 E Preston St, Baltimore, Maryland	0.144415
2205 E North Ave, Baltimore, Maryland	
2209 E North Ave, Baltimore, Maryland	
2209 E Preston St, Baltimore, Maryland	0.19382
2211 E Preston St, Baltimore, Maryland	0.201077
2215 E North Ave, Baltimore, Maryland	
2217 E North Ave, Baltimore, Maryland	
2217 E Preston St, Baltimore, Maryland	
2223 E Preston St, Baltimore, Maryland	
2224 E Oliver St, Baltimore, Maryland	
2225 E North Ave, Baltimore, Maryland	
2225 E Preston St, Baltimore, Maryland	
2229 E Preston St, Baltimore, Maryland	
2231 E North Ave, Baltimore, Maryland	
2233 E North Ave, Baltimore, Maryland	
2233 E Preston St, Baltimore, Maryland	
2239 E Preston St, Baltimore, Maryland	0.995242
2243 E Preston St, Baltimore, Maryland	
2247 E Preston St, Baltimore, Maryland	0.178792
2300 Llewelyn Ave, Baltimore, Maryland	
2303 E Preston St, Baltimore, Maryland	
2306 E Oliver St, Baltimore, Maryland	
2307 E Hoffman St, Baltimore, Maryland	0.126868
2307 E North Ave, Baltimore, Maryland	
2309 E Lafayette Ave, Baltimore, Maryland	
2312 E Preston St, Baltimore, Maryland	
2313 E Preston St, Baltimore, Maryland	0.409916
2316 E Federal St, Baltimore, Maryland	
2321 E Oliver St, Baltimore, Maryland	0.290991
2321 E Hoffman St, Baltimore, Maryland	0.167519

24 S Robinson St, Baltimore, Maryland	0.2963339	2325 E Lafayette Ave, Baltimore, Maryland	
25 N Curley St, Baltimore, Maryland	0.2662845	2326 E Oliver St, Baltimore, Maryland	
25 N East Ave, Baltimore, Maryland		2327 E Lafayette Ave, Baltimore, Maryland	
25 N Glover St, Baltimore, Maryland	0.2788603	2330 E Hoffman St, Baltimore, Maryland	0.517303
25 N Kenwood Ave, Baltimore, Maryland		2400 E Federal St, Baltimore, Maryland	
25 N Linwood Ave, Baltimore, Maryland		2400 E Preston St, Baltimore, Maryland	0.260971
25 N Milton Ave, Baltimore, Maryland		2401 E North Ave, Baltimore, Maryland	
25 N Potomac St, Baltimore, Maryland	0.0047886	2401 E North Ave, Baltimore, Maryland	
25 S East Ave, Baltimore, Maryland		2402 E Hoffman St, Baltimore, Maryland	0.241944
2502 E Baltimore St, Baltimore, Maryland		2402 E Lafayette Ave, Baltimore, Maryland	
2504 E Baltimore St, Baltimore, Maryland		2403 E Federal St, Baltimore, Maryland	
2504 E Fairmount Ave, Baltimore, Maryland		2403 E Hoffman St, Baltimore, Maryland	0.049217
2507 E Fayette St, Baltimore, Maryland		2404 E Federal St, Baltimore, Maryland	
2510 E Baltimore St, Baltimore, Maryland		2404 E Lafayette Ave, Baltimore, Maryland	
2511 E Fairmount Ave, Baltimore, Maryland	0.0441136	2404 E Oliver St, Baltimore, Maryland	0.045177
2511 E Fairmount Ave, Baltimore, Maryland	0.0441136	2404 E Preston St, Baltimore, Maryland	0.260971
2512 E Baltimore St, Baltimore, Maryland		2405 E Hoffman St, Baltimore, Maryland	0.241944
2514 E Baltimore St, Baltimore, Maryland		2405 E Preston St, Baltimore, Maryland	0.016695
2514 E Fairmount Ave, Baltimore, Maryland	0.0644458	2406 E Federal St, Baltimore, Maryland	
2515 E Fairmount Ave, Baltimore, Maryland	0.0644458	2406 E Preston St, Baltimore, Maryland	0.016695
2515 E Fayette St, Baltimore, Maryland	0.0702557	2407 E Hoffman St, Baltimore, Maryland	0.241944
2516 E Baltimore St, Baltimore, Maryland		2408 E Preston St, Baltimore, Maryland	0.016695
2517 E Fairmount Ave, Baltimore, Maryland	0.0644458	2409 E Hoffman St, Baltimore, Maryland	0.14286
2518 E Baltimore St, Baltimore, Maryland		2410 E Hoffman St, Baltimore, Maryland	0.14286
2518 E Fairmount Ave, Baltimore, Maryland		2410 E Preston St, Baltimore, Maryland	
2519 E Fairmount Ave, Baltimore, Maryland		2412 E Hoffman St, Baltimore, Maryland	
2519 E Fayette St, Baltimore, Maryland		2412 E Preston St, Baltimore, Maryland	
2520 E Baltimore St, Baltimore, Maryland		2413 E Hoffman St, Baltimore, Maryland	
2524 E Baltimore St, Baltimore, Maryland		2414 E Hoffman St, Baltimore, Maryland	
2526 E Baltimore St, Baltimore, Maryland		2415 E Hoffman St, Baltimore, Maryland	
2530 E Baltimore St, Baltimore, Maryland		2415 Llewelyn Ave, Baltimore, Maryland	0.457285
2532 E Baltimore St, Baltimore, Maryland		2416 E Preston St, Baltimore, Maryland	
2536 E Baltimore St, Baltimore, Maryland	0.1595237	2418 E Biddle St, Baltimore, Maryland	
2540 E Baltimore St, Baltimore, Maryland		2420 E Biddle St, Baltimore, Maryland	
26 N Ellwood Ave, Baltimore, Maryland	0.1701951	2422 E Federal St, Baltimore, Maryland	0.028633
26 N Glover St, Baltimore, Maryland	0.2788603	2422 E Lafayette Ave, Baltimore, Maryland	
26 N Highland Ave, Baltimore, Maryland		2423 E Oliver St, Baltimore, Maryland	0.089652
26 N Lakewood Ave, Baltimore, Maryland		2424 E Federal St, Baltimore, Maryland	0.065959
26 N Potomac St, Baltimore, Maryland	0.0047886	2425 E Federal St, Baltimore, Maryland	
26 S Decker Ave, Baltimore, Maryland	0.2354238	2427 E Lanvale St, Baltimore, Maryland	
26 S Ellwood Ave, Baltimore, Maryland		2428 E Lafayette Ave, Baltimore, Maryland	0.061653
26 S Highland Ave, Baltimore, Maryland	0.0590022	2429 E Hoffman St, Baltimore, Maryland	
26 S Potomac St, Baltimore, Maryland		2429 E Lafayette Ave, Baltimore, Maryland	0.128483

26 S Robinson St, Baltimore, Maryland	0.2963339	2429 E Oliver St, Baltimore, Maryland	
2601 E Fairmount Ave, Baltimore, Maryland	0.3921204	2433 E Hoffman St, Baltimore, Maryland	
2602 E Baltimore St, Baltimore, Maryland		2433 E Lafayette Ave, Baltimore, Maryland	0.128483
2604 E Baltimore St, Baltimore, Maryland		2434 E Hoffman St, Baltimore, Maryland	
2604 E Fairmount Ave, Baltimore, Maryland		2435 E Federal St, Baltimore, Maryland	0.19518
2606 E Baltimore St, Baltimore, Maryland		2443 E Hoffman St, Baltimore, Maryland	
2606 E Fairmount Ave, Baltimore, Maryland		2443 E Hoffman St, Baltimore, Maryland	
2607 E Fairmount Ave, Baltimore, Maryland		2446 E Preston St, Baltimore, Maryland	
2608 E Baltimore St, Baltimore, Maryland		3211 Leverton Ave, Baltimore, Maryland	
2613 E Fairmount Ave, Baltimore, Maryland	0.0908642	3212 E Baltimore St, Baltimore, Maryland	
2614 E Baltimore St, Baltimore, Maryland		3212 E Lombard St, Baltimore, Maryland	
2615 E Fairmount Ave, Baltimore, Maryland		3212 Leverton Ave, Baltimore, Maryland	
2616 E Baltimore St, Baltimore, Maryland		3213 Leverton Ave, Baltimore, Maryland	
2616 E Fairmount Ave, Baltimore, Maryland		3214 E Baltimore St, Baltimore, Maryland	
2618 E Baltimore St, Baltimore, Maryland		3214 E Lombard St, Baltimore, Maryland	
2620 E Baltimore St, Baltimore, Maryland		3214 Leverton Ave, Baltimore, Maryland	
2620 E Fairmount Ave, Baltimore, Maryland		3215 Esther Pl, Baltimore, Maryland	0.082385
2622 E Baltimore St, Baltimore, Maryland	0.2581656	3216 E Lombard St, Baltimore, Maryland	
2624 E Baltimore St, Baltimore, Maryland		3216 Leverton Ave, Baltimore, Maryland	
27 N Belnord Ave, Baltimore, Maryland	0.1035199	3217 E Baltimore St, Baltimore, Maryland	0.032497
27 N Luzerne Ave, Baltimore, Maryland	0.060104	3219 E Baltimore St, Baltimore, Maryland	0.032497
27 N Milton Ave, Baltimore, Maryland	0.0349388	3219 Esther Pl, Baltimore, Maryland	0.082385
27 N Rose St, Baltimore, Maryland		3219 Leverton Ave, Baltimore, Maryland	
27 S Decker Ave, Baltimore, Maryland	0.2354238	3222 E Baltimore St, Baltimore, Maryland	
27 S East Ave, Baltimore, Maryland		3223 Leverton Ave, Baltimore, Maryland	
2700 E Baltimore St, Baltimore, Maryland		3224 E Fairmount Ave, Baltimore, Maryland	0.158932
2700 E Baltimore St, Baltimore, Maryland		3224 E Lombard St, Baltimore, Maryland	0.127588
2700 E Baltimore St, Baltimore, Maryland		3225 E Baltimore St, Baltimore, Maryland	
2700 E Baltimore St, Baltimore, Maryland		3225 E Fairmount Ave, Baltimore, Maryland	0.064623
2706 E Fairmount Ave, Baltimore, Maryland	0.11468	3225 Esther Pl, Baltimore, Maryland	
2707 E Fayette St, Baltimore, Maryland	0.0874265	3225 Leverton Ave, Baltimore, Maryland	
2708 E Fairmount Ave, Baltimore, Maryland	0.11468	3225 Noble St, Baltimore, Maryland	0.11335
2712 E Fairmount Ave, Baltimore, Maryland		3226 E Fairmount Ave, Baltimore, Maryland	0.064623
2716 E Fairmount Ave, Baltimore, Maryland		3226 E Lombard St, Baltimore, Maryland	0.127588
2717 E Fayette St, Baltimore, Maryland		3227 Esther Pl, Baltimore, Maryland	0.126663
2719 E Fayette St, Baltimore, Maryland		3228 E Baltimore St, Baltimore, Maryland	
2728 E Baltimore St, Baltimore, Maryland	0.0407901	3228 E Fairmount Ave, Baltimore, Maryland	0.064623
2730 E Baltimore St, Baltimore, Maryland		3228 E Lombard St, Baltimore, Maryland	0.079316
2732 E Baltimore St, Baltimore, Maryland		3229 E Baltimore St, Baltimore, Maryland	
2734 E Baltimore St, Baltimore, Maryland	0.0268469	3229 E Fayette St, Baltimore, Maryland	
2742 E Baltimore St, Baltimore, Maryland	0.9949749	3229 Leverton Ave, Baltimore, Maryland	
2746 E Baltimore St, Baltimore, Maryland		3230 E Fairmount Ave, Baltimore, Maryland	
28 N Lakewood Ave, Baltimore, Maryland		3231 E Baltimore St, Baltimore, Maryland	

28 N Luzerne Ave, Baltimore, Maryland		3232 E Lombard St, Baltimore, Maryland	0.079316
28 N Potomac St, Baltimore, Maryland	0.0047886	3232 E Lombard St, Baltimore, Maryland	0.079316
28 S Decker Ave, Baltimore, Maryland	0.2990474	3233 E Baltimore St, Baltimore, Maryland	
28 S East Ave, Baltimore, Maryland		3233 Leverton Ave, Baltimore, Maryland	
28 S Ellwood Ave, Baltimore, Maryland		3234 Leverton Ave, Baltimore, Maryland	
28 S Robinson St, Baltimore, Maryland	0.2963339	3235 E Baltimore St, Baltimore, Maryland	
2800 E Fairmount Ave, Baltimore, Maryland	0.0438857	3235 E Baltimore St, Baltimore, Maryland	
2804 E Baltimore St, Baltimore, Maryland	0.994709	3236 Leverton Ave, Baltimore, Maryland	
2808 E Baltimore St, Baltimore, Maryland		3238 E Baltimore St, Baltimore, Maryland	0.032497
2821 E Fairmount Ave, Baltimore, Maryland		3238 E Lombard St, Baltimore, Maryland	
2826 E Baltimore St, Baltimore, Maryland		3238 Esther Pl, Baltimore, Maryland	0.126663
2830 E Baltimore St, Baltimore, Maryland		3240 E Lombard St, Baltimore, Maryland	
2834 E Baltimore St, Baltimore, Maryland	0.5853659	3241 E Baltimore St, Baltimore, Maryland	0.319296
2836 E Baltimore St, Baltimore, Maryland	0.5853659	3242 E Baltimore St, Baltimore, Maryland	
29 N Kenwood Ave, Baltimore, Maryland		3242 Leverton Ave, Baltimore, Maryland	
29 N Luzerne Ave, Baltimore, Maryland	0.060104	3247 E Baltimore St, Baltimore, Maryland	
29 N Streeper St, Baltimore, Maryland	0.1688578	3248 E Baltimore St, Baltimore, Maryland	
29 S Curley St, Baltimore, Maryland		3257 E Baltimore St, Baltimore, Maryland	
29 S Ellwood Ave, Baltimore, Maryland		3261 E Baltimore St, Baltimore, Maryland	
29 S Robinson St, Baltimore, Maryland	0.1760241	33 N Ellwood Ave, Baltimore, Maryland	0.056232
2900 E Baltimore St, Baltimore, Maryland		33 N Kenwood Ave, Baltimore, Maryland	0.986667
2900 E Baltimore St, Baltimore, Maryland		33 N Luzerne Ave, Baltimore, Maryland	0.101543
2901 E Baltimore St, Baltimore, Maryland		33 S Curley St, Baltimore, Maryland	0.301296
2901 E Baltimore St, Baltimore, Maryland		3300 E Baltimore St, Baltimore, Maryland	
2901 E Baltimore St, Baltimore, Maryland		3300 E Lombard St, Baltimore, Maryland	0.136457
2902 E Pratt St, Baltimore, Maryland		3301 Leverton Ave, Baltimore, Maryland	0.196749
2904 E Pratt St, Baltimore, Maryland		3301 Noble St, Baltimore, Maryland	0.071971
2905 E Baltimore St, Baltimore, Maryland		3302 E Lombard St, Baltimore, Maryland	0.136457
2905 E Baltimore St, Baltimore, Maryland		3303 E Baltimore St, Baltimore, Maryland	0.05347
2906 E Baltimore St, Baltimore, Maryland		3303 Leverton Ave, Baltimore, Maryland	0.196749
2907 E Baltimore St, Baltimore, Maryland		3304 Noble St, Baltimore, Maryland	0.144199
2908 E Baltimore St, Baltimore, Maryland		3305 E Baltimore St, Baltimore, Maryland	0.05347
2908 E Pratt St, Baltimore, Maryland		3305 Noble St, Baltimore, Maryland	
2909 E Baltimore St, Baltimore, Maryland		3306 Leverton Ave, Baltimore, Maryland	0.10131
2910 E Baltimore St, Baltimore, Maryland		3307 E Baltimore St, Baltimore, Maryland	0.05347
2910 E Pratt St, Baltimore, Maryland		3307 Noble St, Baltimore, Maryland	0.071971
2911 E Baltimore St, Baltimore, Maryland		3308 E Lombard St, Baltimore, Maryland	
2912 E Baltimore St, Baltimore, Maryland		3308 Noble St, Baltimore, Maryland	
2912 E Pratt St, Baltimore, Maryland		3309 Noble St, Baltimore, Maryland	
2914 E Baltimore St, Baltimore, Maryland		3310 E Baltimore St, Baltimore, Maryland	
2915 E Baltimore St, Baltimore, Maryland	0.0484355	3310 E Lombard St, Baltimore, Maryland	0.585798
2917 E Baltimore St, Baltimore, Maryland	0.0484355	3310 Leverton Ave, Baltimore, Maryland	
2918 E Baltimore St, Baltimore, Maryland	0.1140385	3317 E Baltimore St, Baltimore, Maryland	

2918 E Pratt St, Baltimore, Maryland	
2920 E Pratt St, Baltimore, Maryland	0.1620187
2921 E Baltimore St, Baltimore, Maryland	0.1229121
2922 E Pratt St, Baltimore, Maryland	0.1620187
2924 E Baltimore St, Baltimore, Maryland	
2924 E Pratt St, Baltimore, Maryland	
2926 E Pratt St, Baltimore, Maryland	
2928 E Baltimore St, Baltimore, Maryland	0.9754902
2929 E Baltimore St, Baltimore, Maryland	0.9754902
2933 E Baltimore St, Baltimore, Maryland	
2935 E Baltimore St, Baltimore, Maryland	
2938 E Baltimore St, Baltimore, Maryland	
3 N Clinton St, Baltimore, Maryland	
3 N Curley St, Baltimore, Maryland	0.3721137
3 N Kenwood Ave, Baltimore, Maryland	
3 N Luzerne Ave, Baltimore, Maryland	
3 N Milton Ave, Baltimore, Maryland	
3 S East Ave, Baltimore, Maryland	0.0706869
3 S Linwood Ave, Baltimore, Maryland	
3 S Potomac St, Baltimore, Maryland	
3 S Robinson St, Baltimore, Maryland	0.2420237
30 N Ellwood Ave, Baltimore, Maryland	0.0605383
30 N Kenwood Ave, Baltimore, Maryland	
30 N Linwood Ave, Baltimore, Maryland	
30 S Curley St, Baltimore, Maryland	0.263082
30 S East Ave, Baltimore, Maryland	
30 S Ellwood Ave, Baltimore, Maryland	
3000 E Pratt St, Baltimore, Maryland	0.0352009
3000 E Pratt St, Baltimore, Maryland	0.0352009
3001 E Baltimore St, Baltimore, Maryland	
3001 E Baltimore St, Baltimore, Maryland	
3002 E Baltimore St, Baltimore, Maryland	
3003 E Baltimore St, Baltimore, Maryland	
3004 E Baltimore St, Baltimore, Maryland	
3005 E Baltimore St, Baltimore, Maryland	
3006 E Baltimore St, Baltimore, Maryland	
3007 E Baltimore St, Baltimore, Maryland	
3009 E Baltimore St, Baltimore, Maryland	
3010 E Baltimore St, Baltimore, Maryland	
3011 E Baltimore St, Baltimore, Maryland	
3013 E Baltimore St, Baltimore, Maryland	
3014 E Pratt St, Baltimore, Maryland	0.0613467
3015 E Baltimore St, Baltimore, Maryland	0.1062652

3317 Noble St, Baltimore, Maryland	
3318 E Baltimore St, Baltimore, Maryland	
3318 Noble St, Baltimore, Maryland	0.141766
3321 Noble St, Baltimore, Maryland	0.141766
3324 E Baltimore St, Baltimore, Maryland	0.05347
3324 Noble St, Baltimore, Maryland	0.085447
3340 E Baltimore St, Baltimore, Maryland	0.29188
3344 E Baltimore St, Baltimore, Maryland	0.340313
3344 E Baltimore St, Baltimore, Maryland	0.340313
3344 E Baltimore St, Baltimore, Maryland	0.340313
34 N Curley St, Baltimore, Maryland	0.145904
34 N East Ave, Baltimore, Maryland	
34 N Ellwood Ave, Baltimore, Maryland	0.056232
34 N Lakewood Ave, Baltimore, Maryland	0.510488
34 N Streeper St, Baltimore, Maryland	0.230558
34 S Decker Ave, Baltimore, Maryland	0.251511
34 S Potomac St, Baltimore, Maryland	0.090558
35 N Belnord Ave, Baltimore, Maryland	0.237828
35 N Curley St, Baltimore, Maryland	0.145904
35 N Lakewood Ave, Baltimore, Maryland	0.510488
35 N Lakewood Ave, Baltimore, Maryland	0.510488
35 N Lakewood Ave, Baltimore, Maryland	0.510488
35 N Lakewood Ave, Baltimore, Maryland	0.510488
35 N Lakewood Ave, Baltimore, Maryland	0.510488
35 N Lakewood Ave, Baltimore, Maryland	0.510488
35 N Lakewood Ave, Baltimore, Maryland	0.510488
35 N Lakewood Ave, Baltimore, Maryland	0.510488
35 N Lakewood Ave, Baltimore, Maryland	0.510488
35 N Linwood Ave, Baltimore, Maryland	
35 N Milton Ave, Baltimore, Maryland	0.029278
35 S Decker Ave, Baltimore, Maryland	0.251511
35 S Potomac St, Baltimore, Maryland	0.090558
36 N Decker Ave, Baltimore, Maryland	0.242824
36 N Lakewood Ave, Baltimore, Maryland	0.01073
36 N Linwood Ave, Baltimore, Maryland	
36 N Luzerne Ave, Baltimore, Maryland	0.101543
36 N Potomac St, Baltimore, Maryland	0.034615
36 S East Ave, Baltimore, Maryland	0.028568
36 S Ellwood Ave, Baltimore, Maryland	
36 S Potomac St, Baltimore, Maryland	0.090558
37 N Decker Ave, Baltimore, Maryland	0.242824
37 N Streeper St, Baltimore, Maryland	0.166391
37 S Decker Ave, Baltimore, Maryland	0.251511

3017 E Baltimore St, Baltimore, Maryland	0.1062652
3018 E Pratt St, Baltimore, Maryland	
3019 E Baltimore St, Baltimore, Maryland	
3020 E Pratt St, Baltimore, Maryland	
3022 E Baltimore St, Baltimore, Maryland	0.074136
3023 E Baltimore St, Baltimore, Maryland	0.074136
3024 E Baltimore St, Baltimore, Maryland	
3027 E Baltimore St, Baltimore, Maryland	
3027 E Baltimore St, Baltimore, Maryland	
3028 E Pratt St, Baltimore, Maryland	
3029 E Baltimore St, Baltimore, Maryland	
3030 E Baltimore St, Baltimore, Maryland	0.5334607
3031 E Baltimore St, Baltimore, Maryland	0.5334607
3035 E Baltimore St, Baltimore, Maryland	
3036 E Baltimore St, Baltimore, Maryland	
3038 E Baltimore St, Baltimore, Maryland	
31 N Ellwood Ave, Baltimore, Maryland	0.0562324
31 N Luzerne Ave, Baltimore, Maryland	0.060104
31 N Milton Ave, Baltimore, Maryland	
31 S Curley St, Baltimore, Maryland	0.263082
31 S East Ave, Baltimore, Maryland	
31 S Ellwood Ave, Baltimore, Maryland	
3101 E Fairmount Ave, Baltimore, Maryland	0.1257677
3102 E Baltimore St, Baltimore, Maryland	
3103 E Baltimore St, Baltimore, Maryland	
3104 E Lombard St, Baltimore, Maryland	
3107 E Fayette St, Baltimore, Maryland	
3116 E Baltimore St, Baltimore, Maryland	
3120 E Baltimore St, Baltimore, Maryland	
3126 E Lombard St, Baltimore, Maryland	0.9880478
3137 E Baltimore St, Baltimore, Maryland	0.1676881
32 N East Ave, Baltimore, Maryland	
32 N Lakewood Ave, Baltimore, Maryland	0.5104881
32 N Potomac St, Baltimore, Maryland	0.0298978
32 S Decker Ave, Baltimore, Maryland	0.2354238
32 S East Ave, Baltimore, Maryland	
32 S Ellwood Ave, Baltimore, Maryland	
32 S Potomac St, Baltimore, Maryland	0.0094983
3200 E Lombard St, Baltimore, Maryland	
3201 Esther Pl, Baltimore, Maryland	
3201 Leverton Ave, Baltimore, Maryland	
3202 E Fairmount Ave, Baltimore, Maryland	0.0633108
3203 E Lombard St, Baltimore, Maryland	0.0316635

38 S Curley St, Baltimore, Maryland	0.301296
38 S Decker Ave, Baltimore, Maryland	0.251721
38 S East Ave, Baltimore, Maryland	0.028568
38 S Ellwood Ave, Baltimore, Maryland	
39 S Decker Ave, Baltimore, Maryland	0.251511
39 S East Ave, Baltimore, Maryland	0.028568
39 S Potomac St, Baltimore, Maryland	0.229945
4 N Clinton St, Baltimore, Maryland	
4 N Decker Ave, Baltimore, Maryland	0.186753
4 N Lakewood Ave, Baltimore, Maryland	
4 N Linwood Ave, Baltimore, Maryland	0.017516
4 N Rose St, Baltimore, Maryland	0.156818
4 S Decker Ave, Baltimore, Maryland	0.212141
4 S East Ave, Baltimore, Maryland	
4 S Potomac St, Baltimore, Maryland	
41 S Decker Ave, Baltimore, Maryland	
41 S East Ave, Baltimore, Maryland	
42 S Decker Ave, Baltimore, Maryland	0.251635
43 S Decker Ave, Baltimore, Maryland	0.251635
5 N Ellwood Ave, Baltimore, Maryland	0.097603
5 N Kenwood Ave, Baltimore, Maryland	
5 N Potomac St, Baltimore, Maryland	
5 N Rose St, Baltimore, Maryland	0.156818
5 S Ellwood Ave, Baltimore, Maryland	
6 N Curley St, Baltimore, Maryland	0.372114
6 N East Ave, Baltimore, Maryland	
6 N Ellwood Ave, Baltimore, Maryland	0.097603
6 N Glover St, Baltimore, Maryland	0.247232
6 N Lakewood Ave, Baltimore, Maryland	0.054429
6 N Linwood Ave, Baltimore, Maryland	
6 N Luzerne Ave, Baltimore, Maryland	
6 N Potomac St, Baltimore, Maryland	
6 N Streeper St, Baltimore, Maryland	0.211248
6 S Ellwood Ave, Baltimore, Maryland	
6 S Robinson St, Baltimore, Maryland	0.229935
7 N Belnord Ave, Baltimore, Maryland	0.14297
7 N Curley St, Baltimore, Maryland	0.20193
7 N Ellwood Ave, Baltimore, Maryland	0.097603
7 N Linwood Ave, Baltimore, Maryland	
7 N Milton Ave, Baltimore, Maryland	
7 S Curley St, Baltimore, Maryland	0.199214
7 S Linwood Ave, Baltimore, Maryland	0.031039
8 N Decker Ave, Baltimore, Maryland	0.309971

3205 E Lombard St, Baltimore, Maryland	0.127588	8 N Lakewood Ave, Baltimore, Maryland	0.054429
3205 Esther Pl, Baltimore, Maryland		8 N Luzerne Ave, Baltimore, Maryland	
3206 E Fairmount Ave, Baltimore, Maryland	0.022243	8 N Potomac St, Baltimore, Maryland	
3207 Esther Pl, Baltimore, Maryland		8 N Rose St, Baltimore, Maryland	
3207 Leverton Ave, Baltimore, Maryland		8 N Streeper St, Baltimore, Maryland	
3208 E Fairmount Ave, Baltimore, Maryland	0.022243	9 N Belnord Ave, Baltimore, Maryland	0.14297
3208 E Lombard St, Baltimore, Maryland		9 N Curley St, Baltimore, Maryland	0.201801
3209 E Baltimore St, Baltimore, Maryland		9 N East Ave, Baltimore, Maryland	0.077948
3209 E Lombard St, Baltimore, Maryland	0.0793156	9 N Ellwood Ave, Baltimore, Maryland	0.176097
3209 Leverton Ave, Baltimore, Maryland		9 S Curley St, Baltimore, Maryland	0.22301
3211 Esther Pl, Baltimore, Maryland		9 S Decker Ave, Baltimore, Maryland	0.223656